Chapter 7

Hydrologic Processes

7.1 INTRODUCTION TO HYDROLOGY

7.1.1 What is Hydrology?

The U.S. National Research Council (1991) presented the following definition of hydrology:

> Hydrology is the science that treats the waters of the Earth, their occurrence, circulation, and distribution, their chemical and physical properties, and their reaction with the environment, including the relation to living things. The domain of hydrology embraces the full life history of water on Earth.

For purposes of this book we are interested in the engineering aspects of hydrology, or what we might call *engineering hydrology*. From this point of view we are mainly concerned with quantifying amounts of water at various locations (spatially) as a function of time (temporally) for surface water applications. In other words, we are concerned with solving engineering problems using hydrologic principles. This chapter is not concerned with the chemical properties of water and their relation to living things.

Books on hydrology include: Bedient and Huber (1992); Bras (1990); Chow (1964); Chow, Maidment, and Mays (1988); Gupta (1989); Maidment (1993); McCuen (1998); Ponce (1989); Singh (1992); Viessman and Lewis (1996); and Wanielista, Kersten, and Eaglin (1997).

7.1.2 The Hydrologic Cycle

The central focus of hydrology is the *hydrologic cycle*, consisting of the continuous processes shown in Figure 7.1.1. Water *evaporates* from the oceans and land surfaces to become water vapor that is carried over the earth by atmospheric circulation. The *water vapor* condenses and *precipitates* on the land and oceans. The precipitated water may be *intercepted* by vegetation, become overland flow over the ground surface, *infiltrate* into the ground, flow through the soil as *subsurface flow*, and discharge as *surface runoff*. Evaporation from the land surface comprises evaporation directly from soil and vegetation surfaces, and *transpiration* through plant leaves. Collectively these processes are called *evapotranspiration*. Infiltrated water may percolate deeper to recharge groundwater and later become *springflow* or *seepage* into streams also to become streamflow.

The hydrologic cycle can be viewed on a global scale as shown in Figure 7.1.2. As discussed by the U.S. National Research Council (1991): "As a global average, only about 57 percent of the precipitation that falls on the land (P_l) returns directly to the atmosphere (E_l) without reaching the ocean. The remainder is runoff (R), which find its way to the sea primarily by rivers but also through subsurface (groundwater) movement and by the calving of icebergs from glaciers and ice shelves
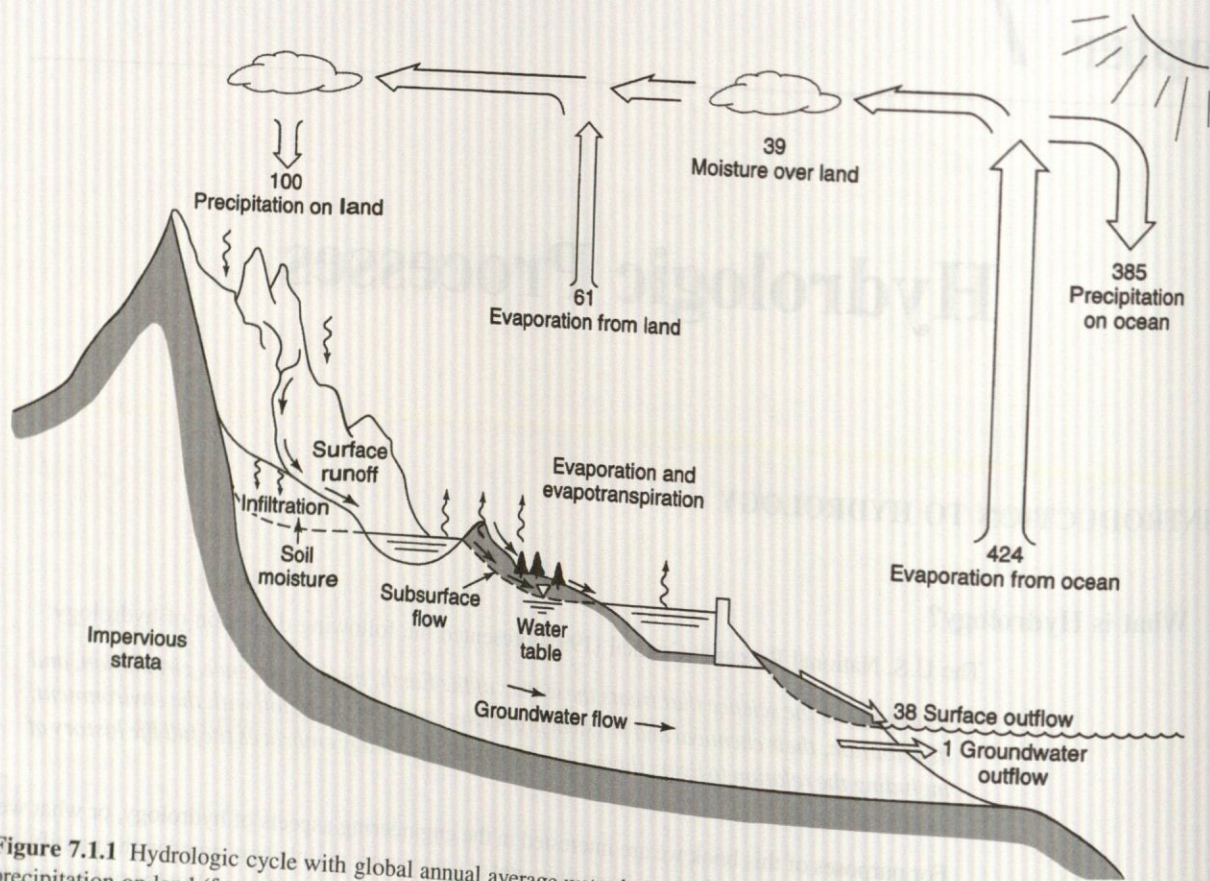
Figure 7.1.1 Hydrologic cycle with global annual average water balance given in units relative to a value of 100 for the rate of precipitation on land (from Chow et al. (1988)).
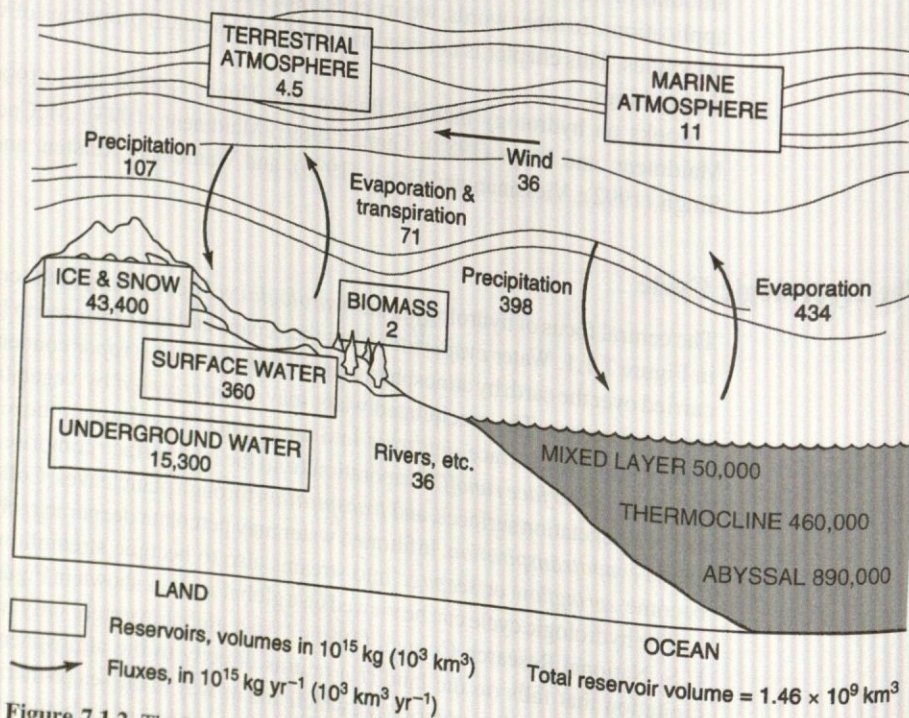

Figure 7.1.2 The hydrologic cycle at global scale (from U.S. National Research Council (1991)).

(*W*). In this gravitationally powered runoff process, the water may spend time in one or more natural storage reservoirs such as snow, glaciers, ice sheets, lakes, streams, soils and sediments, vegetation, and rock. Evaporation from these reservoirs short-circuits the global hydrologic cycle into subcycles with a broad spectrum of scale. The runoff is perhaps the best-known element of the global hydrologic cycle, but even this is subject to significant uncertainty."

7.1.3 Hydrologic Systems

Chow, Maidment, and Mays (1988) defined a *hydrologic system* as a structure or volume in space, surrounded by a boundary, that accepts water and other inputs, operates on them internally, and produces them as outputs. The structure (for surface or subsurface flow) or volume in space (for atmospheric moisture flow) is the totality of the flow paths through which the water may pass as throughput from the point it enters the system to the point it leaves. The boundary is a continuous surface defined in three dimensions enclosing the volume or structure. A *working medium* enters the system as input, interacts with the structure and other media, and leaves as output. Physical, chemical, and biological processes operate on the working media within the system; the most common working media involved in hydrologic analysis are water, air, and heat energy.

The *global hydrologic cycle* can be represented as a system containing three subsystems: the atmospheric water system, the surface water system, and the subsurface water system, as shown in Figure 7.1.3. Another example is the storm-rainfall-runoff process on a watershed, which can be represented as a hydrologic system. The input is rainfall distributed in time and space over the watershed, and the output is streamflow at the watershed outlet. The boundary is defined by the watershed divide and extends vertically upward and downward to horizontal planes.
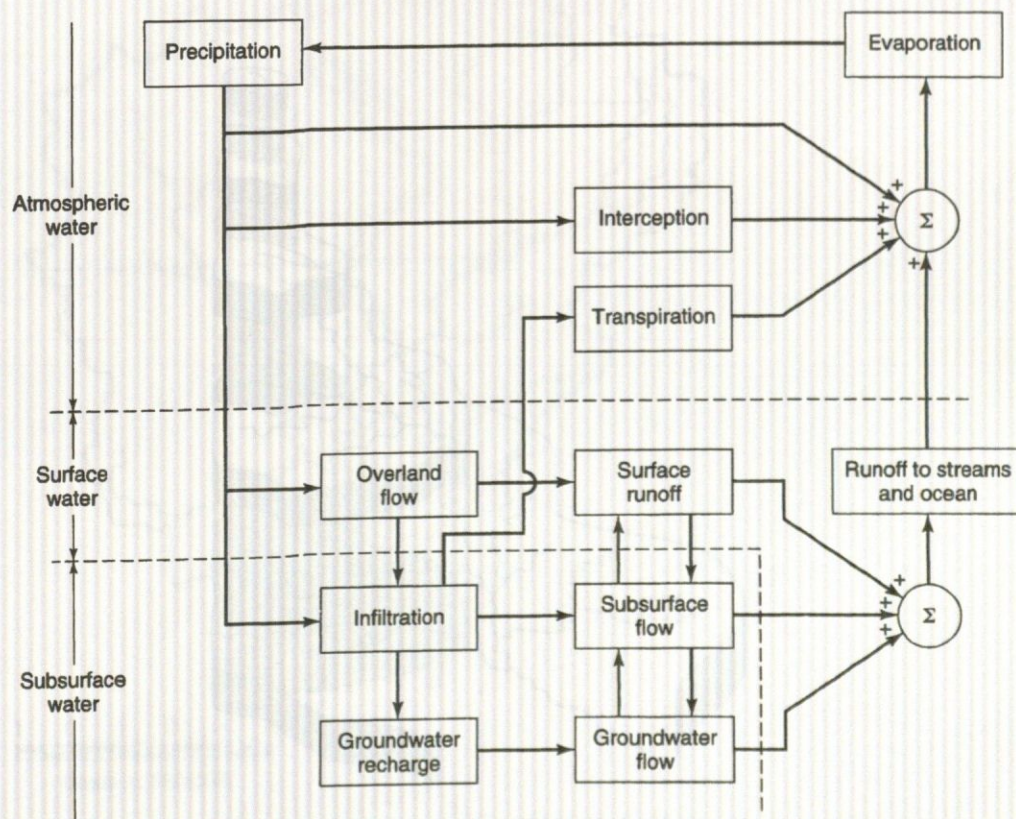

Figure 7.1.3 Block-diagram representation of the global hydrologic system (from Chow et al. (1988)).

Drainage basins, catchments, and *watersheds* are three synonymous terms that refer to the topographic area that collects and discharges surface streamflow through one outlet or mouth. Catchments are typically referred to as small drainage basins, but no specific area limits have been established. Figure 7.1.4 illustrates the drainage basin divide, watershed divide, or catchment divide, which is the line dividing land whose drainage flows toward the given stream from land whose drainage flows away from that stream. Think of drainage basin sizes ranging from the Mississippi
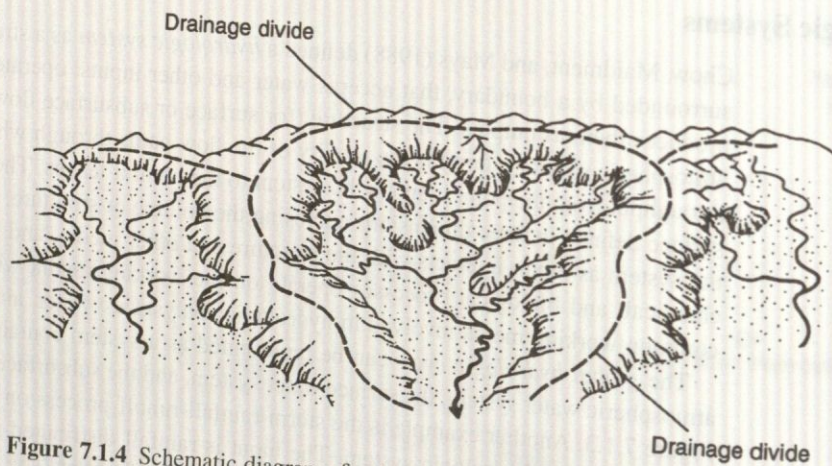

Figure 7.1.4 Schematic diagram of a drainage basin. The high terrain on the perimeter is the drainage divide (from Marsh (1987)).
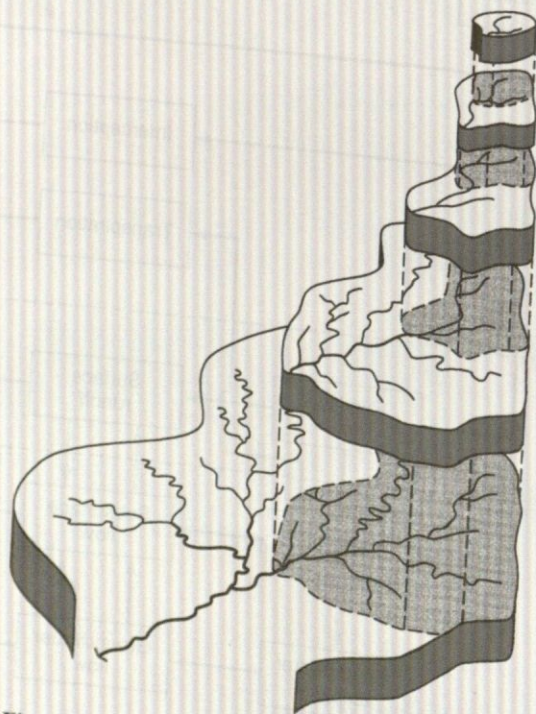

Figure 7.1.5 Illustration of the nested hierarchy of lower-order basins within a large drainage basin (from Marsh (1987)).

River drainage basin to small urban drainage basins in your local community or some small valley in the countryside near you.

As shown in Figure 7.1.5, drainage basins can be pictured in a pyramidal fashion as the runoffs from smaller basins (subsystems) combine to form larger basins (subsystem in system), and the runoffs from these basins in turn combine to form even larger basins, and so on. Marsh (1987) refers to this mode of organization as a *hierarchy* or *nested hierarchy*, as each set of smaller basins is set inside the next layer. A similar concept is that streams that drain small basins combine to form larger streams, and so on.

Figures 7.1.6–7.1.10 illustrate the hierarchy of the Friends Creek watershed located in the Lake Decatur watershed (drainage area upstream of Decatur, Illinois, on the Sangamon River with a drainage area of 925 mi^2 or 2396 km^2). Obviously, the Friends Creek watershed can be subdivided into much smaller watersheds. Figure 7.1.8 illustrates the Illinois River basin (29,000 mi^2) with the Sangamon River. Figure 7.1.9 illustrates the upper Mississippi River basin (excluding the Missouri River) with the Illinois River. Figure 7.1.10 illustrates the entire Mississippi River basin (1.15 million mi^2). This is the largest river basin in the United States, draining about 40 percent of the country. The main stem of the river is about 2400 miles long.
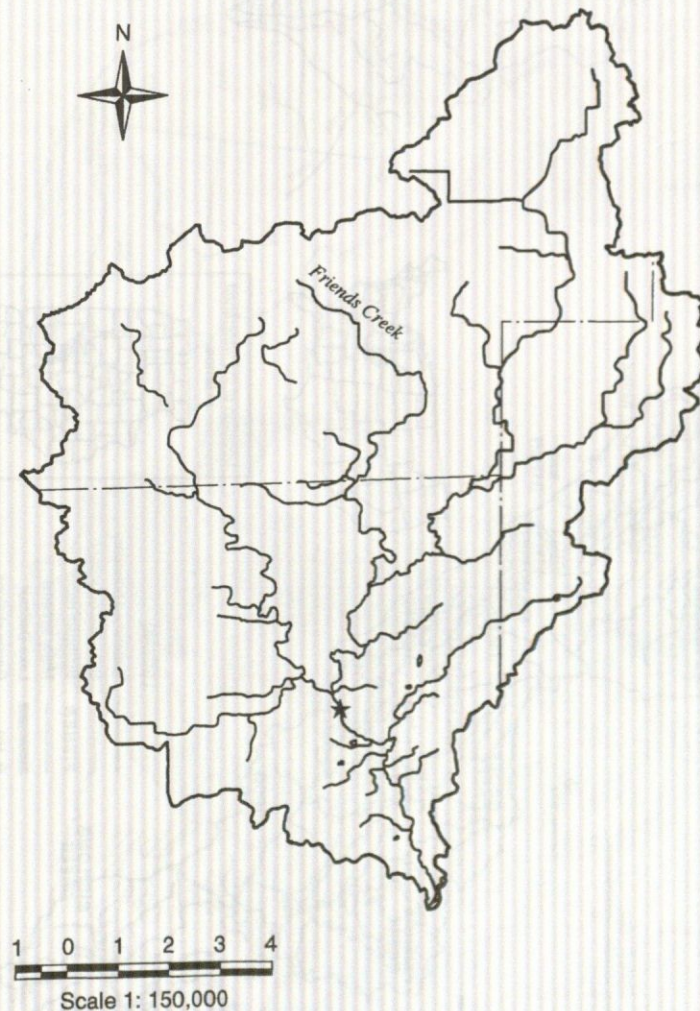

Figure 7.1.6 Friends Creek watershed, subwatershed of the Lake Decatur watershed. (Courtesy of the Illinois State Water Survey, compiled by Erin Hessler Bauer.)
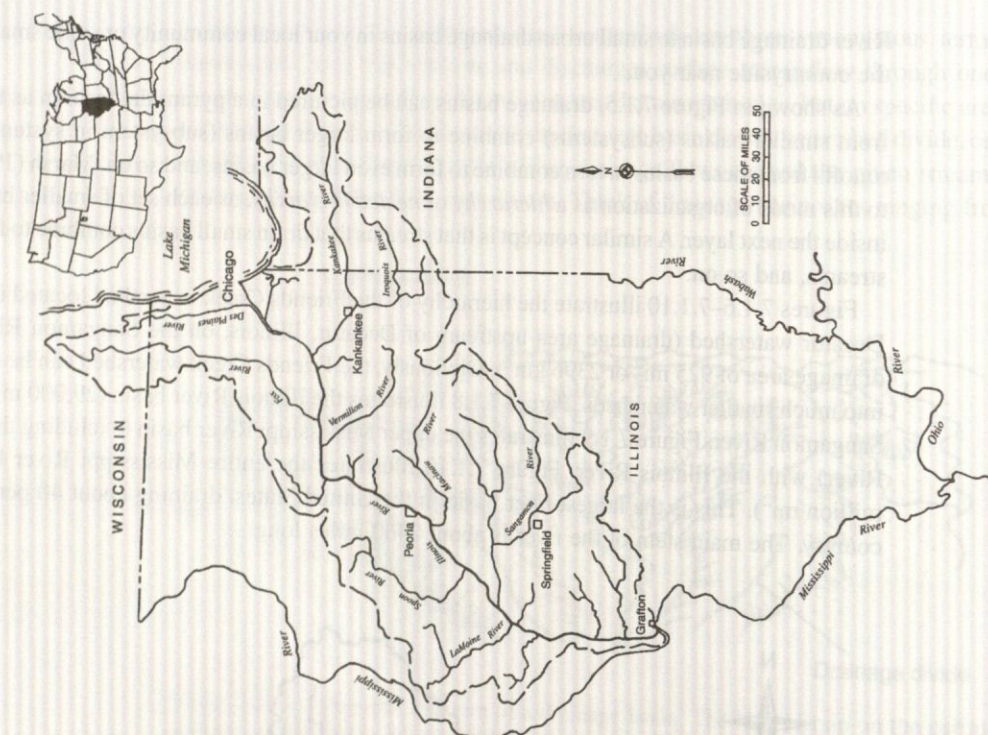
Figure 7.1.8 The Illinois River Basin showing the Sangamon River (from Bhowmik (1998)).

Figure 7.1.7 Lake Decatur watershed in the upper Sangamon River Basin (upstream of Decatur, Illinois). The location of Friends Creek watershed (Figure 7.1.6) is shown (from Demissee and Keefer (1998)).

Figure 7.1.10 The Mississippi River Basin in the United States (from Bhowmik (1998)).

Figure 7.1.9 The Upper Mississippi River excluding the Missouri River. The location of the Illinois River (Figure 7.1.8) is shown (from Bhowmik (1998)).

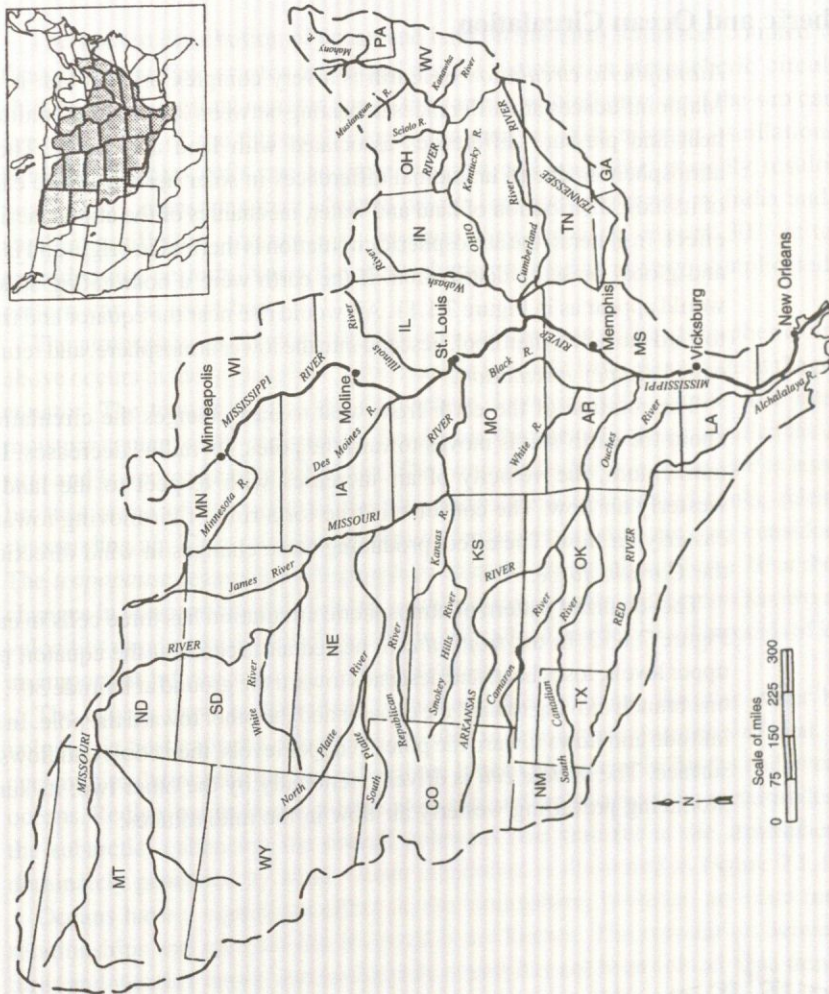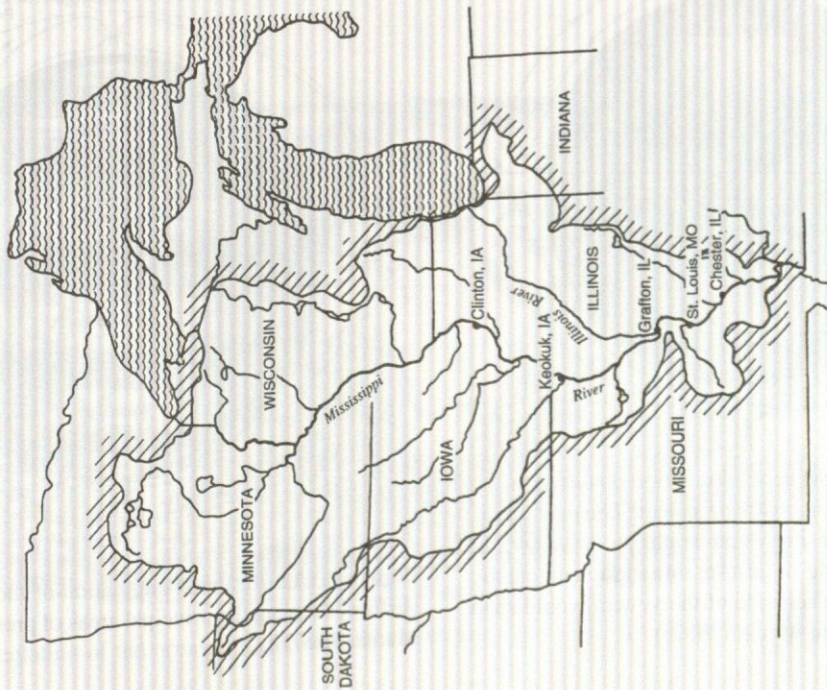## 7.1.4 Atmospheric and Ocean Circulation

Atmospheric circulation on Earth is a very complex process that is influenced by many factors. Major influences are differences in heating between low and high altitudes, the earth's rotation, and heat and pressure differences associated with land and water. The general circulation of the atmosphere is due to latitudinal differences in solar heating of the earth's surface and inclination of its axis, distribution of land and water, mechanics of the atmospheric fluid flow, and the Coriolis effect. In general, the atmospheric circulation is thermal in origin and is related to the earth's rotation and global pressure distribution. If the earth were a nonrotating sphere, atmospheric circulation would appear as in Figure 7.1.11. Air would rise near the equator and travel in the upper atmosphere toward the poles, then cool, descend into the lower atmosphere, and return toward the equator. This is called *Hadley circulation*.

The rotation of the earth from west to east changes the circulation pattern. As a ring of air about the earth's axis moves toward the poles, its radius decreases. In order to maintain angular momentum, the velocity of air increases with respect to the land surface, thus producing a westerly air flow. The converse is true for a ring of air moving toward the equator—it forms an easterly air flow. The effect producing these changes in wind direction and velocity is known as the *Coriolis force*.

The idealized pattern of atmospheric circulation has three cells in each hemisphere, as shown in Figure 7.1.12. In the *tropical cell*, heated air ascends at the equator, proceeds toward the poles at upper levels, loses heat, and descends toward the ground at latitude 30°. Near the ground it branches, one branch moving toward the equator and the other toward the pole. In the *polar cell*, air rises at 60° latitude and flows toward the poles at upper levels, then cools and flows back to 60° near the earth's surface. The *middle cell* is driven frictionally by the other two; its surface flows toward the pole, producing prevailing westerly air flow in the midlatitudes.
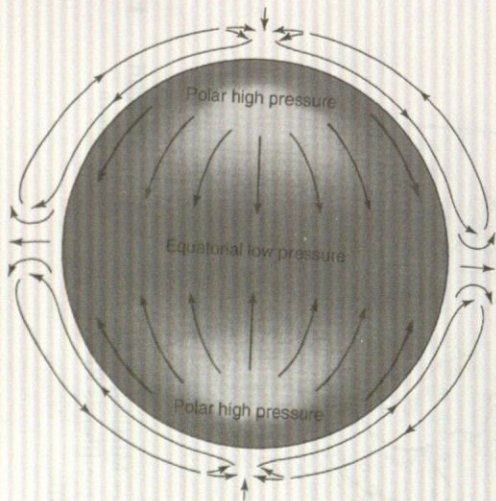
Figure 7.1.11 Atmospheric circulation pattern that would develop on a nonrotating planet. The equatorial belt would heat intensively and would produce low pressure, which would in turn set into motion a gigantic convection system. Each side of the system would span one hemisphere (from Marsh (1987)).
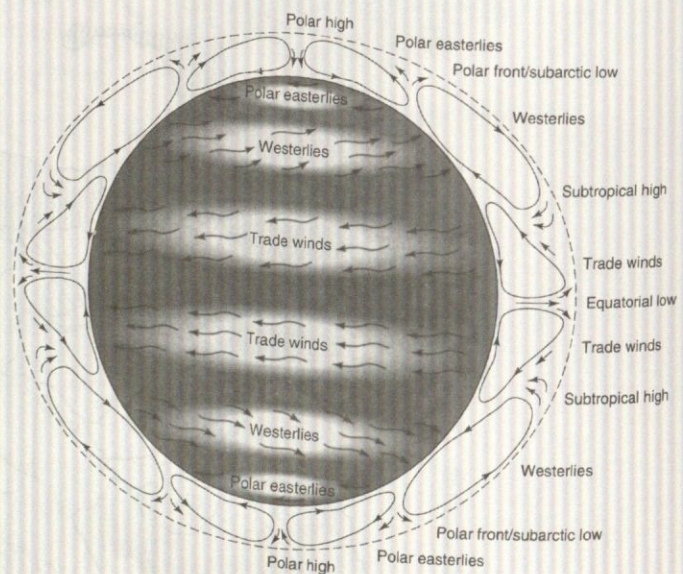

Figure 7.1.12 Idealized circulation of the atmosphere at the earth's surface, showing the principal areas of pressure and belts of winds (from Marsh (1987)).

The uneven distribution of ocean and land on the earth's surface, coupled with their different thermal properties, creates additional spatial variation in atmospheric circulation. The annual shifting of the thermal equator due to the earth's revolution around the sun causes a corresponding oscillation of the three-cell circulation pattern. With a larger oscillation, exchanges of air between adjacent cells can be more frequent and complete, possibly resulting in many flood years. Also, monsoons may advance deeper into such countries as India and Australia. With a smaller oscillation, intense high pressure may build up around 30° latitude, thus creating extended dry periods. Since the atmospheric circulation is very complicated, only the general pattern can be identified.

The atmosphere is divided vertically into various zones. The atmospheric circulation described above occurs in the *troposphere*, which ranges in height from about 8 km at the poles to 16 km at the equator. The temperature in the troposphere decreases with altitude at a rate varying with the moisture content of the atmosphere. For dry air, the rate of decrease is called the *dry adiabatic lapse rate* and is approximately 9.8°C/km. The *saturated adiabatic lapse rate* is less, about 6.5° C/km, because some of the vapor in the air condenses as it rises and cools, releasing heat into the surrounding air. These are average figures for lapse rates that can vary considerably with altitude. The *tropopause* separates the troposphere from the *stratosphere* above. Near the tropopause, sharp changes in temperature and pressure produce strong narrow air currents known as *jet streams*, with velocities ranging from 15 to 50 m/s (30 to 100 m/h). They flow for thousands of kilometers and have an important influence on air-mass movement.

The oceans exert an important control on global climate. Because water bodies have a high volumetric heat capacity, the oceans are able to retain great quantities of heat. Through wave and current circulation, the oceans redistribute heat to considerable depths and even large areas of the oceans. Redistribution is east-west or west-east and is also across the midaltitudes from the tropics to the subarctic, enhancing the overall poleward beat transfer in the atmosphere. Waves are predominately generated by wind. Ocean circulation is illustrated in Figure 7.1.13.

Oceans have a significant effect on the atmosphere; however, an exact understanding of the relationships and mechanisms involved is not known. The correlation between ocean temperatures and weather trends and midlatitude events has not been solved. One trend is the growth and decline of a warm body of water in the equatorial zone of the eastern Pacific Ocean, referred to as
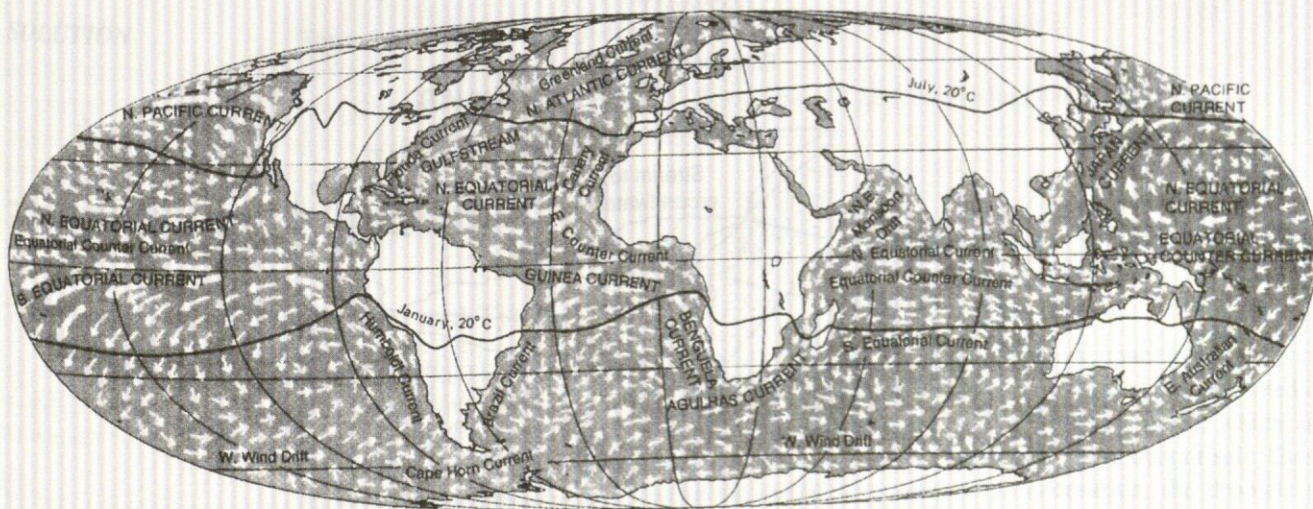

Figure 7.1.13 The actual circulation of the oceans. Major currents are shown with heavy arrows (from Marsh (1987)).

El Niño (meaning "The Infant" in Spanish, alluding to the Christ Child, because the effect typically begins around Christmas). The warm body of water develops and expands every five years or so off the coast of Peru, initiated by changes in atmospheric pressure resulting in a decline of the easterly trade winds. This reduction in wind reduces resistance, causing the eastwardly equatorial countercurrent to rise. As El Niño builds up, the warm body of water flows out into the Pacific and along the tropical west coast of the Americas, displacing the colder water of the California and Humboldt currents. One of the interesting effects of this weather variation is the South Oscillation, which changes precipitation patterns—resulting in drier conditions in areas of normally little precipitation.

7.1.5 Hydrologic Budget

A *hydrologic budget, water budget,* or *water balance* is a measurement of continuity of the flow of water, which holds true for any time interval and applies to any size area ranging from local-scale areas to regional-scale areas or from any drainage area to the earth as a whole. The hydrologists usually must consider an open system, for which the quantification of the hydrologic cycle for that system becomes a mass balance equation in which the change of storage of water (dS/dt) with respect to time within that system is equal to the inputs (I) to the system minus the outputs (O) from the system.

Considering the open system in Figure 7.1.14, the water balance equation can be expressed for the surface water system and the groundwater system in units of volume per unit time separately or, for a given time period and area, in depth.
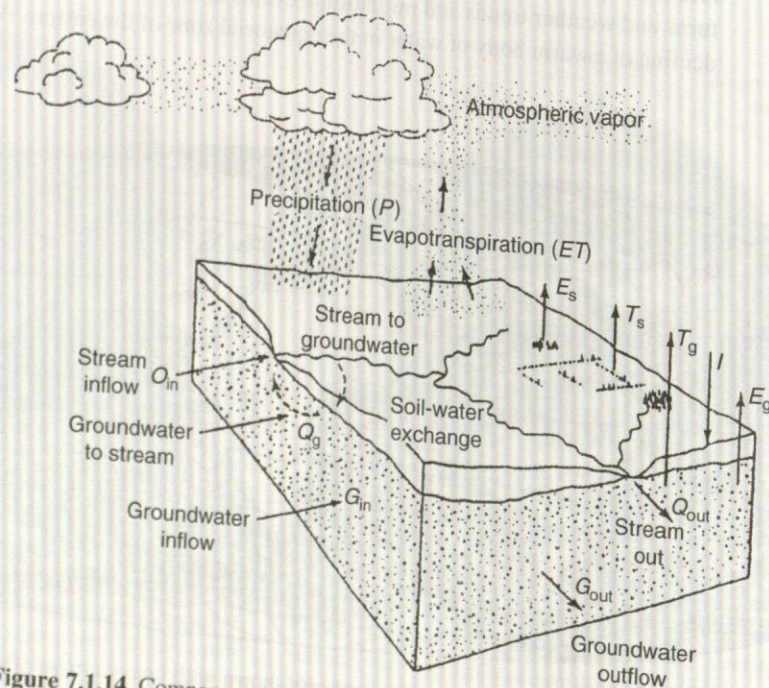

Figure 7.1.14 Components of hydrologic cycle in an open system: the major inflows and outflows of water from a parcel of land (from Marsh and Dozier (1986)) (Courtesy John Wiley & Sons, Inc.)

EXAMPLE 7.1.

SOLUTION

7.2 PRECIP

7.2.1 Precipit

Surface Water System Hydrologic Budget

$$P + Q_{in} - Q_{out} + Q_g - E_s - T_s - I = \Delta S_s \tag{7.1.1}$$

where P is the precipitation, Q_{in} is the surface water flow into the system, Q_{out} is the surface water flow out of the system, Q_g is the groundwater flow into the stream, E_s is the surface evaporation, T_s is the transpiration, I is the infiltration, and ΔS_s is the change in water storage of the surface water system.

Groundwater System Hydrologic Budget

$$I + G_{in} - G_{out} - Q_g - E_g - T_g = \Delta S_g \tag{7.1.2}$$

where G_{in} is the groundwater flow into the system, G_{out} is the groundwater flow out of the system, and ΔS_g is the change in groundwater storage. The evaporation, E_g, and the transpiration, T_g, can be significant if the water table is near the ground surface.

System Hydrologic Budget
The system hydrologic budget is developed by adding the above two budgets together:

$$P - (Q_{out} - Q_{in}) - (E_s + E_g) - (T_s + T_g) - (G_{out} - G_{in}) = \Delta(S_s + S_g) \tag{7.1.3}$$

Using net mass exchanges, the above system hydrologic budget can be expressed as

$$P - Q - G - E - T = \Delta S \tag{7.1.4}$$

EXAMPLE 7.1.1 During January 1996, the water-budget terms for Lake Annie in Florida included precipitation (P) of 1.9 in, evaporation (E) of 1.5 in, surface water inflow (Q_{in}) of 0 in, surface outflow (Q_{out}) of 17.4 in, and change in lake volume (ΔS) of 0 in. Determine the net groundwater flow for January 1996 (the groundwater inflow minus the groundwater outflow).

SOLUTION The water budget equation to define the net groundwater flow for the lake is

$$G = \Delta S - P + E - Q_{in} + Q_{out} = 0 - 1.9 + 1.5 - 0 + 17.4 = 17 \text{ in for January 1996}$$

7.2 PRECIPITATION (RAINFALL)

7.2.1 Precipitation Formation and Types

Even though precipitation includes rainfall, snowfall, hail, and sleet, our concern in this book will relate almost entirely to rainfall. The formation of water droplets in clouds is illustrated in Figure 7.2.1. *Condensation* takes place in the atmosphere on *condensation nuclei*, which are very small particles ($10^{-3} - 10 \, \mu m$) in the atmosphere that are composed of dust or salt. These particles are called *aerosols*. During the initial occurrence of condensation, the droplets or ice particles are very small and are kept aloft by motion of the air molecules. Once droplets are formed they also act as condensation nuclei. These droplets tend to repel one another, but in the presence of an electric field in the atmosphere they attract one another and are heavy enough
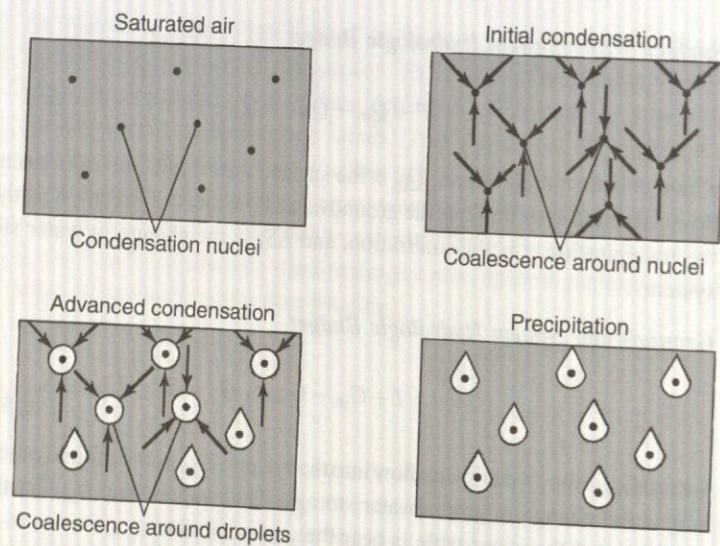
Saturated air

Initial condensation

Condensation nuclei

Coalescence around nuclei

Advanced condensation

Precipitation

Coalescence around droplets

Figure 7.2.1 Precipitation formation. Water droplets in clouds are formed by nucleation of vapor on aerosols, then go through many condensation-evaporation cycles as they circulate in the cloud, until they aggregate into large enough drops to fall through the cloud base (from Marsh (1987)).

(~0.1 mm) to fall through the atmosphere. Some of the droplets evaporate in the atmosphere, some of the droplets decrease in size by evaporation, and some of the droplets increase in size by impact and aggregation.

Basically, the formation of precipitation requires lifting of an air mass in the atmosphere; it then cools and some of its moisture condenses. There are three main mechanisms of air mass lifting: *frontal lifting, orographic lifting*, and *convective lifting*. Frontal lifting (Figure 7.2.2) occurs when warm air is lifted over cooler air by frontal passage, orographic lifting (Figure 7.2.3) occurs when an air mass rises over a mountain range, and convective lifting (Figure 7.2.4) occurs when air is drawn upward by convective action such as a thunderstorm cell.

7.2.2   Rainfall Variability

In order to determine the runoff from a watershed and the resulting stream flow, precipitation is one of the primary inputs. Rainfall varies in space and time as a result of the general pattern of atmospheric circulation and local factors. Figure 7.2.5 shows the mean annual precipitation in the United States, and Figure 7.2.6 shows the normal monthly distribution of precipitation in the United States. Figure 7.2.7 shows the mean annual precipitation of the world.

Rainstorms can vary significantly in space and time. *Rainfall hyetographs* are plots of rainfall depth or intensity as a function of time. Figure 7.2.8a shows examples of two rainfall hyetographs. Cumulative rainfall hyetographs (rainfall mass curve) can be developed as shown in Figure 7.2.8b. *Isohyets* (contours of constant rainfall) can be drawn to develop isohyetal maps of rainfall depth. *Isohyetal maps* are an interpolation of rainfall data recorded at gauged points. An example is shown in Figure 7.2.9 for the Upper Mississippi River Basin storm of January through July 1993. On a much smaller scale, shown in Figure 7.2.10, is the isohyetal map of the May 24–25, 1981 storm in Austin, Texas.

Figure 7.2.11 illustrates the three methods for determining areal average rainfall using rainfall gauge data. These are the *arithmetic-mean method*, the *Thiessen method*, and the *isohyetal method*.

Cross-section from A to B
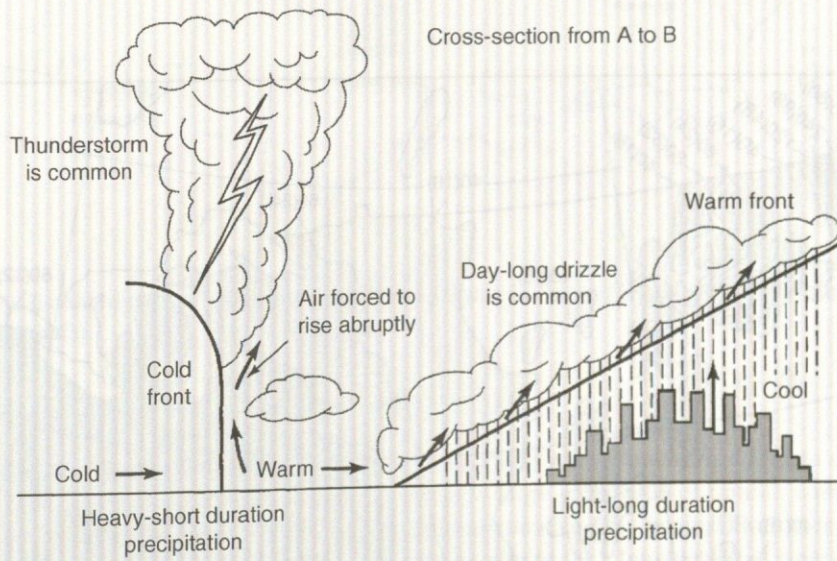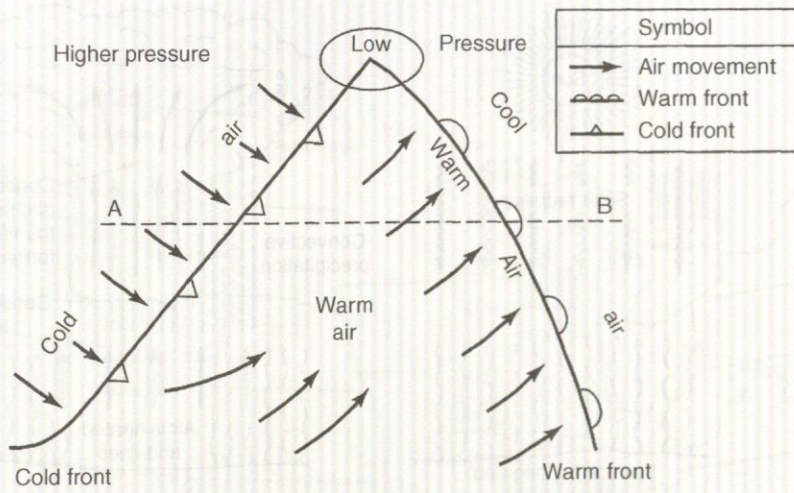
Figure 7.2.2 Cyclonic storms in midlatitude (from Masch (1984)).
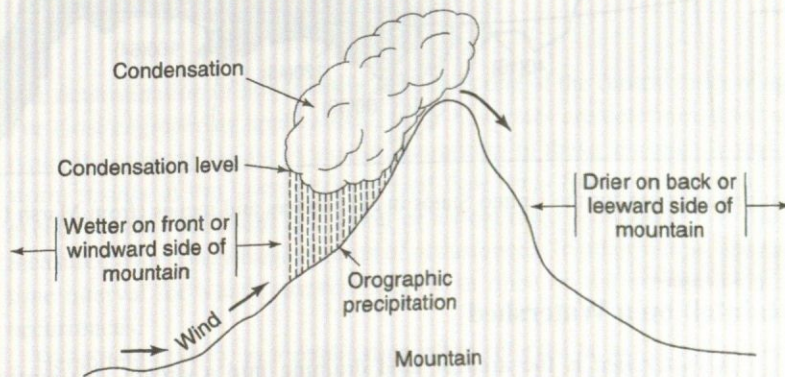
Figure 7.2.3 Orographic storm (from Masch (1984)).
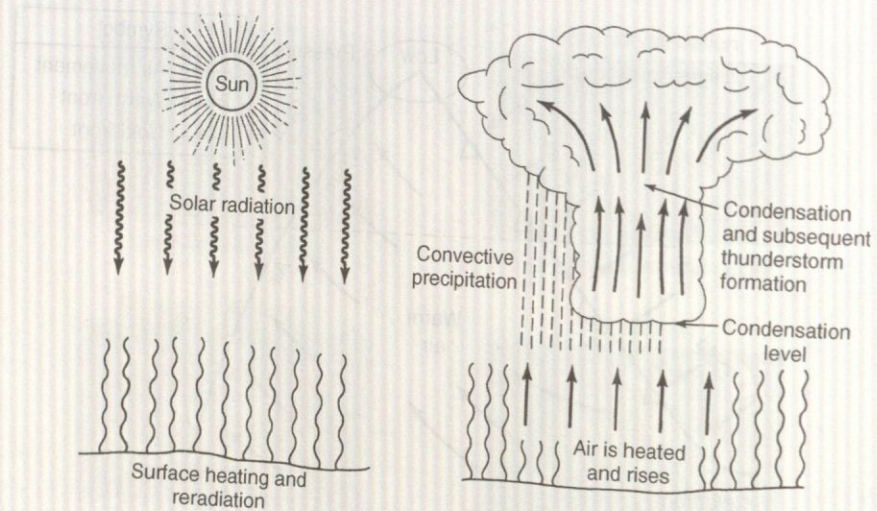
Figure 7.2.4 Convective storm (from Masch (1984)).
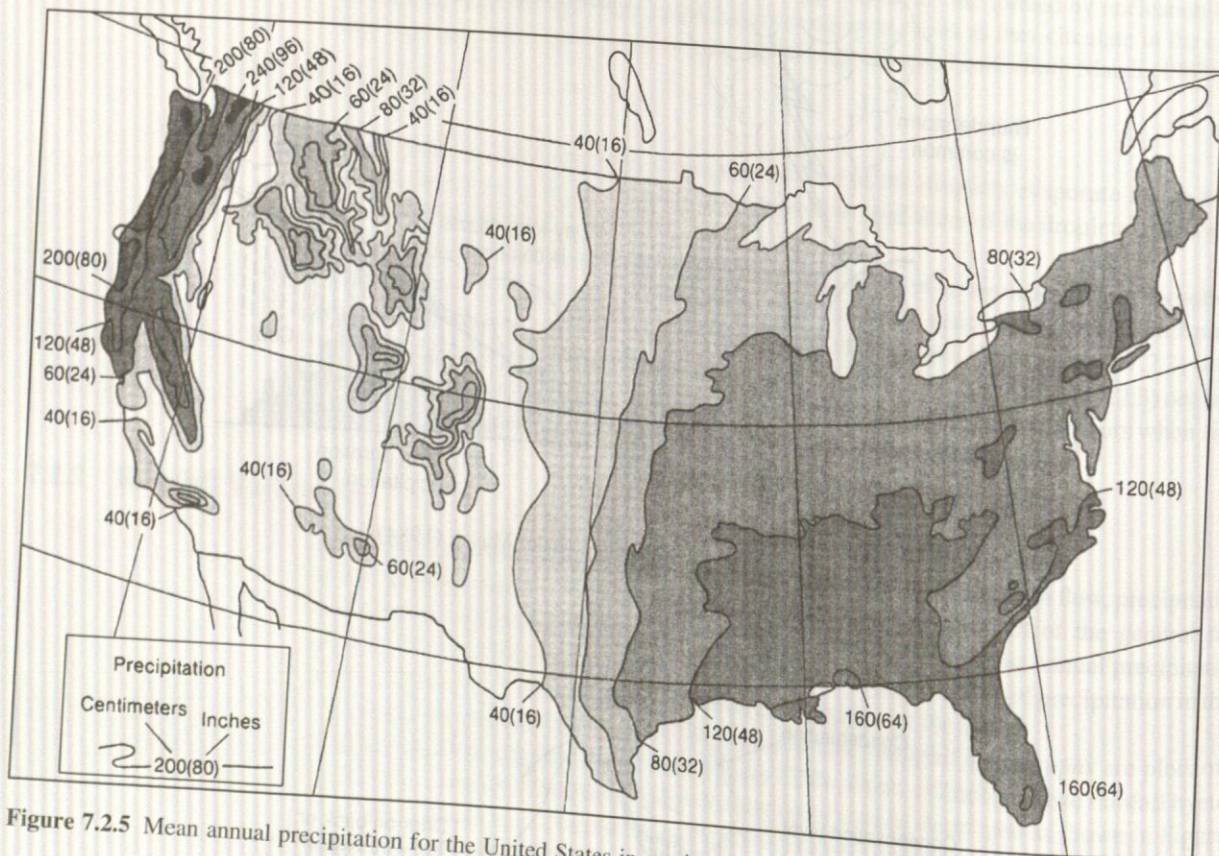
Figure 7.2.5 Mean annual precipitation for the United States in centimeters and inches (from Marsh (1987)).

7.2.3 Disposal of Rainfall on a Watershed

A *watershed* is the area of land draining into a stream at a particular location. The various surface water processes in the hydrologic cycle occur on a watershed. Figure 7.2.12 is a schematic illustration of the disposal of rainfall during a storm on a watershed. This figure
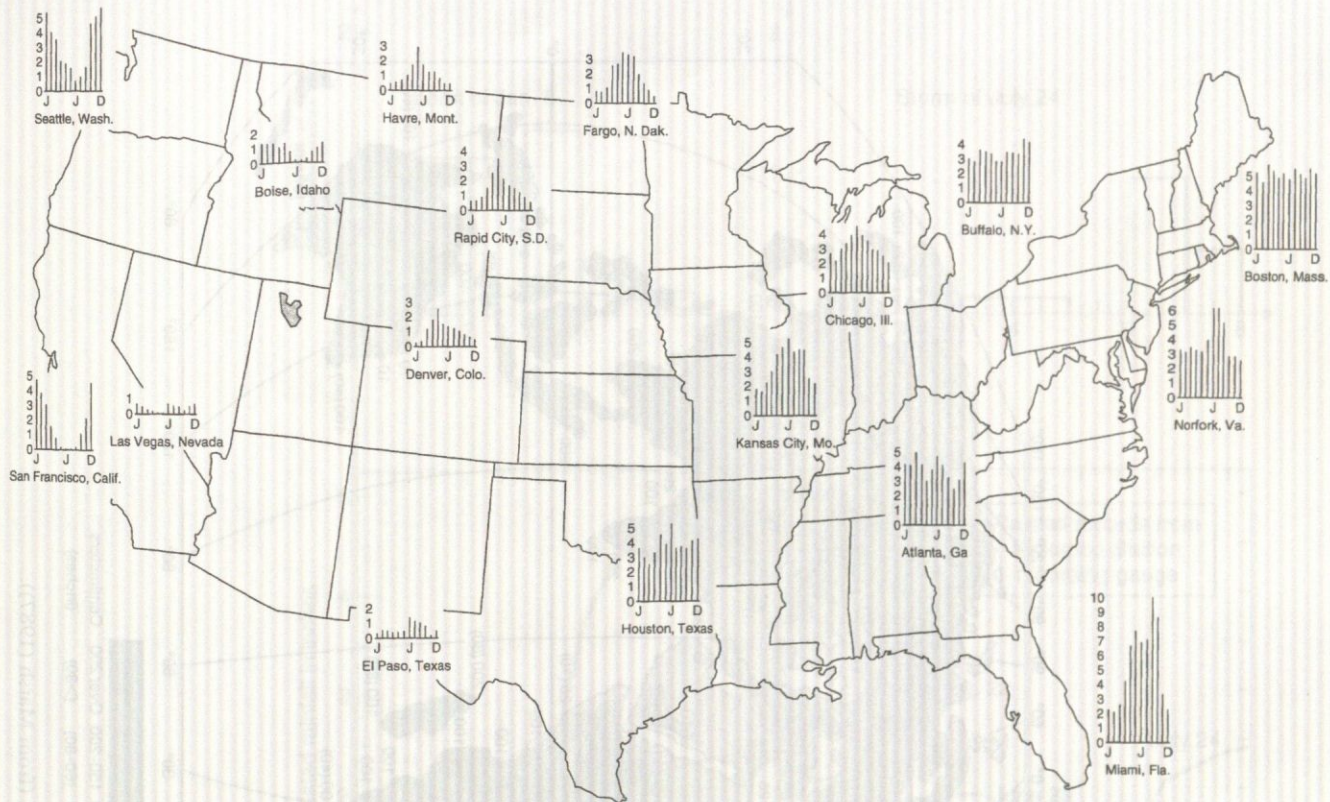
Figure 7.2.6 Normal monthly distribution of precipitation in the United States in inches (1 in = 254 mm) (from U.S. Environmental Data Services (1968)).

illustrates the rate (as a function of time) at which water flows or is added to storage for each of the processes. At the beginning of a storm, a large proportion of rainfall contributes to *surface storage*, and as water infiltrates, the *soil moisture storage* begins. Both *retention storage* and *detention storage* prevail. Retention storage is held for a long period of time and is depleted by evaporation, whereas detention storage is over a short time and is depleted by flow from the storage location.

7.2.4 Design Storms

The determination of flow rates in streams is one of the central tasks of surface water hydrology. For most engineering applications, these flow rates are determined for specified events that are typically extreme events. A major assumption in these analyses is that a certain return period storm results in the same return period flow rates from a watershed. The return period of an event, whether the event is a storm or a flow rate, is the expected value or the average value measured over a very large number of occurrences. In other words, the return period refers to the time interval for which an event will occur once on the average over a very large number of occurrences.

Hershfield (1961), in a publication often referred to as TP-40, presented isohyetal maps of design rainfall depths for the United States for durations from 30 minutes to 24 hours and return periods from 1 to 100 years. The values of rainfall in these isohyetal maps are point precipitation values, which is precipitation occurring at a single point in space (as opposed to areal
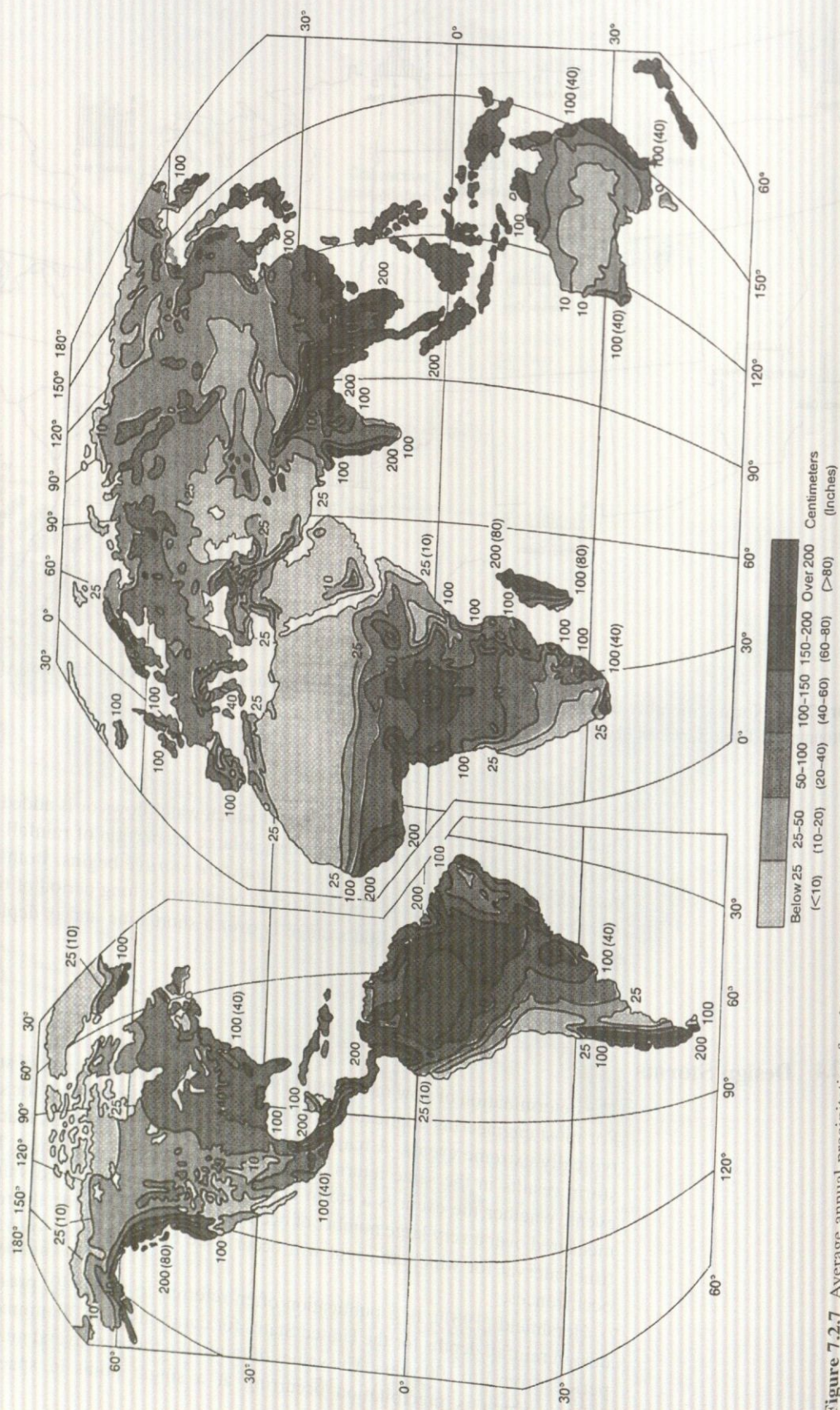
Figure 7.2.7 Average annual precipitation for the world's land areas, except Antarctica (from Marsh (1987)).
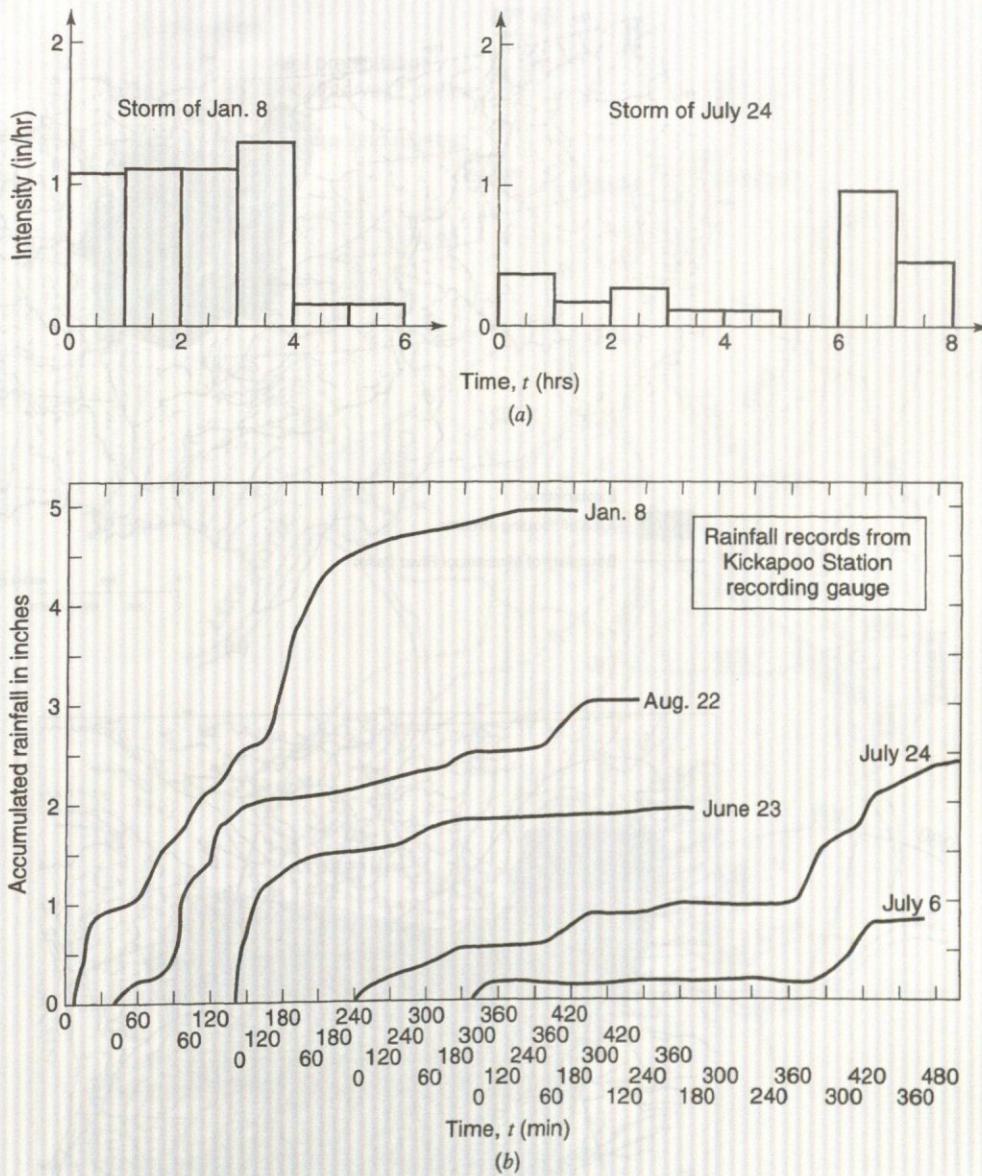
Figure 7.2.8 (*a*) Rainfall hyetographs for Kickapoo Station; (*b*) Mass rainfall curves (from Masch (1984)).

precipitation, which is over a larger area). Figure 7.2.13 is the isohyetal map for 100-year 24-hour rainfall. A later publication, U.S. Weather Bureau (1964), included maps for durations for 2 to 10 days, in what is referred to as TP-49. Miller et al. (1973) presented isohyetal maps for 6- and 24-hour durations for the 11 mountainous states in the western United States, which supersede the corresponding maps in TP-40.

Frederick et al. (1977), in a publication commonly referred to as HYDRO-35, presented isohyetal maps for events having durations from 5 to 60 minutes. The maps of precipitation depths for 5-, 15-, and 60-minutes durations and return periods of 2 and 100 years for the 37 eastern states are presented in Figures 7.2.14 *a–f*. Depths for a return period are obtained by interpolation from the 5-, 15-, and
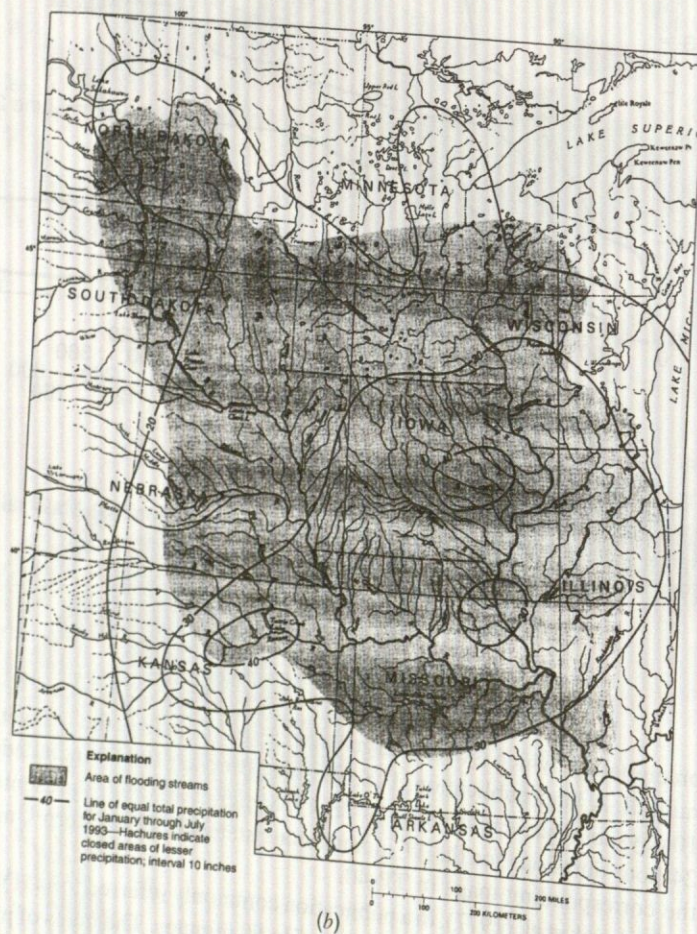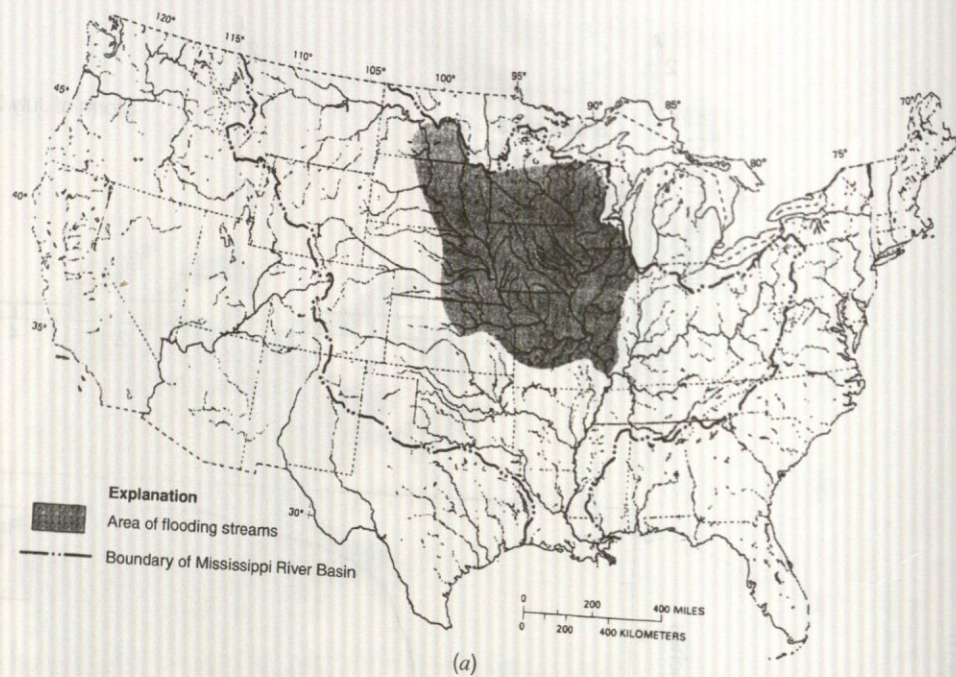
Figure 7.2.9 (*a*) Mississippi River Basin and general area of flooding streams, June through August 1993 (from Parrett et al. (1993)). (*b*) Areal distribution of total precipitation in the area of flooding in the upper Mississippi River Basin, January through May 1993 (from Parrett et al. (1993)).

244
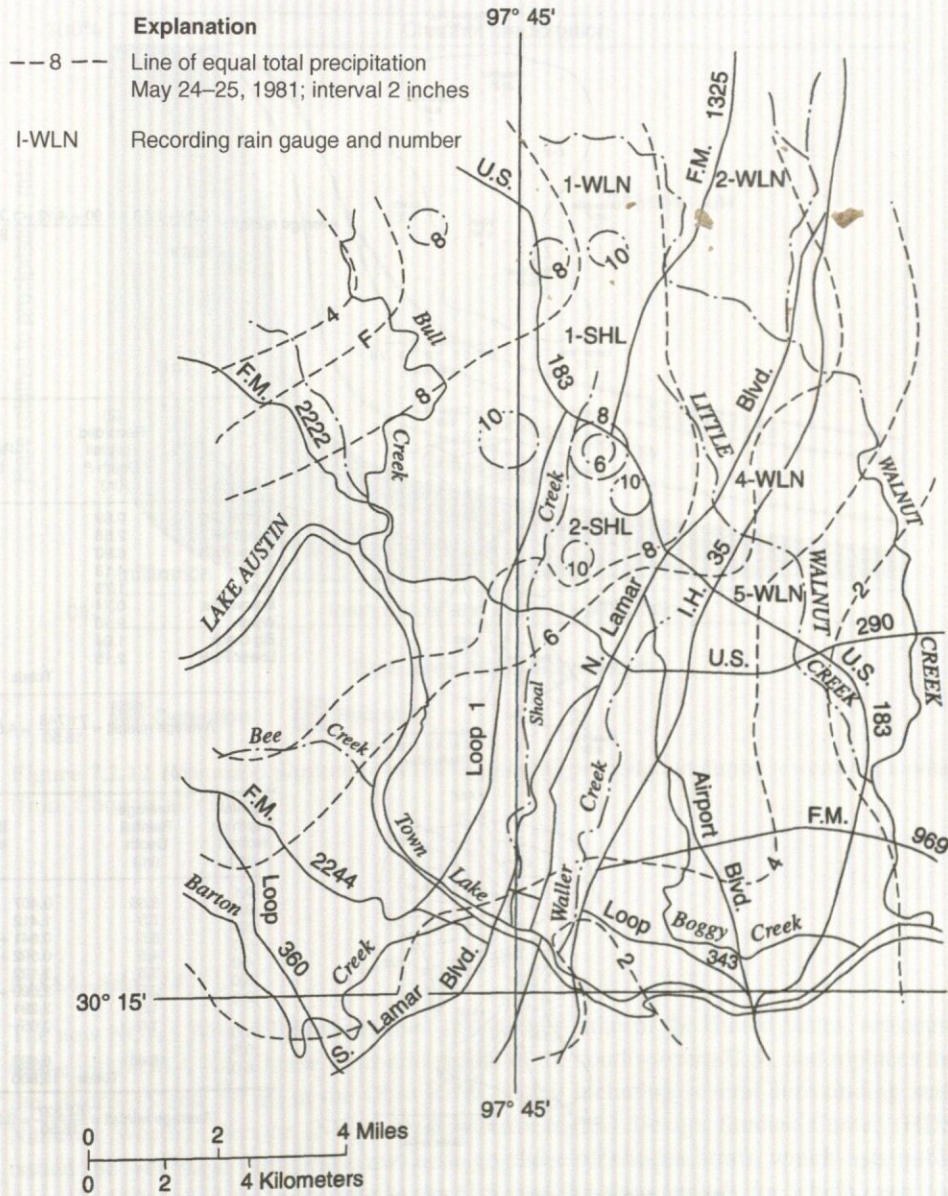
Figure 7.2.10 Isohyetal map of total precipitation (in) on May 24–25, 1981, based on USGS measurements, the City of Austin network, and unofficial precipitation reports (from Moore et al. (1982)).

60-minute data for the same return period:

$$P_{10min} = 0.41 \, P_{5min} + 0.59 \, P_{15min} \tag{7.2.1a}$$

$$P_{30min} = 0.51 \, P_{15min} + 0.49 \, P_{60min} \tag{7.2.1b}$$

To consider return periods other than 2 or 100 years, the following interpolation equation is used:

$$P_{T \, yr} = aP_{2yr} + bP_{100yr} \tag{7.2.2}$$

where the coefficients a and b are found in Table 7.2.1.
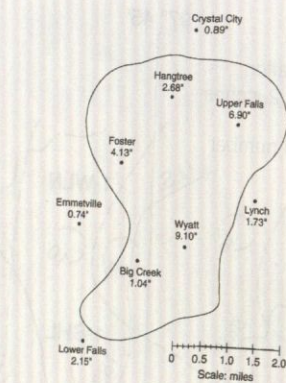
Average rainfall = $\dfrac{0.89 + 2.68 + 6.90 + 4.13 + 1.73 + 0.74 + 1.04 + 9.10 + 2.15}{9}$

= 3.26 in

(a)
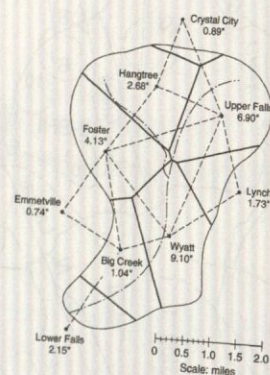
(1) Station	(2) Recorded Rainfall Depth P (in)	(3) Area A Represented by Station (mi^2)	(4) Rainfall Volume (mi^2-in)
Crystal City	0.89	0.21	0.187
Hangtree	2.68	2.82	7.558
Upper Falls	6.90	3.00	20.700
Foster	4.13	2.64	10.903
Lynch	1.73	1.00	1.730
Emmetville	0.74	0	0
Wyatt	9.10	2.94	26.754
Big Creek	1.04	2.07	2.153
Lower Falls	2.15	0.82	1.763
Totals		15.50	71.748

Average rainfall = $\dfrac{71.748}{15.50}$ = 4.63 in

(b)
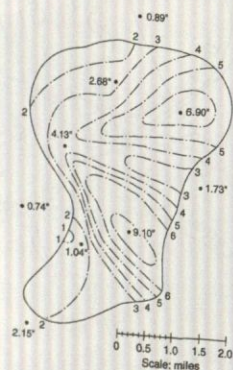
Rainfall Depth on Isohyet (in.)	Average Rainfall Depth (in.)	Area Between Isohyets (mi^2)	Rainfall Volume (mi^2-in.)
9.1			
8.0	8.55	0.407	3.480
6.0	7.0	1.412	9.884
5.0	5.5	0.841 + 1.375 = 2.216	1.219
4.0	4.5	0.592 + 1.697 = 2.289	10.300
3.0	3.5	3.122	10.927
2.0	2.5	2.599 + 0.431 = 3.030	7.575
	1.5	2.281	3.422
1.0	1.0	0.05	0.050
6.9			
6.0	6.45	0.693	4.470
Totals		15.500	51.327

Average rainfall = $\dfrac{51.327}{15.50}$ = 3.31 in.

(c)

Figure 7.2.11 (a) Computation of areal average rainfall by the arithmetic-mean method for a 24-hr storm. This is the simplest method of determining areal average rainfall. It involves averaging the rainfall depths recorded at a number of gauges. This method is satisfactory if the gauges are uniformly distributed over the area and the individual gauge measurements do not vary greatly about the mean (after Roberson et al. (1998)); (b) Computation of areal average rainfall by the Thiessen method for 24-hr storm. This method assumes that at any point in the watershed the rainfall is the same as that at the nearest gauge, so the depth recorded at a given gauge is applied out to a distance halfway to the next station in any direction. The relative weights for each gauge are determined from the corresponding areas of application in a *Thiessen polygon* network, the boundaries of the polygons being formed by the perpendicular bisectors of the lines joining adjacent gauges for J gauges; the area within the watershed assigned to each is A_j and P_j is the rainfall recorded at the jth gauge. The areal average precipitation for the watershed is computed by dividing the total rainfall volume by the total watershed area, as shown in the table (after Roberson et al. (1998)). (c) Computation of areal average rainfall by the isohyetal method for 24-hr storm. This method connects isoyets, using observed depths at rain gauges and interpolation between adjacent gauges. Where there is a dense network of rain gauges, isohyetal maps can be constructed using computer programs for automated contouring. Once the isohyetal map is constructed, the area A_j between each pair of isohyets within the watershed, is measured and multiplied by the average P_j of the rainfall depths of the two boundary isohyets to compute the areal average precipitation (after Roberson et al. (1998)).

246
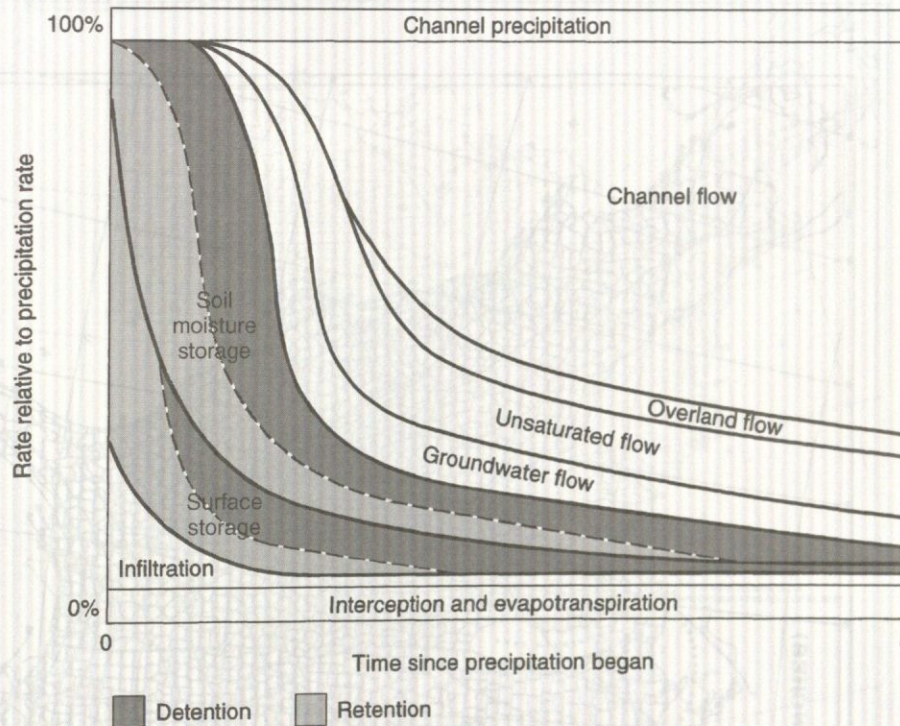
Figure 7.2.12 Schematic illustration of the disposal of precipitation during a storm on a watershed (from Chow et al. (1988)).

NOAA–Atlas 14

The new NOAA Atlas 14, Precipitation – Frequency Atlas of the United States, replaces the use of the old NOAA Atlas in the semi-arid region of the southwestern U.S., and replaces the use of the Hydro-35 and TP 40 in the Ohio River Valley including several surrounding states. The National Weather Service (NWS) Hydrometeorological Design Studies Center (HDSC) has issued the web page (http://hdsc.nws.noaa.gov/hdsc/pfds/index.html), which lists publications that should be used for each state in the U.S. and the time periods for which each should be used (5 min–60 min, 1 hr–24 hr, and 2-day–10-day periods). The two areas of the U.S. that are most impacted by the new NOAA Atlas 14 are the semi-arid southwest and the Ohio River Valley.

Semi-arid Southwest: NOAA-Atlas 2 is no longer valid for the semi-arid southwest, which includes: Arizona, Nevada, New Mexico, Utah, and Southeast California. For these states, NOAA-Atlas 2 (Volumes 4, 6, 7, 8, and part of 11) has been replaced by NOAA Atlas 14, Volume 1 which is available online: http://www.nws.noaa.gov/oh/hdsc/currentpf.htm

Ohio River Valley: Hydro-35 and Tech Paper No. 40 are no longer valid for most states in the Ohio River Valley and surrounding states, which includes: Delaware, Illinois, Indiana, Kentucky, Maryland, New Jersey, North Carolina, Ohio, Pennsylvania, South Carolina, Tennessee, Virginia, West Virginia, and Washington, DC. For these states, Hydro-35 and Tech Paper-40 have been replaced by NOAA Atlas 14, Volume 2, which is available online: http://www.nws.noaa.gov/oh/hdsc/currentpf.htm

Example point precipitation frequency estimates for two locations are presented in Figure 7.2.15. These are Chicago, Illinois and Phoenix, Arizona.

100-YEAR 24-HOUR RAINFALL (INCHES)
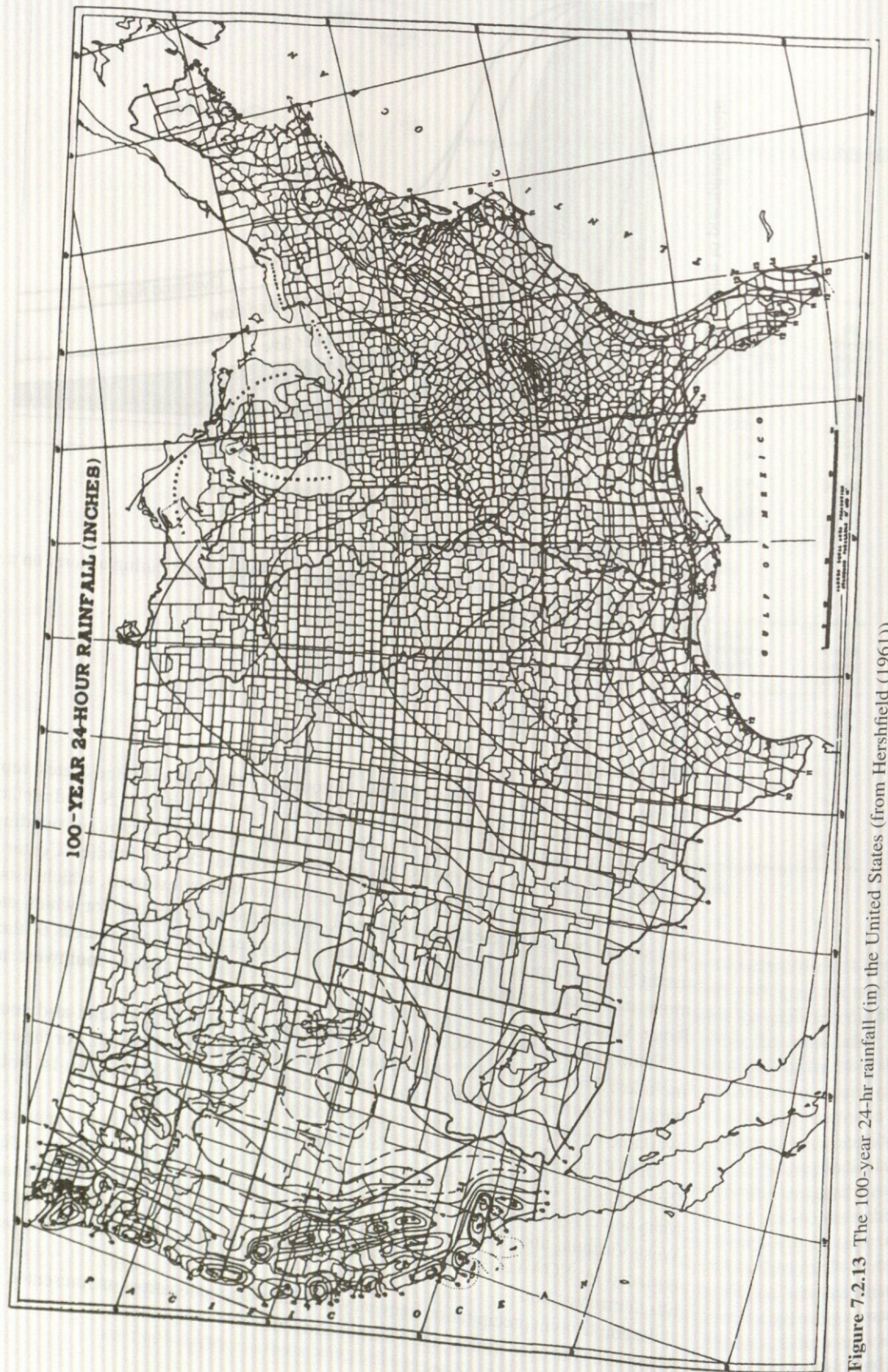
Figure 7.2.13 The 100-year 24-hr rainfall (in) the United States (from Hershfield (1961)).

(a)
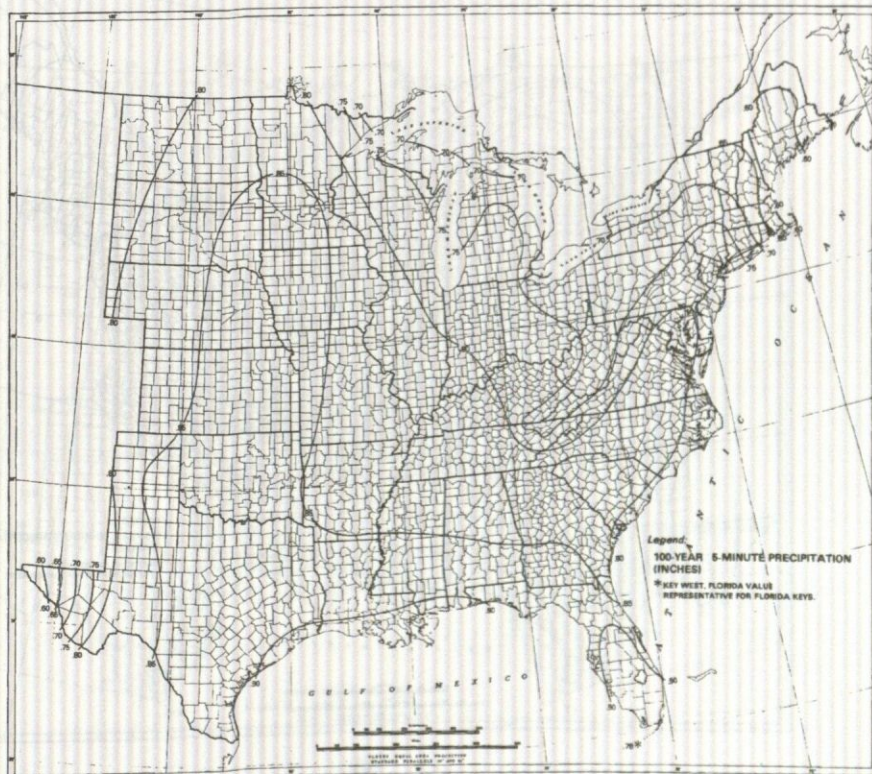
Figure 7.2.14 (a) 2-year 5-min precipitation (in) (from Frederick, Meyers, and Auciello (1977)). (b) 100-year 5-min precipitation (in) (from Frederick, Meyers, and Auciello (1977)). (c) 2-year 15-min precipitation (in) (from Frederick, Meyers, and Auciello (1977)). (d) 100-year 15-min precipitation (in) (from Frederick, Meyers, and Auciello (1977)). (e) 2-year 60-min precipitation (in) (from Frederick, Meyers, and Auciello (1977)). (f) 100-year 60-min precipitation (in) (from Frederick, Meyers, and Auciello (1977)).

(b)
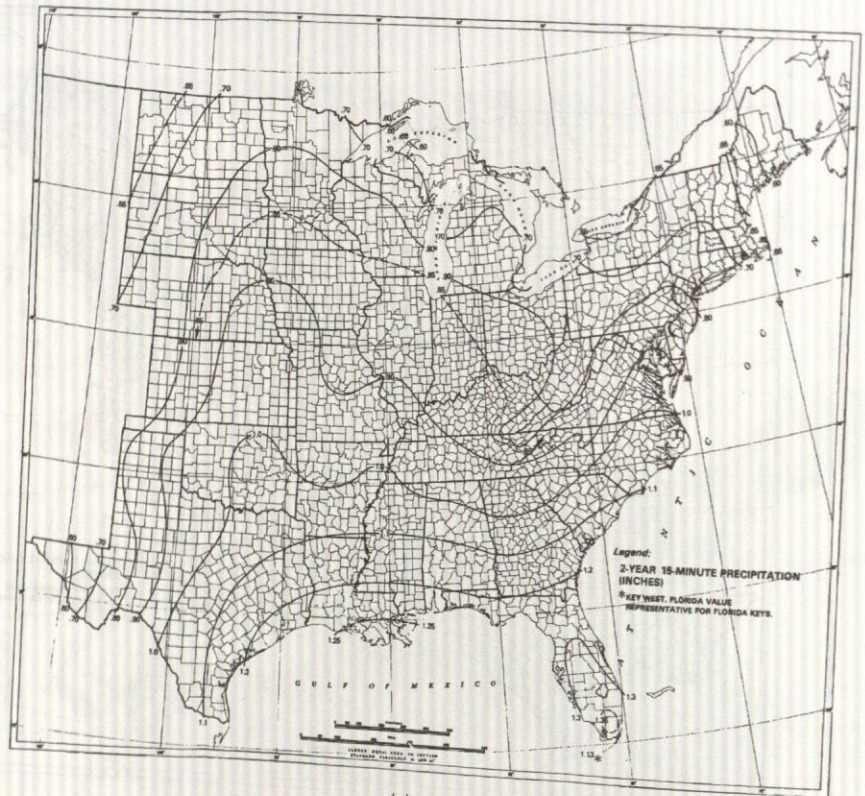
(c)
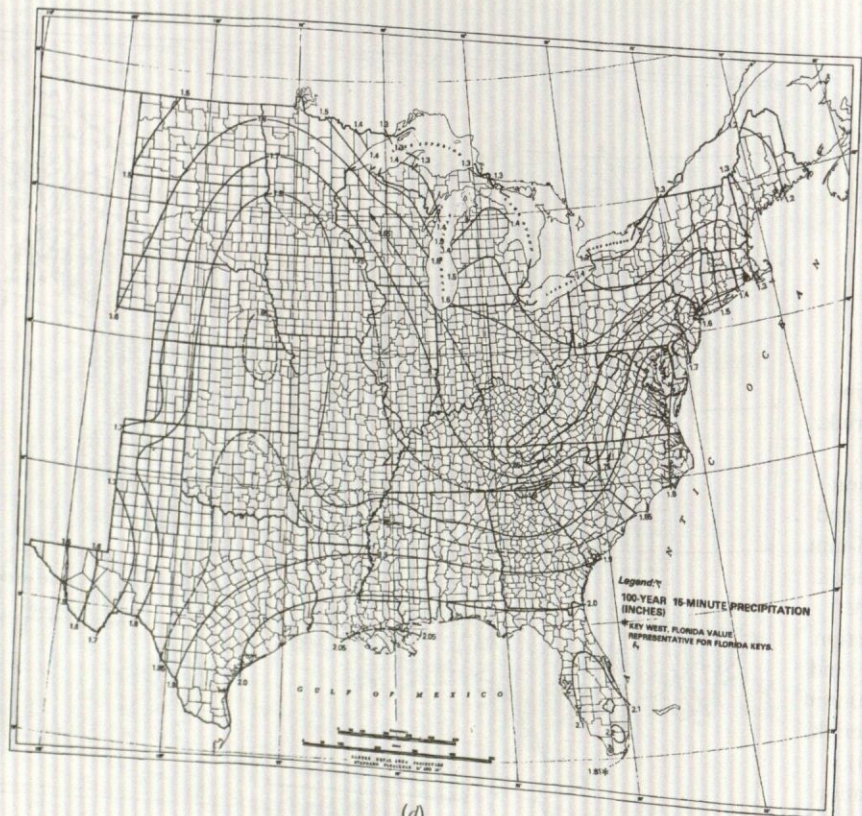
(d)

Figure 7.2.14 (Continued).
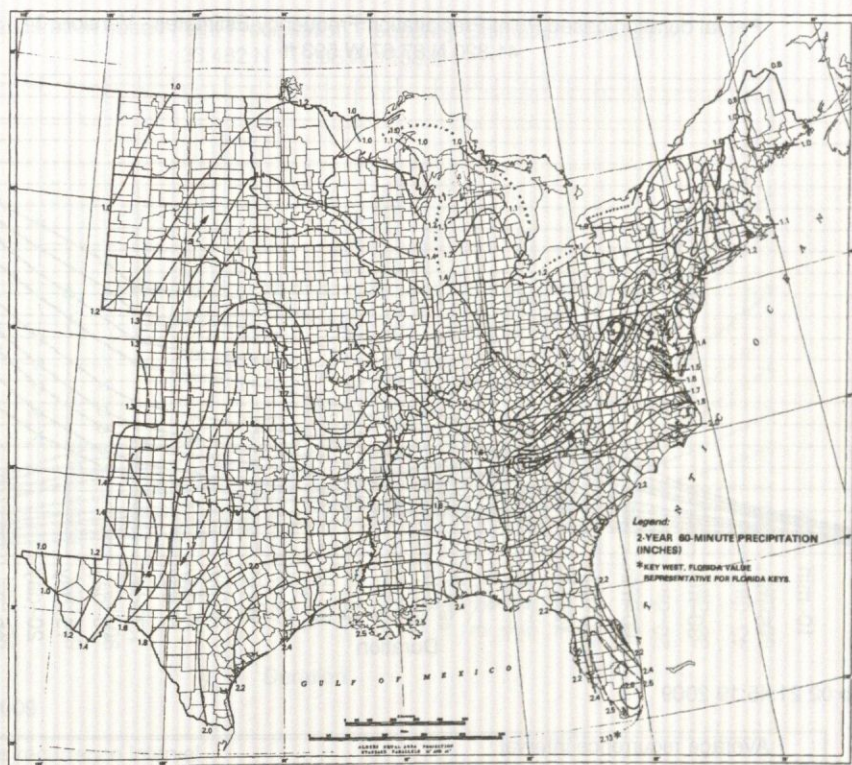
(e)
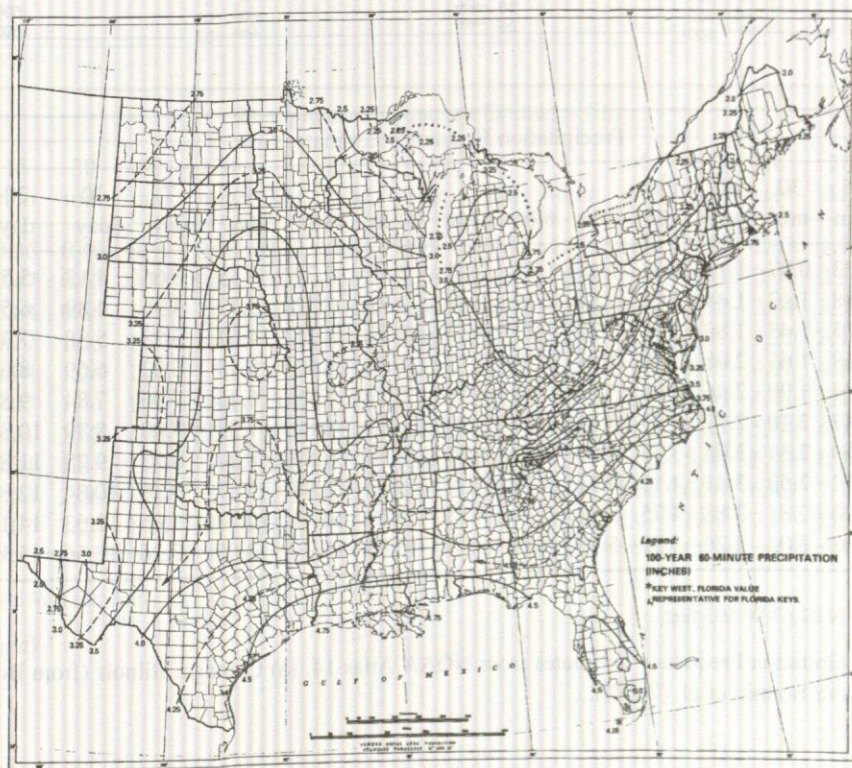
(f)

Figure 7.2.14 (*Continued*)

Partial duration based Point Precipitation Frequency Estimates - Version: 3
41.820 N 87.67 W 593 ft
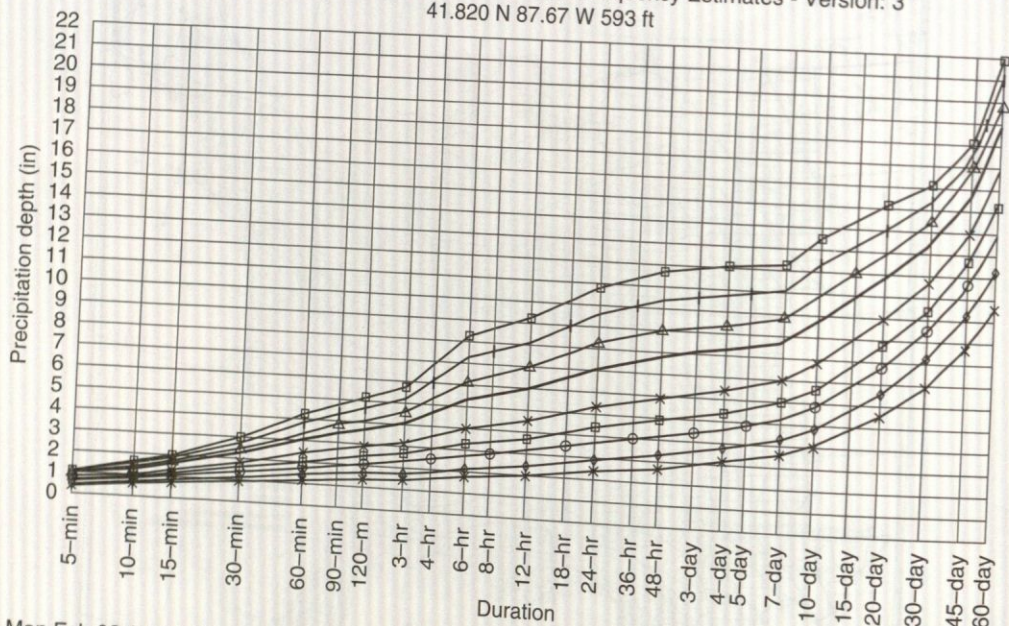
Mon Feb 02 21:45:19 2009

Average recurrence interval (years)

1	2	5	10	25	100	200	500	1000

Precipitation Frequency Estimates (in)

ARI (years)	5 min	10 min	15 min	30 min	60 min	120 min	3 hr	6 hr	12 hr	24 hr	48 hr	4 day	7 day	10 day	20 day	30 day	45 day	60 day
1	0.38	0.60	0.73	0.97	1.18	1.38	1.48	1.77	2.04	2.39	2.74	3.15	3.66	4.13	5.55	6.96	8.73	10.4
2	0.46	0.71	0.88	1.17	1.44	1.68	1.81	2.16	2.48	2.91	3.32	3.77	4.36	4.89	6.56	8.20	10.24	12.2
5	0.55	0.85	1.05	1.43	1.80	2.12	2.30	2.78	3.17	3.72	4.21	4.67	5.28	5.88	7.73	9.49	11.65	13.9
10	0.62	0.96	1.18	1.63	2.08	2.47	2.68	3.30	3.75	4.39	4.93	5.40	6.02	6.69	8.64	10.46	12.69	15.2
25	0.71	1.09	1.34	1.90	2.46	2.94	3.21	4.05	4.58	5.37	5.99	6.46	7.06	7.84	9.88	11.70	13.95	16.7
50	0.78	1.19	1.47	2.10	2.77	3.33	3.64	4.70	5.28	6.20	6.88	7.33	7.90	8.79	10.85	12.62	14.87	17.9
100	0.85	1.28	1.60	2.31	3.08	3.73	4.09	5.40	6.05	7.10	7.83	8.27	8.78	9.78	11.82	13.49	15.71	18.9
200	0.93	1.39	1.72	2.52	3.41	4.15	4.57	6.17	6.89	8.10	8.88	9.27	9.70	10.84	12.80	14.34	16.50	19.9
500	1.03	1.52	1.90	2.81	3.88	4.75	5.24	7.31	8.13	9.58	10.41	10.77	11.06	12.33	14.12	15.42	17.47	21.1
1000	1.11	1.62	2.02	3.04	4.26	5.22	5.78	8.29	9.18	10.83	11.71	12.05	12.26	13.56	15.15	16.20	18.15	21.9

(a) Chicago, Ilinois 41.820 N 87.67 W 593 feet

Figure 7.2.15 Point Precipitation Frequency Estimates from NOAA Atlas 14, (a) Chicago, Illinois (from Bonnin et al. (2004)); (b) Phoenix, Arizona (from Bonnin et al. (2004)).

Partial duration based Point Precipitation Frequency Estimates - Version: 4
33.482 N 112.05 W 1158 ft
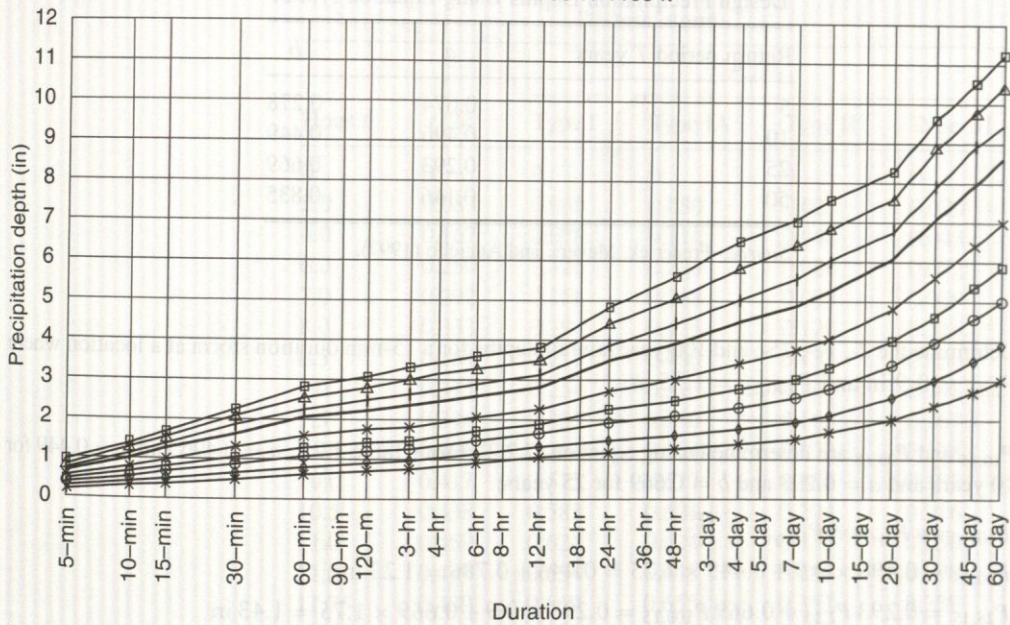
Mon Feb 02 22:31:58 2009

Average recurrence interval (years)				
1		100		
2		200		
5		500		
10		1000		
25				

							Precipitation Frequency Estimates (in)											
ARI (years)	5 min	10 min	15 min	30 min	60 min	120 min	3 hr	6 hr	12 hr	24 hr	48 hr	4 day	7 day	10 day	20 day	30 day	45 day	60 day
1	0.19	0.29	0.36	0.48	0.59	0.68	0.72	0.88	0.99	1.14	1.23	1.36	1.50	1.63	1.98	2.31	2.67	2.95
2	0.25	0.38	0.47	0.63	0.78	0.88	0.93	1.11	1.26	1.45	1.57	1.74	1.91	2.08	2.54	2.97	3.44	3.80
5	0.34	0.51	0.64	0.86	1.06	1.18	1.22	1.43	1.60	1.88	2.06	2.29	2.52	2.74	3.35	3.91	4.53	4.99
10	0.41	0.62	0.77	1.03	1.27	1.41	1.46	1.68	1.86	2.22	2.45	2.74	3.01	3.27	3.96	4.62	5.33	5.85
25	0.50	0.76	0.94	1.26	1.56	1.72	1.78	2.03	2.22	2.69	3.00	3.37	3.71	4.01	4.79	5.57	6.38	6.97
50	0.57	0.86	1.07	1.44	1.78	1.96	2.04	2.30	2.50	3.06	3.44	3.88	4.26	4.61	5.42	6.30	7.16	7.79
100	0.64	0.97	1.21	1.62	2.01	2.20	2.32	2.58	2.78	3.45	3.89	4.42	4.85	5.24	6.05	7.05	7.95	8.62
200	0.71	1.08	1.34	1.81	2.24	2.45	2.60	2.87	3.07	3.85	4.37	5.00	5.48	5.90	6.70	7.81	8.74	9.42
500	0.81	1.23	1.53	2.06	2.54	2.78	2.99	3.26	3.46	4.40	5.04	5.81	6.36	6.82	7.57	8.82	9.76	10.4
1000	0.88	1.34	1.67	2.24	2.78	3.04	3.31	3.57	3.75	4.84	5.57	6.47	7.07	7.57	8.23	9.60	10.53	11.2

(b) Arizona 33.482 N 112.05 W 1158 feet

Figure 7.2.15 (*Continued*)

Table 7.2.1 Coefficients for Interpolating Design Precipitation Depths Using Equation (7.2.2)

Return period T years	a	b
5	0.674	0.278
10	0.496	0.449
25	0.293	0.669
50	0.146	0.835

Source: Frederick, Meyers, and Auciello (1997).

EXAMPLE 7.2.1

Determine the 2-, 10-, 25-, and 100-year rainfall depths for a 15-min duration storm at a location where $P_{2,15} = 0.9$ in and $P_{100,15} = 1.75$ in.

SOLUTION

$P_{10,15}$ and $P_{25,15}$ are determined using equation (7.2.2). From Table 7.2.1, $a = 0.496$ and $b = 0.449$ for 10 years and $a = 0.293$ and $b = 0.669$ for 25 years:

$$P_{10yr} = a\,P_{2yr} + b\,P_{100yr}$$

$$P_{10,15} = 0.496 \times 0.9 + 0.449 \times 1.75 = 0.446 + 0.786 = 1.23 \text{ in}$$

$$P_{25,15} = 0.293\,P_{2,15} + 0.669\,P_{100,15} = 0.293 \times 0.9 + 0.669 \times 1.75 = 1.43 \text{ in}$$

IDF Relationships

In hydrologic design projects, particularly urban drainage design, the use of *intensity-duration-frequency* relationships is recommended. *Intensity* refers to rainfall intensity (depth per unit time), and in some cases depths are used instead of intensity. *Duration* refers to rainfall duration, and *frequency* refers to *return periods*, which is the expected value of the *recurrence interval* (time between occurrences). See Chapter 10 for more details. The intensity-duration-frequency (IDF) relationships are also referred to as *IDF curves*. IDF relationships have also been expressed in equation form, such as

$$i = \frac{c}{T_d^e + f} \tag{7.2.3}$$

where i is the design rainfall intensity in inches per hour, T_d is the duration in minutes, and c, e, and f are coefficients that vary for location and return period. Other forms of these IDF equations include the return period, such as

$$i = \frac{cT^m}{T_d + f} \tag{7.2.4}$$

and

$$i = \frac{cT^m}{T_d^e + f} \tag{7.2.5}$$

where T is the return period. In Chapter 15, these IDF equations are used in urban drainage design. Chow et al. (1988) describe in detail how to derive the coefficients for these relationships using rainfall data.

Synthetic Storm Hyetograph

In many types of hydrologic analysis, such as *rainfall-runoff analysis*, to determine the runoff (discharge) from a watershed the time sequence of rainfall is needed. In such cases it is standard practice to use a *synthetic storm hyetograph*. The United States Department of Agriculture Soil Conservation Service (1973, 1986) developed synthetic storm hyetographs for 6- and 24-hr storms in

EXAMPLE 7.

Table 7.2.2   SCS Rainfall Distributions

		24-hour storm				6-hour storm		
		P_t/P_{24}						
Hour t	$t/24$	Type I	Type IA	Type II	Type III	Hour t	$t/6$	P_t/P_6
0	0	0	0	0	0	0	0	0
2.0	0.083	0.035	0.050	0.022	0.020	0.60	0.10	0.04
4.0	0.167	0.076	0.116	0.048	0.043	1.20	0.20	0.10
6.0	0.250	0.125	0.206	0.080	0.072	1.50	0.25	0.14
7.0	0.292	0.156	0.268	0.098	0.089	1.80	0.30	0.19
8.0	0.333	0.194	0.425	0.120	0.115	2.10	0.35	0.31
8.5	0.354	0.219	0.480	0.133	0.130	2.28	0.38	0.44
9.0	0.375	0.254	0.520	0.147	0.148	2.40	0.40	0.53
9.5	0.396	0.303	0.550	0.163	0.167	2.52	0.42	0.60
9.75	0.406	0.362	0.564	0.172	0.178	2.64	0.44	0.63
10.0	0.417	0.515	0.577	0.181	0.189	2.76	0.46	0.66
10.5	0.438	0.583	0.601	0.204	0.216	3.00	0.50	0.70
11.0	0.459	0.624	0.624	0.235	0.250	3.30	0.55	0.75
11.5	0.479	0.654	0.645	0.283	0.298	3.60	0.60	0.79
11.75	0.489	0.669	0.655	0.357	0.339	3.90	0.65	0.83
12.0	0.500	0.682	0.664	0.663	0.500	4.20	0.70	0.86
12.5	0.521	0.706	0.683	0.735	0.702	4.50	0.75	0.89
13.0	0.542	0.727	0.701	0.772	0.751	4.80	0.80	0.91
13.5	0.563	0.748	0.719	0.799	0.785	5.40	0.90	0.96
14.0	0.583	0.767	0.736	0.820	0.811	6.00	1.0	1.00
16.0	0.667	0.830	0.800	0.880	0.886			
20.0	0.833	0.926	0.906	0.952	0.957			
24.0	1.000	1.000	1.000	1.000	1.000			

Source: U.S. Department of Agriculture Soil Conservation Service (1973, 1986).

the United States. These are presented in Table 7.2.2 and Figure 7.2.16 as cumulative hyetographs. Four 24-hr duration storms, Type I, IA, II, and III, were developed for different geographic locations in the U.S., as shown in Figure 7.2.17. Types I and IA are for the Pacific maritime climate, which has wet winters and dry summers. Type III is for the Gulf of Mexico and Atlantic coastal areas, which have tropical storms resulting in large 24-hour rainfall amounts. Type II is for the remainder of the United States.

In the midwestern part of the United States the Huff (1967) temporal distribution of storms is widely used for heavy storms on areas ranging up to 400 mi^2. Time distribution patterns were developed for four probability groups, from the most severe (first quartile) to the least severe (fourth quartile). Figure 7.2.18a shows the probability distribution of first-quartile storms. These curves are smooth, reflecting average rainfall distribution with time; they do not exhibit the burst characteristics of observed storms. Figure 7.2.18b shows selected histograms of first-quartile storms for 10-, 50-, and 90-percent cumulative probabilities of occurrence, each illustrating the percentage of total storm rainfall for 10 percent increments of the storm duration. The 50 percent histogram represents a cumulative rainfall pattern that should be exceeded in about half of the storms. The 90 percent histogram can be interpreted as a storm distribution that is equaled or exceeded in 10 percent or less of the storms.

EXAMPLE 7.2.2   Using equation (7.2.3), compute the design rainfall intensities for a 10-year return period, 10-, 20-, and 60-min duration storms for $c = 62.5$, $e = 0.89$, and $f = 9.10$.
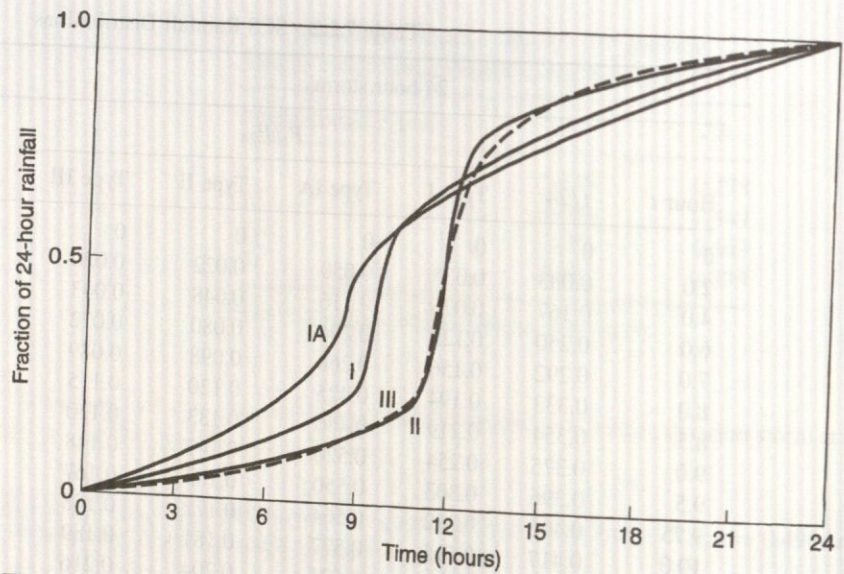
Figure 7.2.16 Soil Conservation Service 24-hour rainfall hyetographs (from U.S. Department of Agriculture Soil Conservation Service (1986)).
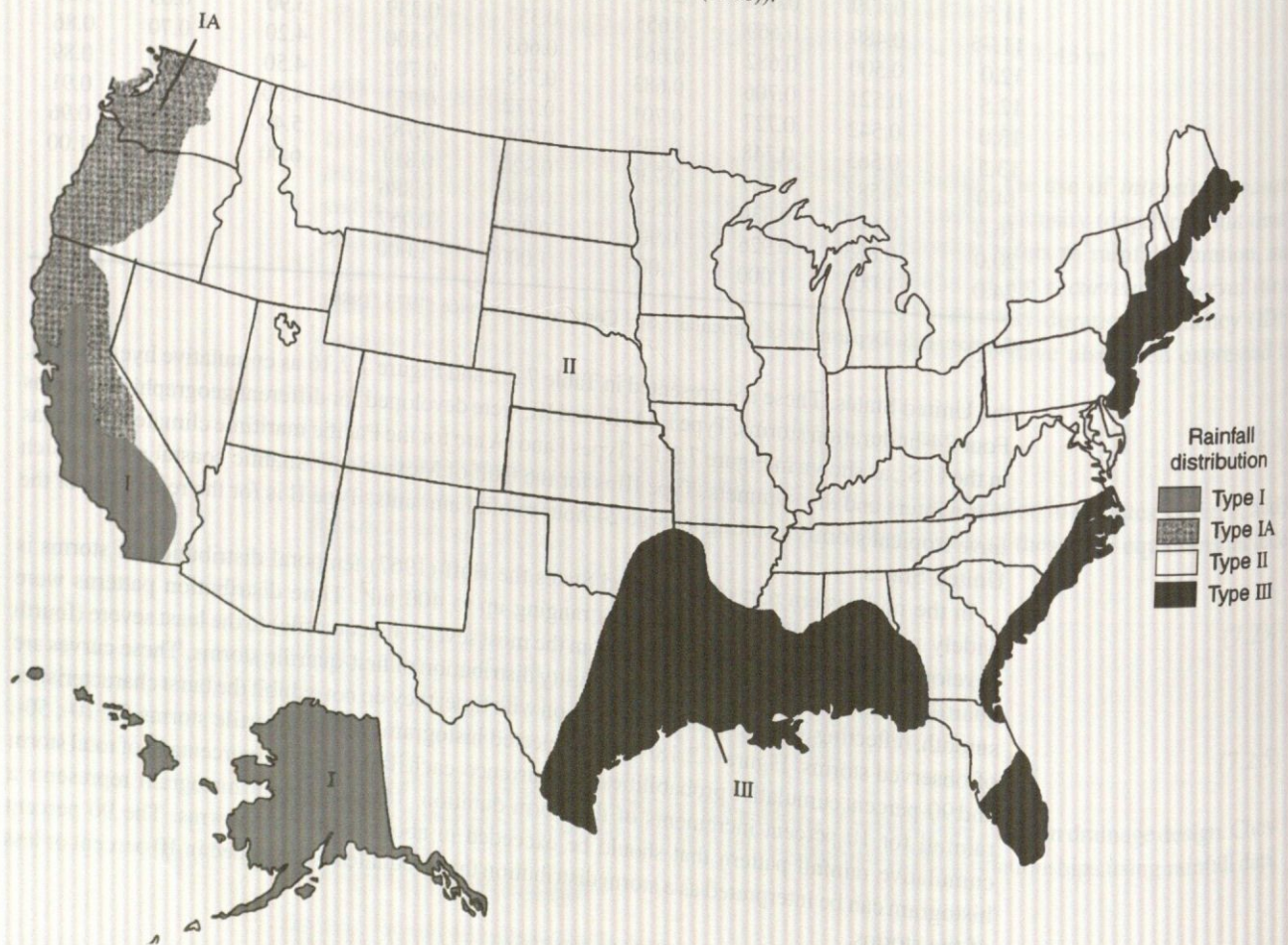
Figure 7.2.17 Location within the United States for application of the SCS 24-hour rainfall hyetographs (from U.S. Department of Agriculture Soil Conservation Service (1986)).
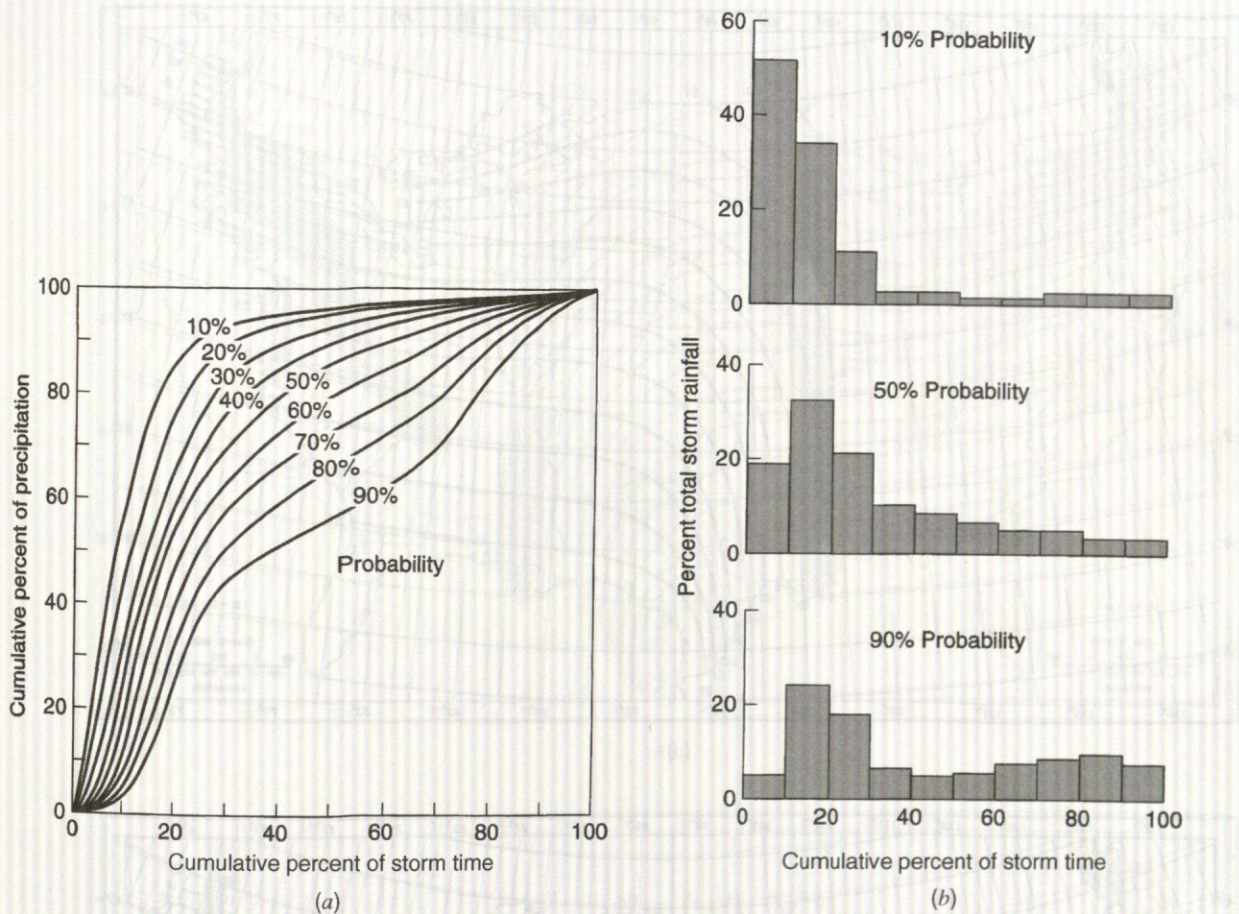
Figure 7.2.18 (a) Time distribution of first-quartile storms. The probability shown is the chance that the observed storm pattern will lie to the left of the curve; (b) Selected histograms for first-quartile storms (from Huff (1967)).

SOLUTION

The rainfall intensity duration frequency relationship is then

$$i = \frac{62.5}{T_d^{0.89} + 9.10}$$

For $T_d = 10$ min, $i = \dfrac{62.5}{10^{0.89} + 9.10} = 3.71$ in/hr. For $T_d = 20$ min, $i = 2.66$ in/hr, and for

$T_d = 60$ min, $i = 1.32$ in/hr.

7.2.5 Estimated Limiting Storms

Estimated limiting values (ELVs) are used for the design of water control structures such as the spillways on large dams. Of particular interest are the *probable maximum precipitation* (PMP) and the *probable maximum storm* (PMS). These are used to derive a *probable maximum flood* (PMF). PMP is a depth of precipitation that is the estimated limiting value of precipitation, defined as the estimated greatest depth of precipitation for a given duration that is physically possible and reasonably characteristic over a particular geographical region at a certain time of year (Chow et al., 1988). Schreiner and Riedel (1978) presented generalized PMP charts for the United States east of the 105th meridian HMR 51. The all-seasons (any time of the year) estimates of PMP are presented in maps as a function of storm area (ranging from 10 to 20,000 mi^2) and storm durations ranging from 6 to 72 hours, as shown in Figure 7.2.19. For regions west of the 105th meridian, the diagram in Figure 7.2.20 shows the appropriate U.S. National Weather Service
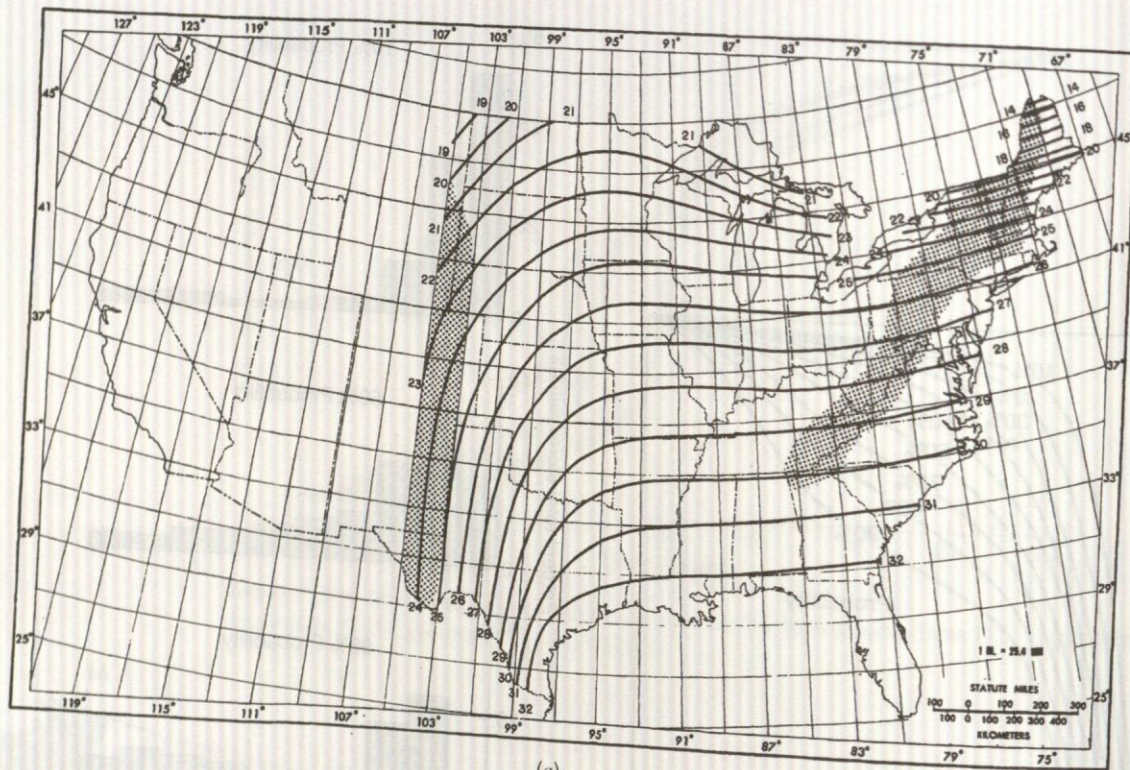
(a)
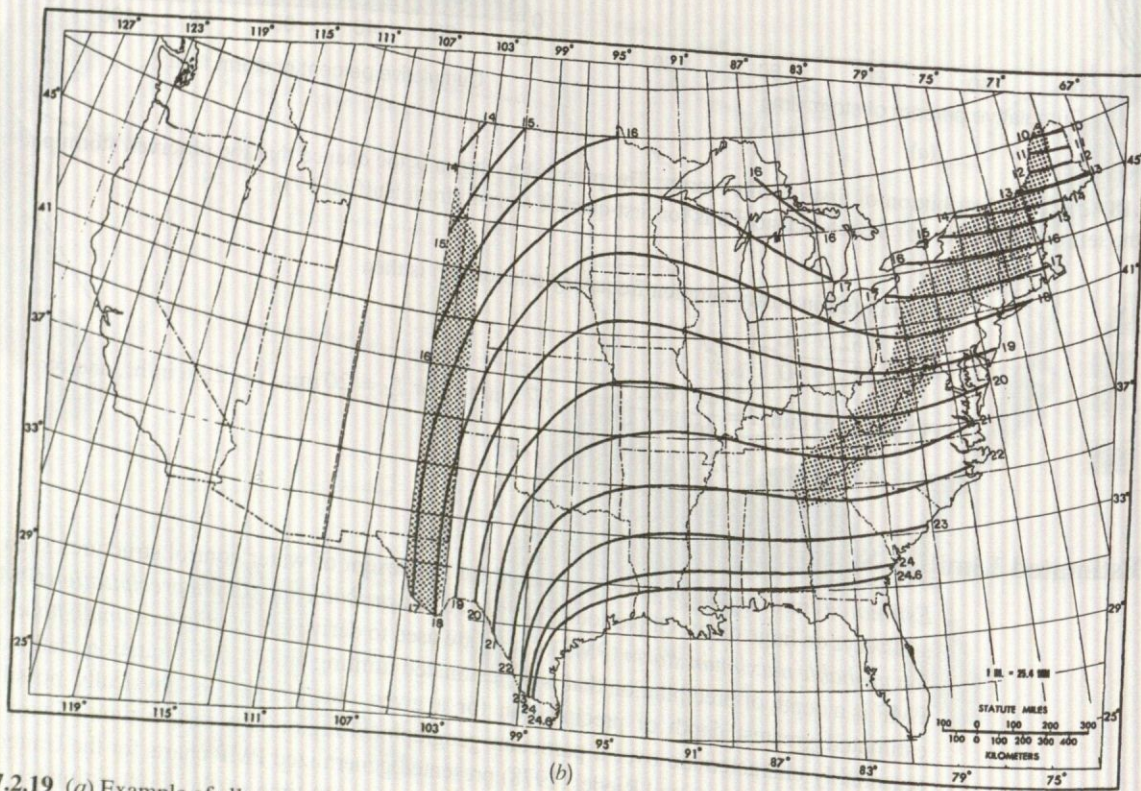
(b)

Figure 7.2.19 (*a*) Example of all-season PMP (in) for 6 hr, 10 mi² (from Schreiner and Riedel, 1978); (*b*) Example of all-season PMP (in) for 6 hr, 200 mi² (from Schreiner and Riedel, 1978).
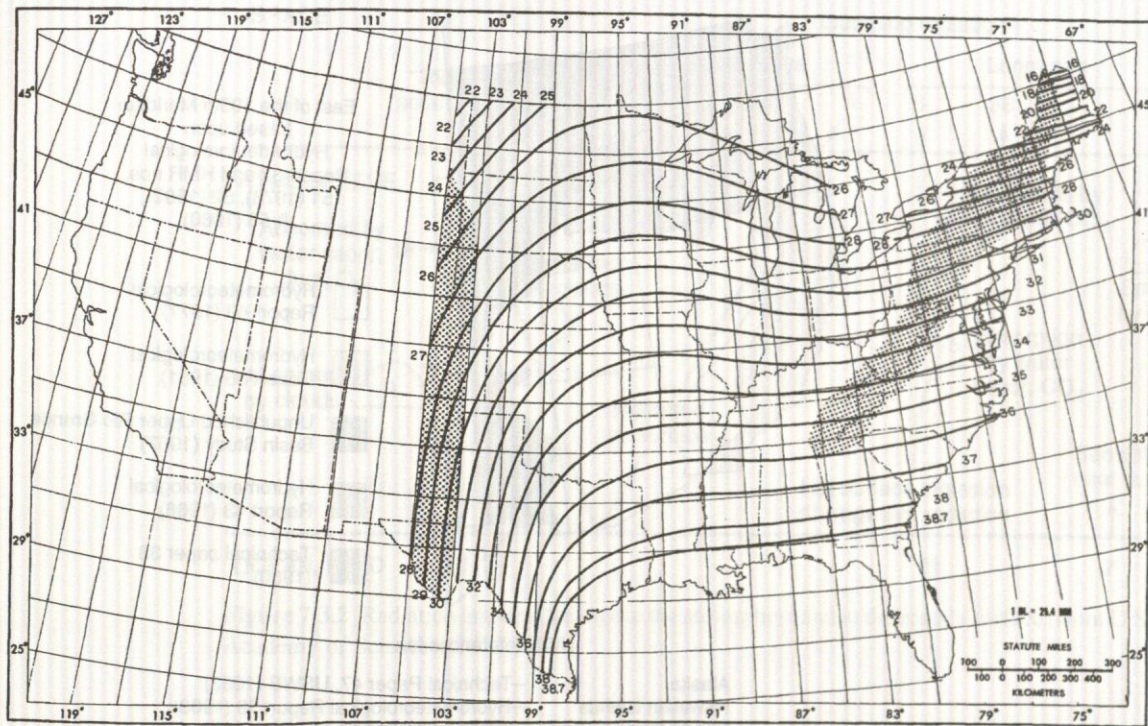
(c)
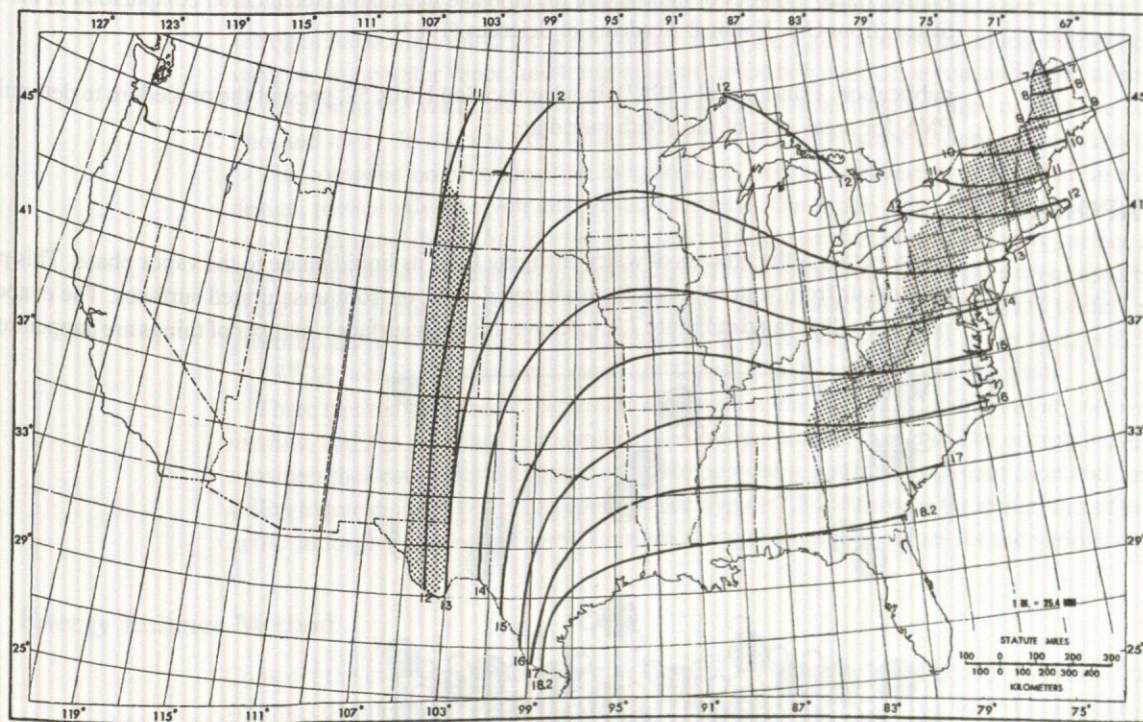
(d)

Figure 7.2.19 (*Continued*) (c) Example of all-season PMP (in) for 12 hr, 10 mi² (from Schreiner and Riedel, 1978); (d) Example of all-season PMP (in) for 6 hr, 1000 mi² (from Schreiner and Riedel, 1978).

East of the 105th Meridian
based upon
Hydrometeorological
Report 33 and HMR nos.
51 (1978), 52 (1982),
& 53 (1980)

Hydrometeorological
Report 49 (1977)

Hydrometeorological
Report 36 (1961)

Unpublished Upper Rio Grande
Basin Study (1967)

Hydrometeorological
Report 43 (1966)

Technical paper 38
(1960)

NWS references for:

Alaska
Hawaiian Islands   –Technical Paper 47, USWB (1963)
Puerto Rico   –Hydrometeorological Report 39 (1963)
and Virgin Islands   –Technical Paper 42, USWB (1961)

Figure 7.2.20 Sources of information for probable maximum precipitation computation in the United States (from U.S. National Academy of Sciences (1983)).

publication. Hansen et al. (1982), in what is called HMR 52, present the procedure to determine the PMS for areas east of the 105th meridian.

7.3 EVAPORATION

Evaporation is the process of water changing from its liquid phase to the vapor phase. This process may occur from water bodies, from saturated soils, or from unsaturated surfaces. The evaporation process is illustrated in Figure 7.3.1. Above the water surface a number of things are happening. First

Water evaporating in air

Oxygen   Hydrogen   Nitrogen

Figure 7.3.1 Evaporation (magnified one billion times) (from Feynman et al. (1963)).

SPACE

Outgoing radiation

Incoming solar radiation 100

Shortwave

Longwave

6   20   4   6   38   26

ATMOSPHERE

Backscattered by air

Absorbed by water vapor, 16 dust, O_3

Reflected by clouds

Absorbed by clouds   3

Absorbed

Reflected by surface

Reflected by surface

Net emission by water vapor, CO_2

Emission by clouds

15 Absorption by water vapor, CO_2

Latent heat flux

Sensible heat flux

Net surface emission of longwave radiation

OCEAN, LAND   51   21   7   23

Figure 7.3.2 Radiation and heat balance in the atmosphere and at the earth's surface (from U.S. National Academy of Sciences (1975)).

of all, there are water molecules in the form of *water vapor*, which are always found above liquid water. In addition, there are some other molecules: (a) two oxygen atoms stuck together by themselves, forming an *oxygen molecule*, and (b) two nitrogen atoms stuck together, forming a nitrogen molecule. Above the water surface is the air, a gas, consisting almost entirely of nitrogen, oxygen, some water vapor, and lesser amounts of carbon dioxide, argon, and other substances. The molecules in the water are always moving around. From time to time, one on the surface gets knocked away. In other words, molecule by molecule, the water disappears or evaporates.

The computation of evaporation in hydrologic analysis and design is important in water supply design, particularly reservoir design an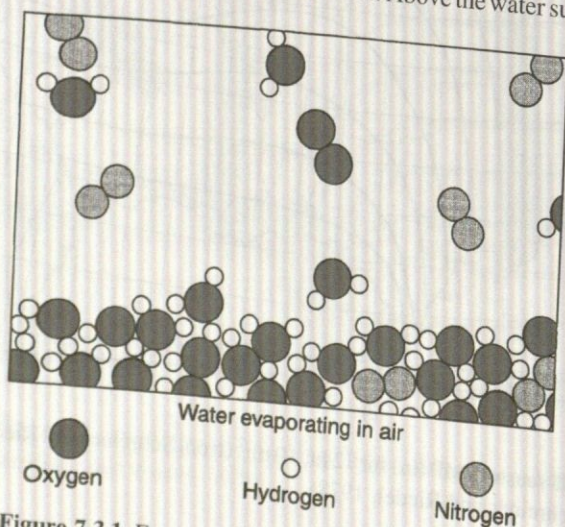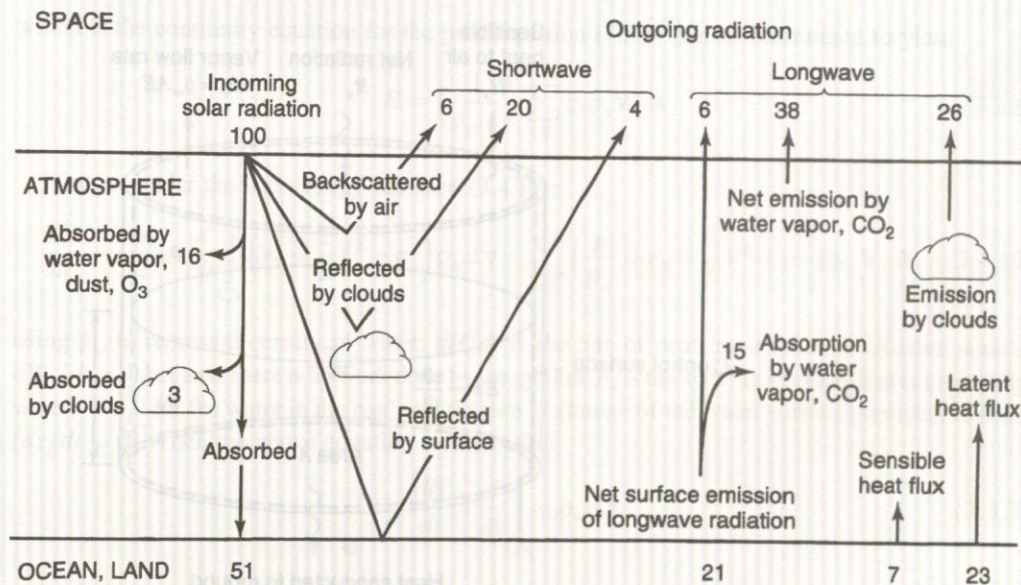d operation. The supply of energy to provide *latent heat of vaporization* and the *ability to transport water vapor away* from the evaporative surface are the two major factors that influence evaporation. *Latent heat* is the heat that is given up or absorbed when a phase (solid, liquid, or gaseous state) changes. *Latent heat of vaporization* (l_v) refers to the heat given up during vaporization of liquid water to water vapor, and is given as $l_v = 2.501 \times 10^6 - 2370T$, where T is the temperature in °C and l_v is in joules (J) per kilogram.

Three methods are used to determine evaporation: *the energy balance method, the aerodynamic method*, and *the combined aerodynamic and energy balance method*. The energy balance method considers the heat energy balance of a hydrologic system, and the aerodynamic method considers the ability to transport away from an open surface. Figure 7.3.2 illustrates the radiation and heat balance in the atmosphere and at the earth's surface along with relative values for the various components.

Energy Balance Method

Consider the evaporation pan shown in Figure 7.3.3 with the defined control volume. This control volume contains water in both the liquid phase and the vapor phase, with densities of ρ_w and ρ_a, respectively. The continuity equation must be written for both phases. For the liquid phase, the extensive property $B = m$ (mass of liquid water), the intensive property $\beta = 1$, and $dB/dt = \dot{m}_v$, which is the mass flow rate of evaporation. Continuity for the liquid phase is then

$$-\dot{m}_v = \frac{d}{dt}\int_{CV}\rho_w \, d\forall + \sum_{CS}\rho_w \mathbf{V}\cdot\mathbf{A} \qquad (7.3.1)$$
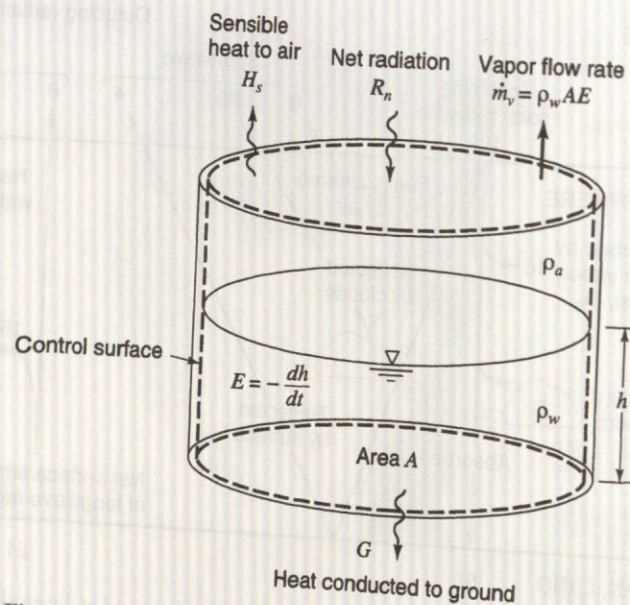
Figure 7.3.3 Control volume defined for continuity and energy equation development for an evaporation pan (from Chow et al. (1988)).

Because the pan has impermeable sides, there is no flow of liquid water across the control surface, so

$$\sum_{CS} \rho_w \mathbf{V} \cdot \mathbf{A} = 0.$$

The rate of change of storage is

$$\frac{d}{dt} \int_{CV} \rho_w \, d\forall = \rho_w A \frac{dh}{dt} \tag{7.3.2}$$

where A is the cross-sectional area of the pan and h is the depth of water. Substituting equation (7.3.2) into (7.3.1) gives

$$-\dot{m}_v = \rho_w A \frac{dh}{dt} \tag{7.3.3a}$$

or

$$\dot{m}_v = \rho_w AE \tag{7.3.3b}$$

where $E = -dh/dt$ is the evaporation rate.

Considering the vapor phase, the extensive property is $B = m_v$ (mass of water vapor), the intensive property is $\beta = q_v$ (specific humidity), and $dB/dt = \dot{m}_v$. Continuity for the vapor phase is

$$\dot{m}_v = \frac{d}{dt} \int_{CV} q_v \rho_a \, d\forall + \sum_{CS} q_v \rho_a \mathbf{V} \cdot \mathbf{A} \tag{7.3.4}$$

Considering steady flow over the pan, the time derivative of water vapor in the control volume is zero, $\dfrac{d}{dt} \int_{CV} q_v \rho_a \, d\forall = 0$, and $\dot{m}_v$ from equation (7.3.3) is substituted into equation (7.3.4) to obtain

$$\rho_w AE \sum_{CS} q_v \rho_a \mathbf{V} \cdot \mathbf{A} \tag{7.3.5}$$

which is the continuity equation for the pan. Equation (7.3.5) can be rearranged to yield

$$E = \left(\frac{1}{\rho_w A}\right) \sum_{CS} q_v \rho_a \mathbf{V} \cdot \mathbf{A} \qquad (7.3.6)$$

Next, consider the heat energy equation (3.4.19):

$$\frac{dH}{dt} - \frac{dW_s}{dt} = \frac{d}{dt} \int_{CV} \left(e_u + \frac{1}{2}V^2 + gz\right)\rho_w d\forall + \sum_{CS}\left(\frac{p}{\rho_w} + e_u + \frac{1}{2}V^2 + gz\right)\rho_w \mathbf{V} \cdot \mathbf{A} \quad (3.4.19)$$

using ρ_w to represent density of water; dH/dt is the rate of heat input from an external source, $dW_s/dt = 0$ because there is no work done by the system; e_u is the specific internal heat energy of the water; $V = 0$ for the water in the pan; and the rate of change of the water surface elevation is small $(dz/dt = 0)$. Then the above equation is reduced to

$$\frac{dH}{dt} = \frac{d}{dt}\int_{CV} e_u \rho_w d\forall \qquad (7.3.7)$$

The rate of heat input from external sources can be expressed as

$$\frac{dH}{dt} = R_n - H_s - G \qquad (7.3.8)$$

where R_n is the *net radiation flux* (watts per meter squared), H_s is the *sensible heat* to the air stream supplied by the water, and G is the *ground heat flux* to the ground surface. Net radiation flux is the net input of radiation at the surface at any instant. The net radiation flux at the earth's surface is the major energy input for evaporation of water, defined as the difference between the radiation absorbed, $R_i(1 - \alpha)$ (where R_i is the *incident radiation* and α is the fraction of radiation reflected, called the *albedo*), and that emitted. R_e:

$$R_n = R_i(1 - \alpha) - R_e \qquad (7.3.9)$$

The amount of radiation emitted is defined by the *Stefan–Boltzmann law*

$$R_e = e\sigma T_p^4 \qquad (7.3.10)$$

where e is the *emissivity* of the surface, σ is the *Stefan-Boltzmann constant* $(5.67 \times 10^{-8} \text{W/m}^2 \cdot \text{K}^4)$, and T_p is the absolute temperature of the surface in degrees Kelvin.

Assuming that the temperature of the water in the control volume is constant in time, the only change in the heat stored within the control volume is the change in the internal energy of the water evaporated $l_v \dot{m}_v$, where l_v is the latent heat of vaporization, so that

$$\frac{d}{dt}\int_{CV} e_u \rho_w d\forall = l_v \dot{m}_v \qquad (7.3.11)$$

Substituting equations (7.3.8) and (7.3.11) into (7.3.7) results in

$$R_n - H_s - G = l_v \dot{m}_v \qquad (7.3.12)$$

From equation (7.3.3b), $\dot{m}_v = \rho_w AE$. Substituting in (7.3.12) with $A = 1 \text{ m}^2$ and solving for E (to denote energy balance) gives the *energy balance equation for evaporation*,

$$E = \frac{1}{l_v \rho_w}(R_n - H_s - G) \qquad (7.3.13)$$

Assuming the sensible heat flux H_s and the ground heat flux G are both zero, then an evaporation rate E_r, which is the rate at which all incoming net radiation is absorbed by evaporation, can be

calculated as

$$E_r = \frac{R_n}{l_v \rho_w} \tag{7.3.14}$$

EXAMPLE 7.3.1

For a particular location the average net radiation is 185 W/m^2, air temperature is 28.5°C, relative humidity is 55 percent, and wind speed is 2.7 m/s at a height of 2 m. Determine the open water evaporation rate in mm/d using the energy method.

SOLUTION

Latent heat of vaporization in joules (J) per kg varies with T (°C), or $l_v = 2.501 \times 10^6 - 2370T$, so $l_v = 2501 - 2.37 \times 28.5 = 2433$ kJ/kg, $\rho_w = 996.3$ kg/m^3. The evaporation rate by the energy balance method is determined using equation (7.3.14) with $R_n = 185$ W/m^2:

$$E_r = R_n/(l_v\rho_w) = 185/(2433 \times 10^3 \times 996.3) = 7.63 \times 10^{-8} \text{ m/s} = 6.6 \text{ mm/d}.$$

7.3.2   Aerodynamic Method

As mentioned previously, the aerodynamic method considers the ability to transport water vapor away from the water surface; that is, generated by the humidity gradient in the air near the surface and the wind speed across the surface. These processes can be analyzed by coupling the equation for mass and momentum transport in the air. Considering the control volume in Figure 7.3.4, the vapor flux $\dot{m}_v$ passing upward by convection can be defined along with the momentum flux (as a function of the humidity gradient and the wind velocity gradient, respectively) (see Chow et al., 1988). The ratio of the vapor flux and the momentum flux can be used to define the *Thornthwaite–Holzman equation* for vapor transport (Thornthwaite and Holzman, 1939). Chow et al. (1988) present details of this derivation. The final form of the evaporation equation for the aerodynamic method expresses the evaporation rate E_a as a function of the difference of the vapor pressure at the surface e_{as}, which is the *saturation vapor pressure* at ambient air temperature (when the rate of evaporation and condensation are equal), and the vapor pressure at a height z_2 above the water surface, which is taken as the ambient vapor pressure in air e_a.

$$E_a = B(e_{as} - e_a) \tag{7.3.15}$$

where E_a has units of mm/day and B is the vapor transfer coefficient with units of mm/day · Pa, given as

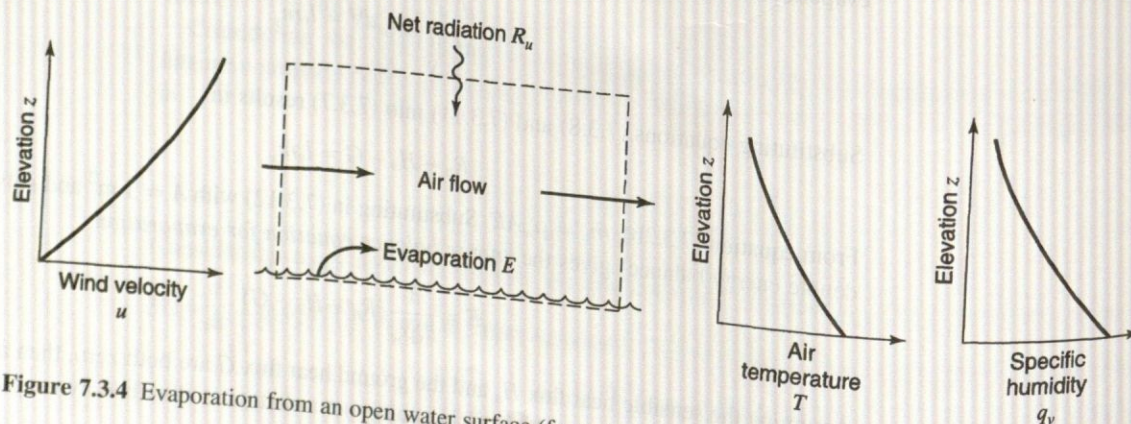**Figure 7.3.4** Evaporation from an open water surface (from Chow et al. (1988)).

$$B = \frac{0.102u_2}{[\ln(z_2/z_0)]^2} \tag{7.3.16}$$

where u_2 is the wind velocity (m/s) measured at height z_2 (cm) and z_0 is the roughness height (0.01–0.06 cm) of the water surface. The vapor pressures have units of Pa (N/m^2). The saturation vapor pressure is approximated as

$$e_{as} = 611 \exp\left(\frac{17.27T}{237.3+T}\right) \tag{7.3.17}$$

and the vapor pressure is

$$e_a = R_h e_{as} \tag{7.3.18}$$

where T is the air temperature in °C and R_h is the relative humidity ($R = e_a/e_{as}$) and ($0 \le R_h \le 1$).

EXAMPLE 7.3.2

Solve example 7.3.1 using the aerodynamic method, by using a roughness height $z_0 = 0.03$ cm.

SOLUTION

From equation (7.3.17), the saturated vapor pressure is

$$e_{as} = 611 \exp[17.27T/(237.3+T)] = 611 \exp[17.27 \times 28.5/(237.3+28.5)]$$
$$= 3893 \text{ Pa}$$

The ambient vapor pressure e_a is determined from equation (7.3.18); for a relative humidity $R_h = 0.55$, $e_a = e_{as}R_h = 3893 \times 0.55 = 2141$ Pa. The vapor transfer coefficient B is given by equation (7.3.16) in which $u_2 = 2.7$ m/s, $z_2 = 2$ m, and $z_0 = 0.03$ cm for an open water surface, so that $B = 0.102u_2/[\ln(zz/z0)]^2 = 0.102 \times 2.7/[\ln(200/0.03)]^2 = 0.0036$ mm/d·Pa; then the evaporation rate by the aerodynamic method is given by equation (7.3.15):

$$E_a = B(e_{as} - e_a) = 0.0036(3893 - 2141) = 6.31 \text{ mm/d}.$$

7.3.3 Combined Method

When the energy supply is not limiting, the aerodynamic method can be used, and when the vapor transport is not limiting, the energy balance method can be used. However, both of these factors are not normally limiting, so a combination of these methods is usually required. The combined method equation is

$$E = \left(\frac{\Delta}{\Delta+\gamma}\right)E_r + \left(\frac{\gamma}{\Delta+\gamma}\right)E_a \tag{7.3.19}$$

in which ( )E_r is the vapor transport term and ( )E_a is the aerodynamic term. γ is the *psychrometric constant* (approximately 66.8 Pa/°C) and Δ is the *gradient of the saturated vapor pressure curve* $\Delta = de_{as}/dT$ at air temperature T_α given as

$$\Delta = \frac{4098e_{as}}{(237.3+T_\alpha)} \tag{7.3.20}$$

in which e_{as} is the *saturated vapor pressure* (the maximum moisture content the air can hold for a given temperature).

The combination method is best for application to small areas with detailed climatological data including net radiation, air temperature, humidity, wind speed, and air pressure. For very large areas, energy (vapor transport) largely governs evaporation. Priestley and Taylor (1972) discovered that the aerodynamic term in equation (7.3.19) is approximately 30 percent of the energy term, so that

equation (7.3.19) can be simplified to

$$E = 1.3 \left(\frac{\Delta}{\Delta + \gamma} \right) E_r \qquad (7.3.21)$$

which is known as the *Priestley–Taylor evaporation equation.*

EXAMPLE 7.3.3   Solve example 7.3.1 using the combined method.

SOLUTION

The gradient of the saturated vapor pressure curve is, from equation (7.3.20),

$$\Delta = 4098 e_{as}/(237.3 + T)^2 = 4098 \times 3893/(237.3 + 28.5)^2 = 225.8 \text{ Pa/°C}$$

The psychrometric constant γ is approximately 66.8 Pa/°C; then E_r and E_a may be combined according to equation (7.3.19) to give

$$\begin{aligned} E &= \Delta/(\Delta + \gamma)E_r + \gamma/(\Delta + \gamma)E_a \\ &= (225.8/(225.8 + 66.8))6.6 + (66.8/(225.8 + 66.8))6.31 = 0.772(6.6) + 0.228(6.31) \\ &= 5.10 + 1.44 = 6.54 \text{ mm/d} \end{aligned}$$

EXAMPLE 7.3.4   Solve example 7.3.1 using the Priestley–Taylor method.

SOLUTION

The evaporation is computed using equation (7.3.21):

$$E = 1.3 \left(\frac{\Delta}{\Delta + \gamma} \right) E_r = 1.3 \left(\frac{225.8}{225.8 + 66.8} \right) 6.6$$

$$= 6.62 \text{ mm/d}$$

7.4   INFILTRATION

The process of water penetrating into the soil is *infiltration.* The rate of infiltration is influenced by the condition of the soil surface, vegetative cover, and soil properties including porosity, hydraulic conductivity, and moisture content. In order to discuss infiltration, we must first consider the division of subsurface water (see Figure 6.1.2) and the various subsurface flow processes shown in Figure 7.4.1. These processes are infiltration of water to become *soil moisture, subsurface flow* (unsaturated flow) through the soil, and *groundwater flow* (saturated flow). *Unsaturated flow* refers to flow through a porous medium when some of the voids are occupied by air. *Saturated flow* occurs when the voids are filled with water. The *water table* is the interface between the saturated and unsaturated flow, where atmospheric pressure prevails. Saturated flow occurs below the water table and unsaturated flow occurs above the water table.
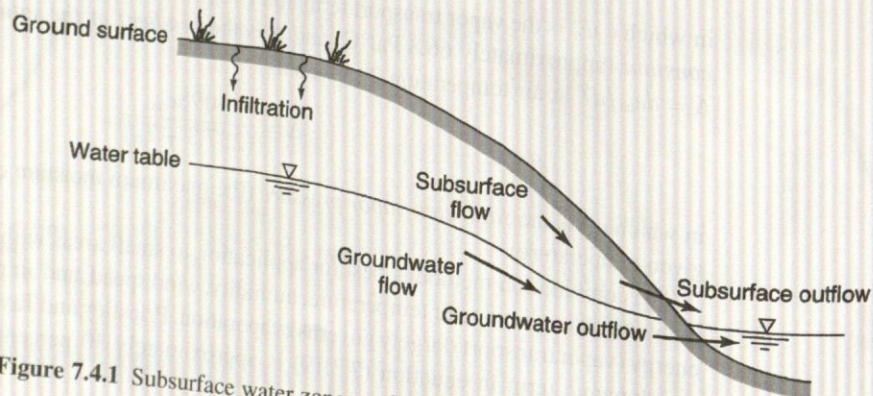
Figure 7.4.1 Subsurface water zones and processes (from Chow et al. (1988)).

7.4.1   Unsaturated Flow

The cross-section through an unsaturated porous medium (Figure 7.4.2*a*) is now used to define *porosity*, η:

$$\eta = \frac{\text{volume of voids}}{\text{total volume}} \tag{7.4.1}$$

in which η is $0.25 < \eta < 0.40$, and the *soil moisture content,* θ,

$$\theta = \frac{\text{volume of water}}{\text{total volume}} \tag{7.4.2}$$

in which θ is $0 \leq \theta \leq \eta$. For saturated conditions, $\theta = \eta$.

Consider the control volume in Figure 7.4.2*b* for an unsaturated soil with sides of lengths *dx*, *dy*, and *dz*, with a volume of *dxdydz*. The volume of water contained in the control volume is θ*dxdydz*. Flow through the control volume is defined by the *Darcy flux, q = Q/A*, which is the volumetric flow rate per unit of soil area. For this derivation, the horizontal fluxes are ignored and only the vertical (*z*) direction is considered, with *z* positive upward.

(a)

(b)
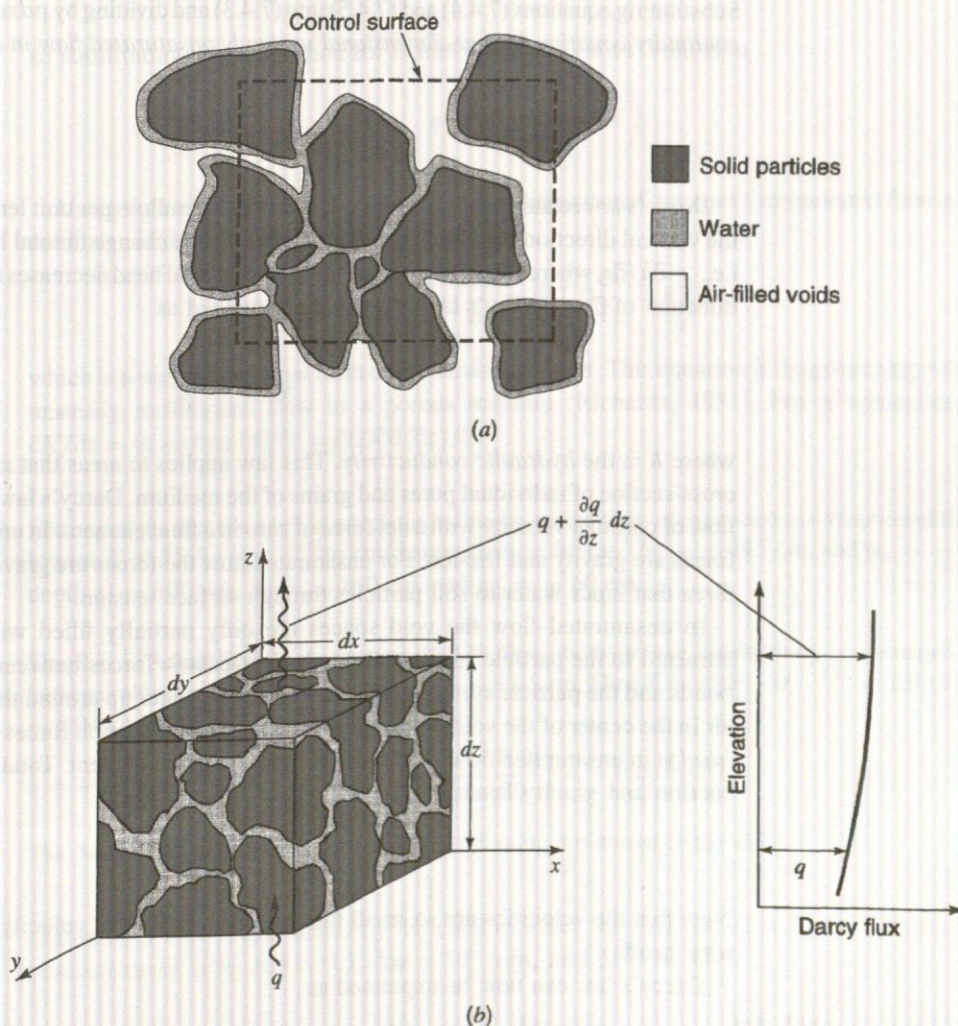
Figure 7.4.2 (*a*) Cross-section through an unsaturated porous medium; (*b*) Control volume for development of the continuity equation in an unsaturated porous medium (from Chow et al. (1988)).

With the control volume approach, the extensive property B is the mass of soil water, so the intensive property $\beta = dB/dm = 1$ and $dB/dt = 0$, because no phase changes are occurring in water. The general control volume equation for continuity, equation (3.3.1), is applicable:

$$0 = \frac{d}{dt} \int_{CV} \rho \, d\forall + \int_{CS} \rho \mathbf{V} \cdot d\mathbf{A} \tag{7.4.3}$$

The time rate of change of mass stored in the control volume is

$$\frac{d}{dt} \int_{CV} \rho \, d\forall = \frac{d}{dt} (\rho\theta dxdydz) = \rho dxdydz \frac{\partial \theta}{\partial t} \tag{7.4.4}$$

where the density is assumed constant. The net outflow of water is the difference between the volumetric inflow at the bottom $(qdxdy)$ and the volumetric outflow at the top $[q + (\partial q/\partial z)dz]dxdy$, so

$$\int_{CV} \rho \mathbf{V} \cdot d\mathbf{A} = \rho \left(q + \frac{\partial q}{\partial z} dz \right) dxdy - \rho q dxdy = \rho dxdydz \frac{\partial q}{\partial z} \tag{7.4.5}$$

Substituting equations (7.4.4) and (7.4.5) into (7.4.3) and dividing by $\rho dxdydz$ results in the following continuity equation for one-dimensional unsteady unsaturated flow in a porous medium:

$$\frac{\partial \theta}{\partial t} + \frac{\partial q}{\partial z} = 0 \tag{7.4.6}$$

Darcy's law relates the *Darcy flux q* to the rate of headloss per unit length of medium. For flow in the vertical direction the headloss per unit length is the change in total head ∂h over a distance, ∂z, i.e., $-\partial h/\partial z$, where the negative sign indicates that total head decreases (as a result of friction) in the direction of flow. Darcy's law can now be expressed as

$$q = -K \frac{\partial h}{\partial z} \tag{7.4.7}$$

where K is the *hydraulic conductivity*. This law applies to areas that are large compared with the cross-section of individual pores and grains of the medium. Darcy's law describes a steady uniform flow of constant velocity with a net force of zero in a fluid element. In unconfined saturated flow, the forces are gravity and friction. For unsaturated flow the forces are gravity, friction, and the *suction force* that binds water to soil particles through surface tension.

In unsaturated flow the void spaces are only partially filled with water, so that water is attracted to the particle surfaces through electrostatic forces between the water molecule polar bonds and the particle surfaces. This in turn draws water up around the particle surfaces, leaving air in the center of the voids. The energy due to the soil suction forces is referred to as the *suction head* ψ in unsaturated flow, which varies with moisture content. Total head is then the sum of the suction and gravity heads:

$$h = \psi + z \tag{7.4.8}$$

Note that the velocities are so small that there is no term for velocity head in this expression for total head.

Darcy's law can now be expressed as

$$q = -K \frac{\partial(\psi + z)}{\partial z} \tag{7.4.9}$$

EXAMPLE 7.4.

SOLUTION

EXAMPLE 7.4.

SOLUTION

Darcy's law was originally conceived for saturated flow and was extended by Richards (1931) to unsaturated flow with the provision that the hydraulic conductivity is a function of the suction head, i.e., $K = K(\psi)$. Also, the hydraulic conductivity can be related more easily to the degree of saturation, so that $K = K(\theta)$. Because the soil suction head varies with moisture content and moisture content varies with elevation, the *suction gradient* can be expanded by using the chain rule to obtain

$$\frac{\partial \psi}{\partial z} = \frac{d\psi}{d\theta}\frac{\partial \theta}{\partial z} \tag{7.4.10}$$

in which $\partial \theta / \partial z$ is the *wetness gradient*, and the reciprocal of $d\psi/d\theta$, i.e., $d\theta/d\psi$, is the *specific water capacity*. Now equation (7.4.9) can be modified to

$$q = -K\left(\frac{\partial \psi}{\partial z} + \frac{\partial z}{\partial z}\right) = -K\left(\frac{\partial \psi}{\partial \theta}\frac{\partial \theta}{\partial z} + 1\right) = -\left(K\frac{d\psi}{d\theta}\frac{\partial \theta}{\partial z} + K\right) \tag{7.4.11}$$

The *soil water diffusivity* $D(L^2/T)$ is defined as

$$D = K\frac{d\psi}{d\theta} \tag{7.4.12}$$

so substituting this expression for D into equation (7.4.11) results in

$$q = -\left(D\frac{\partial \theta}{\partial z} + K\right) \tag{7.4.13}$$

Using the continuity equation (7.4.6) for one-dimensional, unsteady, unsaturated flow in a porous medium yields

$$\frac{\partial \theta}{\partial t} = -\frac{\partial q}{\partial z} = \frac{\partial}{\partial z}\left(D\frac{\partial \theta}{\partial z} + K\right) \tag{7.4.14}$$

which is a one-dimensional form of *Richards' equation*. This equation is the governing equation for unsteady unsaturated flow in a porous medium (Richards, 1931). For a homogeneous soil, $\partial K / \partial z = 0$, so that $\partial \theta / \partial t = \partial(D\partial \theta/\partial z)/\partial z$.

EXAMPLE 7.4.1

Determine the flux for a soil in which the hydraulic conductivity is expressed as a function of the suction head as $K = 250(-\psi)^{-2.11}$ in cm/d at depth $z_1 = 80$ cm, $h_1 = -145$ cm, and $\psi_1 = -65$ cm at depth $z_2 = 100$ cm, $h_2 = -160$ cm, and $\psi_2 = -60$ cm.

SOLUTION

The flux is determined using equation (7.4.7). First the hydraulic conductivity is computed using an average value of $\psi = [-65 + (-60)]/2 = -62.5$ cm. Then $K = 250(-\psi)^{-2.11} = 250(62.5)^{-2.11} = 0.041$ cm/d. The flux is then

$$q = -K\left(\frac{h_1 - h_2}{z_1 - z_2}\right) = -0.041\left[\frac{-145 - (-160)}{-80 - (-100)}\right] = -0.03 \text{ cm/d}$$

The flux is negative because the moisture is flowing downward in the soil.

EXAMPLE 7.4.2

Determine the soil water diffusivity for a soil in which $\theta = 0.1$ and $K = 3 \times 10^{-11}$ mm/s from a relationship of $\psi(\theta)$ at $\theta = 0.1$, $\Delta\psi = 10^7$ mm, and $\Delta\theta = 0.35$.

SOLUTION

Using equation (7.4.12), the soil water diffusivity is $D = Kd\psi/d\theta = (3 \times 10^{-11}$ mm/s$)(10^7 \text{ mm}/0.35) = 8.57 \times 10^{-4}$ mm/s.

7.4.2   Green-Ampt Method

Figure 7.4.3 illustrates the distribution of soil moisture within a soil profile during downward movement. These moisture zones are the *saturated zone*, the *transmission zone*, a *wetting zone*, and a *wetting front*. This profile changes as a function of time as shown in Figure 7.4.4.

The *infiltration rate f* is the rate at which water enters the soil surface, expressed in in/hr or cm/hr. The *potential infiltrate rate* is the rate when water is ponded on the soil surface, so if no ponding occurs the actual rate is less than the potential rate. Most infiltration equations describe a potential infiltration rate. *Cumulative infiltration F* is the accumulated depth of water infiltrated, defined mathematically as

$$F(t) = \int_0^t f(\tau)d\tau \qquad (7.4.15)$$

and the infiltration rate is the time derivative of the cumulative infiltration given as

$$f(t) = \frac{dF(t)}{dt} \qquad (7.4.16)$$

Figure 7.4.5 illustrates a rainfall hyetograph with the infiltration rate and cumulative infiltration curves. (See Section 8.2 for further details on the rainfall hyetograph.)

Green and Ampt (1911) proposed the simplified picture of infiltration shown in Figure 7.4.6. The *wetting front* is a sharp boundary dividing soil with moisture content θ_i below from saturated soil
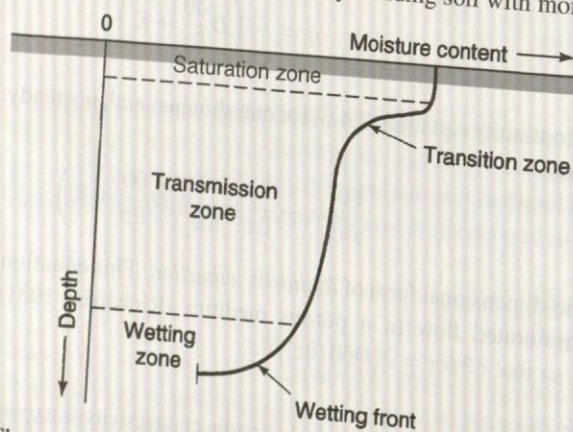

Figure 7.4.3 Moisture zones during infiltration (from Chow et al. (1988)).
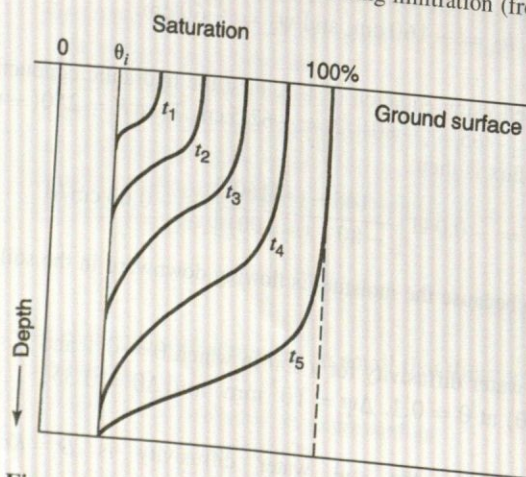

Figure 7.4.4 Moisture profile as a function of time for water added to the soil surface.
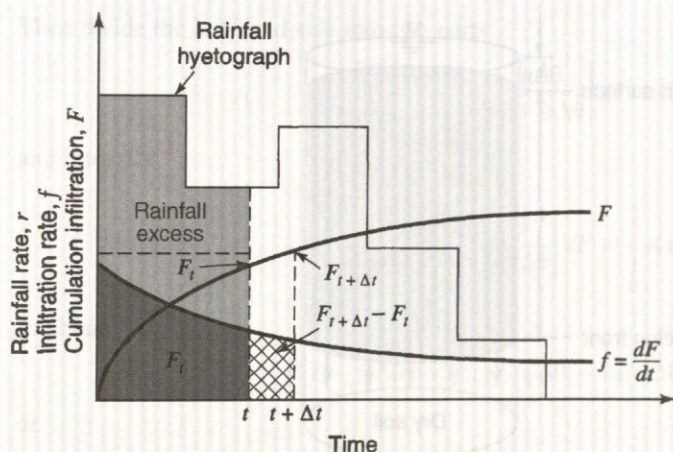
Figure 7.4.5 Rainfall infiltration rate and cumulative infiltration. The rainfall hyetograph illustrates the rainfall pattern as a function of time. The cumulative infiltration at time t is F_t or $F(t)$ and at time $t + \Delta t$ is $F_{t+\Delta t}$ or $F(t + \Delta t)$ and are computed using equation (7.4.15). The increase in cumulative infiltration from time t to $t + \Delta t$ is $F_{t+\Delta t} - F_t$ or $F(t + \Delta t) - F(t)$, as shown in the figure. Rainfall excess is defined in Chapter 8 as that rainfall that is neither retained on the land surface nor infiltrated into the soil.
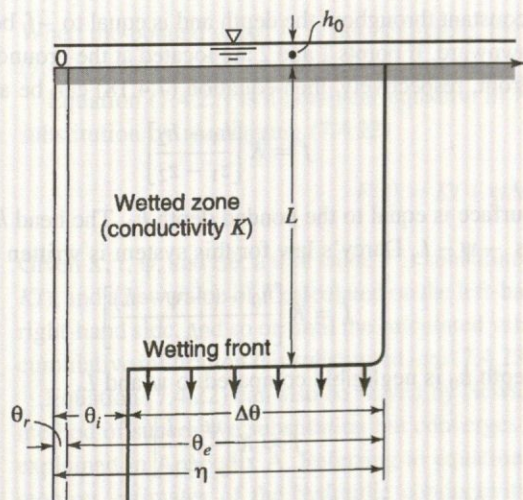
Figure 7.4.6 Variables in the Green–Ampt infiltration model. The vertical axis is the distance from the soil surface; the horizontal axis is the moisture content of the soil (from Chow et al. (1988)).

with moisture content η above. The wetting front has penetrated to a depth L in time t since infiltration began. Water is ponded to a small depth h_0 on the soil surface.

Consider a vertical column of soil of unit horizontal cross-sectional area (Figure 7.4.7) with the control volume defined around the wet soil between the surface and depth L. For a soil initially of moisture content θ_i throughout its entire depth, the *moisture content* will increase from θ_i to η (the porosity) as the wetting front passes. The moisture content θ is the ratio of the volume of water to the total volume within the control surface. $L(\eta - \theta_i)$ is then the increase in the water stored within the control volume as a result of infiltration, through a unit cross-section. By definition this quantity is equal to F, the cumulative depth of water infiltrated into the soil, so that

$$F(t) = L(\eta - \theta_i) = L\Delta\theta \qquad (7.4.17)$$

where $\Delta\theta = (\eta - \theta_i)$.
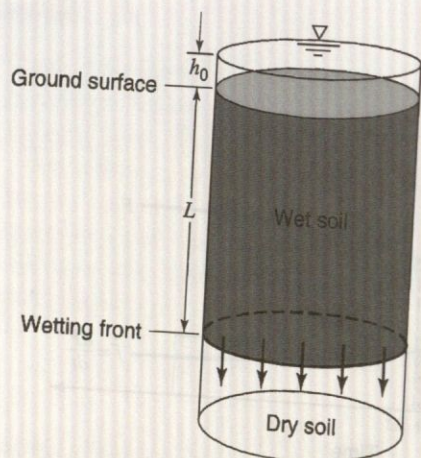
Figure 7.4.7 Infiltration into a column of soil of unit cross-sectional area for the Green–Ampt model (from Chow et al. (1988)).

Darcy's law may be expressed (using equation (7.4.7)) as

$$q = K\frac{\partial h}{\partial z} = -K\frac{\Delta h}{\Delta z} \tag{7.4.18}$$

The Darcy flux q is constant throughout the depth and is equal to $-f$, because q is positive upward while f is positive downward. If points 1 and 2 are located at the ground surface and just on the dry side of the wetting front, respectively, then equation (7.4.18) can be approximated by

$$f = K\left[\frac{h_1 - h_2}{z_1 - z_2}\right] \tag{7.4.19}$$

The head h_1 at the surface is equal to the ponded depth h_0. The head h_2, in the dry soil below the wetting front, equals $-\psi - L$. Darcy's law for this system is written as

$$f = K\left[\frac{h_0 - (-\psi - L)}{L}\right] \tag{7.4.20a}$$

and if the ponded depth h_0 is negligible compared to ψ and L,

$$f \approx K\left[\frac{\psi + L}{L}\right] \tag{7.4.20b}$$

This assumption ($h_0 = 0$) is usually appropriate for surface water hydrology problems because it is assumed that ponded water becomes surface runoff.

From equation (7.4.17), the wetting front depth is $L = F/\Delta\theta$, and assuming $h_0 = 0$, substitution into equation (7.4.20) gives

$$f = K\left[\frac{\psi\Delta\theta + F}{F}\right] \tag{7.4.21}$$

Since $f = dF/dt$, equation (7.4.21) can be expressed as a differential equation in the one unknown F as

$$\frac{dF}{dt} = K\left[\frac{\psi\Delta\theta + F}{F}\right]$$

To solve for F, cross-multiply to obtain

$$\left[\frac{F}{F + \psi\Delta\theta}\right]dF = Kdt$$

Then divide the left-hand side into two parts

$$\left[\frac{F+\psi\Delta\theta}{F+\psi\Delta\theta}-\frac{\psi\Delta\theta}{F+\psi\Delta\theta}\right]dF=Kdt$$

and integrate

$$\int_{0}^{F(t)}\left[1-\frac{\psi\Delta\theta}{F+\psi\Delta\theta}\right]dF=\int_{0}^{t}Kdt$$

to obtain

$$F(t)-\psi\Delta\theta\{\ln[F(t)+\psi\Delta\theta]-\ln(\psi\Delta\theta)\}=Kt \qquad (7.4.22a)$$

or

$$F(t)-\psi\Delta\theta\ln\left(1+\frac{F(t)}{\psi\Delta\theta}\right)=Kt \qquad (7.4.22b)$$

Equation (7.4.22) is the *Green–Ampt equation* for cumulative infiltration. Once F is computed using equation (7.4.22), the infiltration rate f can be obtained from equation (7.4.21) or

$$F(t)=K\left[\frac{\psi\Delta\theta}{F(t)}+1\right] \qquad (7.4.23)$$

When the ponded depth h_0 is not negligible, the value of $\psi+h_0$ is substituted for ψ in equations (7.4.22) and (7.4.23).

Equation (7.4.22) is a nonlinear equation in F that can be solved by the method of successive substitution by rearranging (7.4.22)

$$F(t)=Kt+\psi\Delta\theta\ln\left(1+\frac{F(t)}{\psi\Delta\theta}\right) \qquad (7.4.24)$$

Given K, t, ψ, and $\Delta\theta$, a trial value F is substituted on the right-hand side (a good trial value is $F=Kt$), and a new value of F calculated on the left-hand side, which is substituted as a trial value on the right-hand side, and so on until the calculated values of F converge to a constant. The final value of cumulative infiltration F is substituted into (7.4.23) to determine the corresponding infiltration rate f.

Equation (7.4.22) can also be solved by Newton's method, which is more complicated than the method of successive substitution but converges in fewer iterations. Newton's iteration method is explained in Appendix A. Referring to equation (7.4.24), application of the Green–Ampt model requires estimates of the hydraulic conductivity K, the wetting front soil suction bead ψ (see Table 7.4.1), and $\Delta\theta$.

The *residual moisture content* of the soil, denoted by θ_r, is the moisture content after it has been thoroughly drained. The *effective saturation* is the ratio of the available moisture $(\theta-\theta_r)$ to the maximum possible available moisture content $(\eta-\theta_r)$, given as

$$s_e=\frac{\theta-\theta_r}{\eta-\theta_r} \qquad (7.4.25)$$

where $\eta-\theta_r$ is called the *effective porosity* θ_e.

The effective saturation has the range $0\le s_e\le 1.0$, provided $\theta_r\le\theta\le\eta$. For the initial condition, when $\theta=\theta_i$, cross-multiplying equation (7.4.25) gives $\theta_i-\theta_r=s_e\theta_e$, and the change in the moisture content when the wetting front passes is

$$\Delta\theta=\eta-\theta_i=\eta-(s_e\theta_e+\theta_r)$$
$$\Delta\theta=(1-s_e)\theta_e \qquad (7.4.26)$$

Table 7.4.1   Green–Ampt Infiltration Parameters for Various Soil Classes*

Soil class	Porosity η	Effective porosity θ_e	Wetting front soil suction head ψ (cm)	Hydraulic conductivity K (cm/h)
Sand	0.437 (0.374–0.500)	0.417 (0.354–0.480)	4.95 (0.97–25.36)	11.78
Loamy sand	0.437 (0.363–0.506)	0.401 (0.329–0.473)	6.13 (1.35–27.94)	2.99
Sandy loam	0.453 (0.351–0.555)	0.412 (0.283–0.541)	11.01 (2.67–45.47)	1.09
Loam	0.463 (0.375–0.551)	0.434 (0.334–0.534)	8.89 (1.33–59.38)	0.34
Silt loam	0.501 (0.420–0.582)	0.486 (0.394–0.578)	16.68 (2.92–95.39)	0.65
Sandy clay loam	0.398 (0.332–0.464)	0.330 (0.235–0.425)	21.85 (4.42–108.0)	0.15
Clay loam	0.464 (0.409–0.519)	0.309 (0.279–0.501)	20.88 (4.79–91.10)	0.10
Silty clay loam	0.471 (0.418–0.524)	0.432 (0347–0.517)	27.30 (5.67–131.50)	0.10
Sandy clay	0.430 (0.370–0.490)	0.321 (0.207–0.435)	23.90 (4.08–140.2)	0.06
Silty clay	0.479 (0.425–0.533)	0.423 (0.334–0.512)	29.22 (6.13–139.4)	0.05
Clay	0.475 (0.427–0.523)	0.385 (0.269–0.501)	31.63 (6.39–156.5)	0.03

* The numbers in parentheses below each parameter are one standard deviation around the parameter value given.

Source: Rawls, Brakensiek, and Miller (1983).

A logarithmic relationship between the effective saturation s_e and the soil suction head ψ can be expressed by the *Brooks–Corey equation* (Brooks and Corey, 1964):

$$s_e = \left[\frac{\psi_b}{\psi}\right]^{\lambda}$$

(7.4.27)

in which ψ_b and λ are constants obtained by draining a soil in stages, measuring the values of s_e and ψ at each stage, and fitting equation (7.4.27) to the resulting data.

Brakensiek et al. (1981) presented a method for determining the Green–Ampt parameters using the Brooks–Corey equation. Rawls et al. (1983) used this method to analyze approximately 5000 soil horizons across the United States and determined average values of the Green–Ampt parameters η, θ_e, ψ, and K for different soil classes, as listed in Table 7.4.1. As the soil becomes finer, moving from sand to clay, the wetting front soil suction head increases while the hydraulic conductivity decreases. Table 7.4.1 also lists typical ranges for η, θ_e, and ψ. The ranges are not large for η and θ_e, but ψ can vary over a wide range for a given soil. K varies along with ψ, so the values given in Table 7.4.1 for both ψ and K should be considered typical values that may show a considerable degree of variability in application (American Society of Agricultural Engineers, 1983; Devanrs and Gifford, 1986).

Table 7.4.2 Infiltration Computations Using the Green–Ampt Method

Time t (hr)	0.0	0.1	0.2	0.3	0.4	0.5	1.0	1.5	2.0	2.5	3.0	3.5	4.0	4.5	5.0	5.5	6.0
Infiltration rate f (cm/hr)	∞	1.78	1.20	0.97	0.84	0.75	0.54	0.44	0.39	0.35	0.32	0.30	0.28	0.27	0.26	0.25	0.24
Infiltration depth F (cm)	0.00	0.29	0.43	0.54	0.63	0.71	1.02	1.26	1.47	1.65	1.82	1.97	2.12	2.26	2.39	2.51	2.64

EXAMPLE 7.4.3

Use the Green–Ampt method to evaluate the infiltration rate and cumulative infiltration depth for a silty clay soil at 0.1-hr increments up to 6 hr from the beginning of infiltration. Assume an initial effective saturation of 20 percent and continuous ponding.

SOLUTION

From Table 7.4.1, for a silty clay soil, $\theta_e = 0.423$, $\psi = 29.22$ cm, and $K = 0.05$ cm/hr. The initial effective saturation is $s_e = 0.2$, so $\Delta\theta = (1 - s_e)$, $\theta_e = (1 - 0.20)0.423 = 0.338$, and $\psi\Delta\theta = 29.22 \times 0.338 = 9.89$ cm. Assuming continuous ponding, the cumulative infiltration F is found by successive substitution in equation (7.4.24):

$$F = Kt + \psi\Delta\theta \ln[1 + F/(\psi\Delta\theta)] = 0.05t + 9.89 \ln[1 + F/9.89]$$

For example, at time $t = 0.1$ hr, the cumulative infiltration converges to a final value $F = 0.29$ cm. The infiltration rate f is then computed using equation (7.4.23):

$$f = K(1 + \psi\Delta\theta/F) = 0.05(1 + 9.89/F)$$

As an example, at time $t = 0.1$ hr, $f = 0.05(1 + 9.89/0.29) = 1.78$ cm/hr. The infiltration rate and the cumulative infiltration are computed in the same manner between 0 and 6 hr at 0.1-hr intervals; the results are listed in Table 7.4.2.

EXAMPLE 7.4.4

Ponding time t_p is the elapsed time between the time rainfall begins and the time water begins to pond on the soil surface. Develop an equation for ponding time under a constant rainfall intensity i, using the Green–Ampt infiltration equation (see Figure 7.4.8).

SOLUTION

The infiltration rate f and the cumulative infiltration F are related in equation (7.4.22). The cumulative infiltration at ponding time t_p is $F_p = it_p$, in which i is the constant rainfall intensity (see Figure 7.4.8). Substituting $F_p = it_p$ and the infiltration rate $f = i$ into equation (7.4.23) yields

$$i = K\left(\frac{\psi\Delta\theta}{it_p} + 1\right)$$

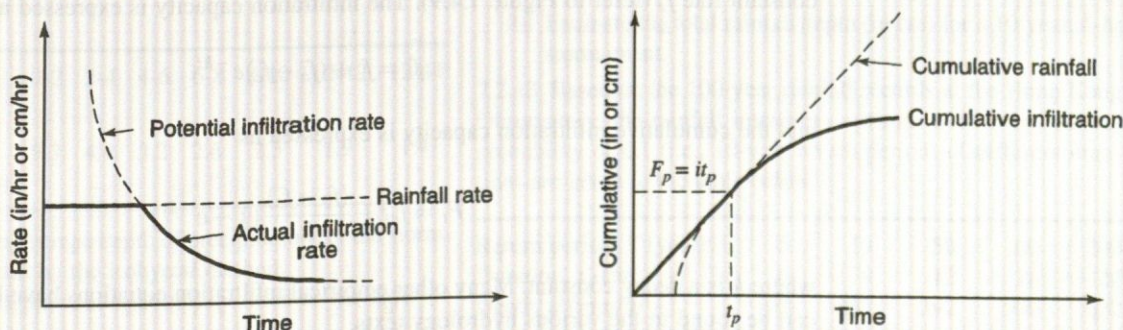

Figure 7.4.8 Ponding time. This figure illustrates the concept of ponding time for a constant intensity rainfall. Ponding time is the elapsed time between the time rainfall begins and the time water begins to pond on the soil surface.
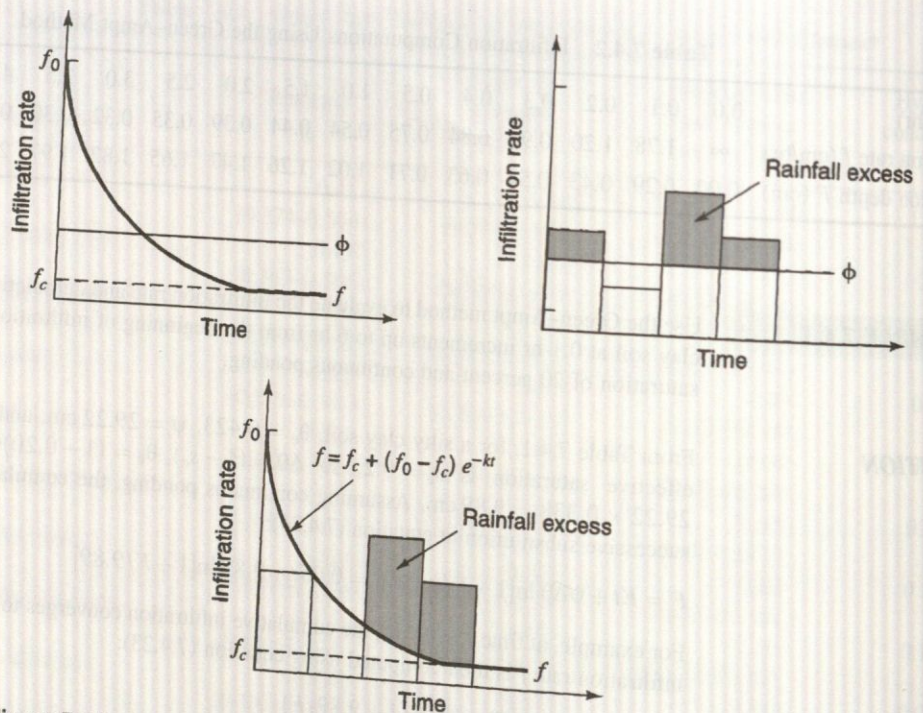
Figure 7.4.9 Φ-index and Horton's equation.

and solving, we get

$$t_p = \frac{K\psi\Delta\theta}{i(i-K)}$$

which is the ponding time for a constant rainfall intensity.

7.4.3 Other Infiltration Methods

The simplest accounting of abstraction is the Φ-*index* (refer to Figure 7.4.9 and Section 8.2), which is a constant rate of abstraction (in/h or cm/h). Other cumulative infiltration and infiltration rate equations include Horton's and the SCS method. Horton's equation (Horton, 1933) is an empirical relation that assumes infiltration begins at some rate f_o and exponentially decreases until it reaches a constant rate f_c (refer to Figure 7.4.9). The infiltration capacity is expressed as

$$f_t = f_c + (f_o - f_c)e^{-kt}$$

(7.4.28)

and the cumulative infiltration capacity is expressed as

$$F_t = f_c t + \frac{(f_0 - f_c)}{k}(1 - e^{-kt})$$

(7.4.29)

where k is a decay constant. Many other empirical infiltration equations have been developed that can be found in the various hydrology texts.

Richard's equation can be solved (Philip, 1957, 1969) under less restrictive conditions by assuming that K and D (equation 7.4.14) can vary with moisture content. Philip used the Boltzmann transformation $B(\theta) = zt^{-1/2}$ to convert Richard's equation (7.4.14) into an ordinary differential equation in B and solved to obtain an intimate series for cumulative infiltration F_t, approximated as

$$F_t = St^{1/2} + Kt \tag{7.4.30}$$

in which S is the sorptivity, a parameter that is a function of the soil suction potential, and K is the hydraulic conductivity. Differentiating $f(t) = df/dt$, the infiltration rate is defined as

$$f(t) = \frac{1}{2} St^{-1/2} + K \tag{7.4.31}$$

As $t \to \infty$, $f(t) \to K$. The two terms S and K represent the effects of soil suction head and gravity head.

There are many other infiltration methods, including the SCS method described in Sections 8.6–8.8. In summary, the Green–Ampt and the SCS are both used in the U.S. Army Corps of Engineers HEC-1 and HEC-HMS models, and both are used widely in the United States.

PROBLEMS

7.2.1 Determine the 25-year return period rainfall depth for a 30-min duration in Chicago, Illinois.

7.2.2 Determine the 2-, 10-, 25-, and 100-year precipitation depths for a 15-min duration storm in Memphis, Tennessee.

7.2.3 Determine the 2- and 25-year intensity-duration-frequency curves for Memphis, Tennessee.

7.2.4 Determine the 10- and 50-year intensity-duration-frequency curves for Chicago, Illinois.

7.2.5 Determine the 2-, 5-, 10-, 25-, 50-, and 100-year depths for a 1-hr duration storm in Phoenix, Arizona. Repeat for a 6-hr duration storm.

7.2.6 Develop the Type I, IA, II, and III 24-hour storms for a 24-hour rainfall of 20 in. Plot and compare these storms.

7.2.7 Develop the SCS 6-hr storm for a 6-hr rainfall of 12 in.

7.2.8 Determine the design rainfall intensities (mm/hr) for a 25-year return period, 60-min duration storm using equation (7.2.5) with $c = 12.1$, $m = 0.25$, $e = 0.75$, and $f = 0.125$.

7.2.9 What is the all-season 6-hr PMP (in) for 200 mi^2 near Chicago, Illinois?

7.2.10 Tabulated are the data derived from a drainage basin of 21,100 hectares, given the areas covered with each of the rainfall isohyetal lines.

Interval of isohyets (cm)	0-2	2-4	4-6	6-8	8-10	10-42	12-44
Enclosed area (hectares × 1000)		5.3	4.4	3.2	2.6	2.3	1.9	1.4

(a) Determine the average depth of precipitation for the storm within the basin by the isohyetal method.
(b) Develop the depth-area relationship based on the data.

7.2.11 For a particular 24-hr storm event on a river basin, an isohyetal map was developed. The corresponding isohyets and area relationship is given in the table below. Based on the given information, (a) develop the depth-area relationship in tabular form for the basin and (b) assuming the maximum point rainfall

is 145 mm, estimate the parameters in the following dimensionless depth-area equation that best fit the existing data, $\dfrac{\bar{P}_A}{P_{max}} = \exp(-k \times A^n)$, where $\bar{P}_A$ = equivalent uniform rainfall depth for an area of A; P_{max} = maximum point rainfall depth; and k and n = parameters.

Isohyet (mm)	130	120	110	100	90
Incremental area between isohyets (km^2)	143	245	258	290	484

7.2.12 Based on the 100-year rainfall records at the Hong Kong Observatory, the rainfall intensities with an annual exceedance probability of 0.1 (i.e., 10-yr return period) of different durations are given in the table below.

Duration, t_d (min)	15	30	60	120
Intensity, i (mm/h)	161	132	103	74

(a) Determine the least-squares estimates of coefficients a and c in the following rainfall intensity-duration equation and the associated R^2 value, $i = \dfrac{a}{(t_d + 4.5)^c}$, in which i = rainfall intensity (in mm/h) and t_d = storm duration in (minutes).
(b) Estimate the total rainfall depth (in cm) for a 10-year, 4-hr storm event.

7.2.13 Based on the 100-year rainfall records at the Hong Kong Observatory, the rainfall intensities with an annual exceedance probability of 0.1 (i.e., 10-year return period) of different durations are given in the table below.

Return period, T (year)	5	10	50	100	200
Duration, t_d (hr)	6	8	12	18	24
Depth, d (mm/h)	192	255	392	500	622

Consider the following empirical model to be used to fit the above rainfall intensity-duration-frequency (IDF) data, $d(T, t_d) = \dfrac{aT^m}{(t_d + b)^c}$, in which d = rainfall depth (in mm) corres-

ponding to a storm event of return period T-year and duration t_d-hr.

(a) Describe a least-squares-based procedure to optimally estimate the coefficients a, b, c, and m in the above rainfall IDF model.

(b) Assuming $b = 4.0$, determine the least-squares estimates of coefficients a, c, and m in the above rainfall intensity-duration equation and the associated R^2 value.

(c) Estimate the average rainfall intensity (in mm/hr) for the 25-year, 4-hr storm event.

7.2.14 Consider a rainfall event having 5-min cumulative rainfall record given below:

Time (min)	0	5	10	15	20	25	30
Cumulative rainfall (mm)	0	7	14	23	34	45	58
Time (min)	35	40	45	50	55	60	65
Cumulative rainfall (mm)	70	81	91	100	110	119	125
Time (min)	70	75	80	85	90		
Cumulative rainfall (mm)	131	136	140	140	140		

(a) What is the duration of the entire rainfall event and the corresponding total rainfall amount?

(b) Find the rainfall depth hyetograph (in tabular form) with 10-min time interval for the storm event.

(c) Find the maximum 10-min and 20-min average rainfall intensities (in mm/hr) for the storm event.

7.2.15 Based on available rainfall records at a location, the rainfall intensity with an annual exceedance probability of 0.1 (i.e., 10-year return period) of different durations are given in the table below.

Duration, t_d (min)	15	30	60	120
Intensity, i (mm/h)	160	132	105	75

(a) Determine the least-squares estimates of coefficients a and c in the following rainfall intensity-duration equation and calculate the corresponding R^2 value, $i = \dfrac{a}{(t_d + 4.5)^c}$ in which i = rainfall intensity (in mm/h) and t_d = storm duration (in minutes).

(b) Estimate the total rainfall depth (in mm) for a 10-year, 90-min storm event.

7.2.16 Based on the available rainfall records at the Hong Kong Observatory, the rainfall intensities corresponding to different durations with an annual exceedance probability of 0.1 (i.e. 10-year return period) are given in the table below.

| Duration, t_d (min)	15	30	60	120
Intensity, i (mm/h)	161	132	103	74

(a) Determine the least-squares estimates of coefficients a and c in the following rainfall intensity-duration equation, $i = \dfrac{a}{(t_d + 45)^c}$ in which i = rainfall intensity (in mm/h) and t_d = storm duration (in minutes).

(b) Estimate the total rainfall depth (in cm) for a 10-year, 4-hr storm event.

7.2.17 An experimental rectangular plot of 10 km × 12 km has five rain gauge stations as shown in the figure. The storm rainfall and coordinates of the stations are given in the table.

Station	(x, y)	Mean annual rainfall (cm)	Storm rainfall (cm)
A	(1, 3)	128	12.0
B	(8, 11)	114	11.4
C	(3, 10)	136	13.2
D	(5, 8)	144	14.6
E	(7, 5)	109	?

(a) Estimate the missing rainfall amount at station E.

(b) Based on the position of the five rain gauges, construct the Thiessen polygon for them.
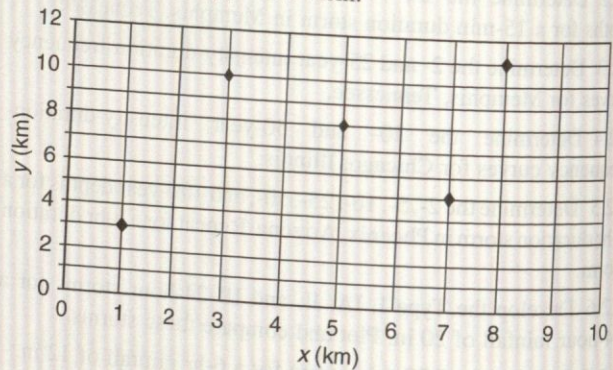
7.3.1 Solve example 7.3.1 for an average net radiation of 92.5 W/m^2. Compare the resulting evaporation rate with that in example 7.3.1.

7.3.2 Solve example 7.3.2 for a roughness height $z_0 = 0.04$ cm. Compare the resulting evaporation rate with that in example 7.3.2.

7.3.3 Solve example 7.3.3 for an average net radiation of 92.5 W/m^2. Compare the resulting evaporation rate with that in example 7.3.3.

7.3.4 Solve example 7.3.4 for an average net radiation of 92.5 W/m^2. Compare the resulting evaporation rate with that in example 7.3.4.

7.3.5 At a certain location during the winter, the average air temperature is 10°C and the net radiation is 40 W/m^2 and during the summer the net radiation is 200 W/m^2 and the temperature is 25°C Compute the evaporation rates using the Priestley–Taylor method.

7.3.6 The average weather conditions are net radiation = 40 W/m^2; air temperature = 28.5° C; relative humidity = 55 percent; and wind speed = 2.7 m/s at a height of 2 m. Calculate the open water evaporation rate in millimeters per day using the energy method, the aerodynamic method, the combination method, and

the Priestley–Taylor method. Assume standard atmospheric pressure is 101 kPa and z_o is 0.03 cm.

7.3.7 A 600-hectare farm land receives annual rainfall of 2500 mm. There is a river flowing through the farm land with inflow rate of 5 m³/s and outflow rate of 4 m³/s. The annual water storage in the farm land increases by 2.5×10^6 m³. Based on the hydrologic budget equation, determine the annual evaporation amount (in mm). [Note: 1 hectare $= 10,000$ m²]

7.4.1 Determine the infiltration rate and cumulative infiltration curves (0 to 5 h) at 1-hr increments for a clay loam soil. Assume an initial effective saturation of 40 percent and continuous ponding.

7.4.2 Rework problem 7.4.1 using an initial effective saturation of 20 percent.

7.4.3 Rework example 7.4.3 for a sandy loam soil.

7.4.4 Compute the ponding time and cumulative infiltration at ponding for a sandy clay loam soil with a 30-percent initial effective saturation, subject to a rainfall intensity of 2 cm/h.

7.4.5 Rework problem 7.4.4 for a silty clay soil.

7.4.6 Determine the cumulative infiltration and the infiltration rate on a sandy clay loam after 1 hr of rainfall at 2 cm/hr if the initial effective saturation is 25 percent. Assume the ponding depth is negligible in the calculations.

7.4.7 Rework problem 7.4.6 assuming that any ponded water remains stationary over the soil so that the ponded depth must be accounted for in the calculations.

7.4.8 Derive the equation for cumulative infiltration using Horton's equation.

7.4.9 Use the Green–Ampt method to compute the infiltration rate and cumulative infiltration for a silty clay soil ($\eta = 0.479$, $\psi = 29.22$ cm, $K = 0.05$ cm/hr) at 0.25-hr increments up to 4 hr from the beginning of infiltration. Assume an initial effective saturation of 30 percent and continuous ponding.

7.4.10 The parameters for Horton's equation are $f_0 = 3.0$ in/h, $f_c = 0.5$ in/h, and $K = 4.0\,h^{-1}$. Determine the infiltration rate and cumulative infiltration at 0.25-hr increments up to 4 hr from the beginning of infiltration. Assume continuous ponding.

7.4.11 Derive an equation for ponding time using Horton's equation.

7.4.12 Compute the ponding time and cumulative infiltration at ponding for a sandy clay loam soil of 25 percent initial effective saturation for a rainfall intensity of (a) 2 cm/h, (b) 3 cm/h, and (c) 5 cm/h.

7.4.13 Rework problem 7.4.12 considering a silt loam soil.

7.4.14 Consider a soil with porosity $\eta = 0.43$ and suction $\psi = 11.0$ cm. Before the rainfall event, the initial moisture content $\theta_i = 0.3$. It is known that after one hour of rainfall, the total infiltrated water is 2.0 cm.

(a) Determine the hydraulic conductivity in the Green–Ampt infiltration model.
(b) Estimate the potential total infiltration amount 1.5 hr after the beginning of the storm.

(c) Determine the instantaneous potential infiltration rate at $t = 1.5$ hr.

7.4.15 The following experimental data are obtained from an infiltration study. The objective of the study is to establish a plausible relationship between infiltration rate (f_t) and time (t).

Time, t (mm)	3	15	30	60	90
Infiltration rate, f_t (cm/hr)	8.5	7.8	7.0	6.1	5.6

From the scatter plot of infiltration rate and time, the following relationship between f_t and t is plausible, $f_t = 5.0 + (f_o - 5.0)\exp(-k \times t)$, where f_o is the initial infiltration rate (in cm/hr) and k is the decay constant (in min⁻¹).

(a) Determine the values of the two constants, i. e., f_o and k, by the least-squares method.
(b) Based on the result in part (a), estimate the infiltration rate at time $t = 150$ min.

7.4.16

(a) For a sandy loam soil, using Green–Ampt equation to calculate the infiltration rate (cm/h) and cumulative infiltration depth (cm) after 1, 60, and 150 min if the effective saturation is 40 percent. Assume a continuously ponded condition.
(b) Take the infiltration rates computed in Part (a) at 1 min and 150 min as the initial and ultimate infiltration rates in Horton's equation, respectively. Determine the decay constant, k.
(c) Use the decay constant, k, found in Part (b) to compute the cumulative infiltration at $t = 60$ min by Horton's equation.

7.4.17 Assume that ponded surface occurs at the beginning of a storm event.

(a) Calculate the potential infiltration rates (cm/hr) and potential cumulative infiltration depth (cm) by the Green–Ampt model for loamy sand at times 30 and 60 min. The initial effective saturation is 0.2.
(b) Based on the infiltration rates or cumulative infiltration depth computed in Part (a), determine the two parameters S and K in the following Philip two-term infiltration model.

$$F(t) = S\,t^{1/2} + K\,t; \quad f(t) = 0.5\,S\,t^{0.5} + K$$

(c) Based on the S and K computed in Part (b), determine the effective rainfall hyetograph for the following total hyetograph of a storm event.

Time (min)	0-30	30-60	60-90	90-120
Intensity (cm/hr)	8.0	15.0	5.0	3.0

(d) Find the value of the Φ-index and the corresponding effective rainfall hyetograph having the total effective rainfall depth obtained in Part (c).

7.4.18 Consider the sandy loam soil with effective porosity $\theta_e = 0.43$, suction $\psi = 11.0$ cm, and hydraulic conductivity $K = 1.1$ cm/h. Before the rainfall event, the initial effective saturation is $S_e = 0.3$. It is known that, after 1 hr of rainfall, the total infiltrated water is 2.0 cm.

(a) Estimate the potential total infiltration amount 1.5 hr after the beginning of the storm event by the Green–Ampt equation.

(b) Also, determine the instantaneous potential infiltration rate at $t = 1.5$ hr.

7.4.19 Considering a plot of land with sandy loam soil, use the Green–Ampt equation to calculate the infiltration rate (cm/h) and cumulative infiltration depth (cm) at $t = 30$ min under the initial degree of saturation of 40 percent and continuously ponding condition. The relevant parameters are: suction head = 6.0 cm; porosity = 0.45; and hydraulic conductivity = 3.00 cm/h.

7.4.20 Suppose that the infiltration of water into a certain type of soil can be described by Horton's equation with the following parameters: initial infiltration rate = 50 mm/h; ultimate infiltration rate = 10 mm/h; and decay constant = 4 h⁻¹. A rain storm event has occurred and its pattern is given below.

Time (min)	0	15	30	45	60	75	90
Cumu. rain (mm)	0	15	25	30	32	33	33

(a) Determine the effective rainfall intensity hyetograph (in mm/h) from the storm event.

(b) What is the percentage of total rainfall infiltrated into the ground?

(c) What assumption(s) do you use in the Part (a) calculation? Justify them.

7.4.21 Consider a 2-hr storm event with a total rainfall amount of 80 mm. The measured direct runoff volume produced by the storm is 40 mm.

(a) Determine the decay constant k in Horton's infiltration model knowing that the initial and ultimate infiltration rates are 30 mm/hr and 2 mm/hr, respectively.

(b) Use the Horton equation developed in Part (a) to determine the effective rainfall intensity hyetograph for the following storm event.

Time (min)	0-10	10-20	20-30
Incremental rainfall depth (mm)	5	20	10

7.4.22 An infiltration study is to be conducted. A quick site investigation indicates that the soil has an effective porosity $\theta_e = 0.40$ and the initial effective saturation $S_e = 0.3$. Also, from the double-ring infiltrometer test, we learn that the cumulative infiltration amounts at $t = 1$ hr and $t = 2$ hr are 1 cm and 1.6 cm, respectively.

(a) It is decided that the Green–Ampt equation is to be used. Determine the parameters suction (ψ) and hydraulic conductivity (K) from the test data. (You can use an iterative procedure or apply simple approximation using $\ln(1+x) = 2x/(2+x)$ for a direct solution.)

(b) Also, determine the cumulative infiltration and the corresponding instantaneous potential infiltration rate at $t = 3$ hr. (You can use the Newton method to obtain the solution with accuracy within 0.1mm or the most accurate direct solution approach.)

7.4.23 You are working on a proposal to do some rainfall runoff modeling for a small city nearby. One of the things the city does not have is a hydrology manual. You must decide upon an infiltration methodology for the analysis. You are going to consider methods such as the Φ-index method, empirical methods (such as Horton's and Holtan's), the SCS method, and the Green–Ampt method. Would you choose the Green–Ampt method over the others? Why?

REFERENCES

American Society of Agricultural Engineers, "Advances in Infiltration," in *Proc. National Conf. on Advances in Infiltration*, Chicago, IL, ASAE Publication 11–83, St. Joseph, MI 1983.

Bedient, P. B., and W. C. Huber, *Hydrology and Floodplain Analysis*, second edition, Addison-Wesley, Reading, MA, 1992.

Bhowmik, N., "River Basin Management: An Integrated Approach" *Water International*, International Water Resources Association, vol. 23, no. 2, pp. 84–90, June 1998.

Bonnin, G. M., D. Martin, B. Lin, T. Parzybok, M. Yekta, and D. Riley, "Precipitation-Frequency Atlas of the United States," NOAA Atlas 14, vol. 2, version 3, NOAA, National Weather Service, Silver Spring, MD, 2004.

Bonnin, G. M., D. Martin, B. Lin, T. Parzybok, M. Yekta, and D. Riley, "Precipitation-Frequency Atlas of the United States," NOAA Atlas 14, vol. 1, version 4, NOAA, National Weather Service, Silver Spring, MD, 2006.

Brakensiek, D. L., R. L. Engleman, and W. J. Rawls, "Variation within Texture Classes of Soil Water Parameters," *Trans. Am. Soc. Agric. Eng.*, vol. 24, no. 2, pp. 335–339, 1981.

Bras, R. L., *Hydrology: An Introduction to Hydrologic Science*, Addison-Wesley, Reading, MA, 1990.

Brooks, R. H., and A. T. Corey, "Hydraulic Properties of Porous Media," *Hydrology Papers*, no. 3, Colorado State University, Fort Collins, CO, 1964.

Chow, V. T., *Handbook of Applied Hydrology*, McGraw Hill, New York 1964.

Chow, V. T., D. R. Maidment, and L. W. Mays, *Applied Hydrology*, McGraw-Hill, New York, 1988.

Demissee, M., and L. Keefer, "Watershed Approach for the Protection of Drinking Water Supplies in Central Illinois," *Water International*, IWRA, vol. 23, no. 4, pp. 272–277, 1998.

Devanrs, M., and G. F. Gifford, "Applicability of the Green and Ampt Infiltration Equation to Rangelands," *Water Resource Bulletin*, vol. 22, no. 1, pp. 19–27, 1986.

Feynman, R. P., R. B. Leighton, and M. Sands, *The Feynman Lecture Notes on Physics*, vol. I, Addison-Wesley, Reading, MA, 1963.

Frederick, R. H., V. A. Meyers, and E. P. Auciello, "Five to 60-Minute Precipitation Frequency for the Eastern and Central United States," NOAA Technical Memo NWS HYDRO-35, National Weather Service, Silver Spring, MD, June 1977.

Green, W. H., and G. A. Ampt, "Studies on Soil Physics. Part I: The Flow of Air and Water Through Soils," *J. Agric. Sci.*, vol. 4, no. 1, pp. 1–24, 1911.

Gupta, R. S., *Hydrology and Hydraulic Systems*, Prentice-Hall, Englewood Cliffs, NJ, 1989.

Hansen, E. M., L. C. Schreiner, and J. F. Miller, "Application of Probable Maximum Precipitation Estimates—United States East of 105th Meridian," NOAA Hydrometeorological Report 52, U.S. National Weather Service, Washington, DC, 1982.

Hershfield, D. M., "Rainfall Frequency Atlas of the United States for Durations from 30 Minutes to 24 Hours and Return Periods from 1 to 100 Years," Tech. Paper 40, U.S. Department of Commerce, Weather Bureau, Washington, DC, 1961.

Horton, R. E., "The Role of Infiltration in the Hydrologic Cycle," *Trans. Am. Geophysical Union*, vol. 14, pp. 446–460, 1933.

Huff, F. A., "Time Distribution of Rainfall in Heavy Storms," *Water Resources Research*, vol. 3, no. 4, pp. 1007–1019, 1967.

Maidment, D. R. (editor-in-chief), *Handbook of Hydrology*, McGraw-Hill, New York, 1993.

Marsh, W. M., *Earthscape: A Physical Geography*, John Wiley & Sons, New York, 1987.

Marsh, W. M., and J. Dozier, *Landscape: An Introduction to Physical Geography*, John Wiley & Sons, New York, 1986.

Masch, F. D., *Hydrology*, Hydraulic Engineering Circular No. 19, FHWA-10-84-15, Federal Highway Administration, U.S. Department of the Interior, McLean, VA, 1984.

McCuen, R. H., *Hydrologic Analysis and Design*, 2nd edition Prentice-Hall, Englewood Cliffs, NJ, 1998.

Miller J. F., R. H. Frederick, and R. J. Tracey, *Precipitation Frequency Atlas of the Coterminous Western United States (by States)*, NOAA Atlas 2, 11 vols., National Weather Service, Silver Spring, MD, 1973.

Moore, W. L., E. Cook, R. S. Gooch, and C. F. Nordin, Jr., "The Austin, Texas, Flood of May, 24-25, 1981," National Research Council, Committee on Natural Disasters, Commission on Engineering and Technical Systems National Academy Press, Washington, DC, 1982.

Parrett, C., N. B. Melcher, and R. W. James, Jr., "Flood Discharges in the Upper Mississippi River Basin," in *Floods in the Upper Mississippi River Basin*," U.S. Geological Survey Circular, 1120-A U.S. Government Printing Office, Washington, DC, 1993.

Philip, J. R., "Theory of Infiltration: 1. The Infiltration Equation and Its Solution," *Soil Science* 83, pp. 345–357, 1957.

Philip, J. R., "The Theory of Infiltration," in *Advances in Hydro Sciences*, edited by V. T. Chow, vol. 5, pp. 215–296, 1969.

Ponce, V. M., *Engineering Hydrology: Principles and Practices*, Prentice-Hall, Englewood Cliffs, NJ, 1989.

Priestley, C. H. B., and R. J. Taylor, "On the Assessment of Surface Heat Flux and Evaporation Using Large-Scale Parameter," *Monthly Weather Review*, vol. 100, pp. 81–92, 1972.

Rawls, W. J., D. L. Brakensiek, and N. Miller, "Green-Ampt Infiltration Parameters from Soils Data," *J. Hydraulic Div., ASCE*, vol. 109, no. 1, pp. 62–70, 1983.

Richards, L. A., "Capillary Conduction of Liquids Through Porous Mediums," *Physics*, vol. 1, pp. 318–333, 1931.

Roberson, J. A., J. J. Cassidy, and M. H. Chaudhry, *Hydraulic Engineering*, 2nd edition, John Wiley & Sons, New York, 1998.

Schreiner, L. C., and J. T. Riedel, Probable Maximum Precipitation Estimates, United States East of the 105th Meridian, NOAA Hydrometeorological Report no. 51, National Weather Service, Washington, DC, June 1978.

Singh, V. P., *Elementary Hydrology*, Prentice-Hall, Englewood Cliffs, NJ, 1992.

Thornthwaite, C. W., and B. Holzman, "The Determination of Evaporation from Land and Water Surface," *Monthly Weather Review*, vol. 67, pp. 4–11, 1939.

U.S. Army Corps of Engineers, Hydrologic Engineering Center, HEC-1, *Flood Hydrograph Package*, User's Manual, Davis, CA, 1990.

U.S. Department of Agriculture Soil Conservation Service, *A Method far Estimating Volume and Rate of Runoff in Small Watersheds*, Tech. Paper 149, Washington, DC, 1973.

U.S. Department of Agriculture Soil Conservation Service, *Urban Hydrology for Small Watersheds*, Tech. Release no. 55, Washington, DC, 1986.

U.S. Department of Commerce, *Probable Maximum Precipitation Estimates, Colorado River and Great Basin Drainages*, Hydrometeorological Report no 49, NOAA, National Weather Service, Silver Spring, MD, 1977.

U.S. Environmental Data Services, *Climate Atlas of the US.*, U.S. Environment Printing Office, Washington, DC, pp. 43–44, 1968.

U.S. National Academy of Sciences, *Understanding Climate Change*, National Academy Press, Washington, DC, 1975.

U.S. National Academy of Sciences, *Safety of Existing Dams; Evaluation and Improvement*, National Academy Press, Washington, DC, 1983.

U.S. National Research Council, *Global Change in the Geosphere-Biosphere*, National Academy Press, Washington, DC, 1986.

U.S. National Research Council, Committee on Opportunities in the Hydrologic Science, Water Science and Technology Board, *Opportunities in the Hydrologic Sciences*, National Academy Press, Washington, DC, 1991.

U.S. Weather Bureau, *Two- to Ten-Day Precipitation for Return Periods of 2 to 100 Years in the Contiguous United States*, Tech. Paper 49, Washington, DC, 1964.

Viessman, W. Jr., and G. L. Lewis, *Introduction to Hydrology*, 4th edition, Harper and Row, New York, 1996.

Wanielista, M., R. Kersten, and R. Eaglin, *Hydrology: Water Quantity and Quality Control*, John Wiley & Sons, New York, 1997.